論文 / 著書情報
Article / Book Information

題目(和文)	
Title(English)	Effects of Simple Electrolytes on the Conformation of Poly(L-glutamic acid) in Aqueous Solution
著者(和文)	佐藤満
Author(English)	MITSURU SATOH
出典(和文)	学位:工学博士, 学位授与機関:東京工業大学, 報告番号:甲第1166号, 授与年月日:1980年3月26日, 学位の種別:課程博士, 審査員:
Citation(English)	Degree:Doctor of Engineering, Conferring organization: Tokyo Institute of Technology, Report number:甲第1166号, Conferred date:1980/3/26, Degree Type:Course doctor, Examiner:
学位種別(和文)	博士論文
Type(English)	Doctoral Thesis

Effects of Simple Electrolytes on the Conformation of Poly(L-glutamic acid) in Aqueous Solution

By Mitsuru Satoh

M. Eng., Tokyo Institute of Technology, 1977

A Dissertation Presented to the Faculty
of the Graduate School of Tokyo Institute
of Technology in Candidacy for the Degree
of Doctor of Engineering, 1980

CONTENTS

CHAPTER I

Introduction

Poly(L-glutamic acid)(PLG) is a polyelectrolyte which transforms its conformation from coil to helix according to experimental conditions, e.g., temperature, solvent, pH, salt concentration and so on, and the helix-coil transition has been extensively studied[1-12] in order to throw light on the conformational transitions of proteins. Much more attentions have been paid to the pH induced helix-coil transition rather than the temperature or solvent induced transition since PLG has weak acidic groups and in most cases water is chosen as the solvent.

This polyaminoacid assumes random coil conformation in a certain range of the charge density, where the polymer may be considered as a simple polyelectrolyte. Decrease in the charge density causes the decrease of the dimension of the chain and eventually the transition from a random coil to an α-helix. A change of helix content in a process of the transition gives rise to variation of the flexibility and the dimension of the polymer. In this connection the information of the dimension of the polymer in random coil will be useful for understanding the conformational transition.

As PLG is a polyelectrolyte, the interaction - specific and/or nonspecific - with counter-ions is one of the most important factors that determine the conformation and the dimension of the polymer chain. Hence investigation on this subject will be also necessary.

Here it may be of interest to review some theoretical and experimental studies related to these aspects; (i) dimension of polymers and polyelectrolytes, (ii) interaction of polyelectrolytes with small ions, (iii) helix-coil transition of nonionic and ionic polypeptides. Interrelations among (i), (ii) and (iii) will be also referred to.

(i) The intrinsic viscosity of nonionic and ionic polymers in solution[13-19] has been used as a measure of the dimension of these polymer chains which are perturbed by hydrodynamic interaction. Theories on the intrinsic viscosity have been developed based on two models; one is the hydrodynamically equivalent sphere model given by Debye[20] and the other the pearl-necklace model given by Kirkwood-Riseman[21]. These theories, however, should be applied to an ideal chain having no excluded volume, of which effect was introduced by Flory[22] into the viscosity theory.

Considering the difference between two expansion factors, statistical and hydrodynamical ones, Stockmayer and Fixman[13] proposed next equation,

$$[\eta]/M^{1/2} = K_0 + 0.51\Phi_0 B\cdot M^{1/2} \qquad (1)$$

which relates the intrinsic viscosity $[\eta]$ and the molecular weight M of a polymer. The unperturbed dimension and the excluded volume of the polymer chain can be evaluated from K_0 and B, respectively.

Recently, Tan and Gasper used eq.(1) to obtain the unperturbed dimensions of a random copolymer of ethyl acrylate and acrylic acid[14] and a homopolymer, sodium poly(3-methacryloyloxypropane-1-sulfonate)[15]. The authors obtained a common intercept in the plots of eq.(1) for each polymer in aq. solutions of various ionic strength.

Morcellet and Loucheux[16] have reported the viscosities of poly(L-glutamic acid) in water and water-dioxane mixtures. They also obtained the unperturbed effective bond length using eq.(1).

Noda et al.[17)] determined the intrinsic viscosity of sodium poly(acrylate) as a function of the molecular weight and the degree of ionization. These authors expressed the apparent long range interaction parameter B in eq.(1) as a sum of the terms due to the nonelectrostatic and electrostatic interactions.

Light scattering measurement has extensively been performed to study the dimension of polyelectrolyte, and numerous investigations[14,15,23-25)] have been made to examine the agreements of experimental results on statistics of polymer chains (dimensions, expansion factors, second virial coefficients) with theories. For example, Nagasawa-Kagawa[26)], Hermans-Overbeek[27)], Flory[28)] and Rice-Harris[29)] estimated the statistical expansion of a spherical polyelectrolyte by considering the electrostatic potential. Most of the theories, however, used binding constant of counter-ion or effective dielectric constant as a parameter to fit with experimental data.

(ii) Strauss et al.[30)] explored the nature of the binding of some alkali cations and tetramethylammonium cation by polyphosphates by means of electrophoresis, salting out and viscosity measurements. They concluded that alkali cations such as Li^+, Na^+ or K^+, but not tetrametylammonium cation are site-bound by the charged group of the polyelectrolyte. Strauss et al.[31)] explained the differential intrinsic viscosities of polyphosphates in the presence of various alkali salts in terms of the specific solvent incompatibilities of site-bound ion pairs. Further Strauss and coworkers[32,33] used the dilatometric data as a criterion for site binding of counter-ions and found the site binding of alkali and alkaline earth metal ions take place to varying degrees with polyelectrolytes.

On the other hand, many efforts have been made to explain non-specific counter-ion binding by solving the Poisson-Boltzmann equation based on a cylinder or a rodlike model for a polyelectrolyte. Fuoss et al.[34] and Alfley et al.[35] have shown that this equation can be exactly solved for an infinitely long rodlike polyion with counter-ions in a cylindrical free volume. When the Poisson-Boltzmann eq. is solved based on a realistic structural model, the Debye-Hückel approximation can be used to solve the equation in a closed form. Otherwise, the nonlinear equation must be solved numerically. This approximation should be used only when the kinetic energy is sufficiently larger than the electrostatic energy. Hence in the region close to the surface of the charged cylinder, "Gouy region", the nonlinear equation should be used to describe the charge density and potential.

Stigter[36] reported the charge-potential relation, the electric free energy of the highly charged colloidal cylinder, the potential-distance relation in the Gouy double layer and the interaction of the cylinder with electrolyte, obtained by numerical solution of the Poisson-Boltzmann equation calculated with a computer. The results were given using a correction factor of an analytical expression derived from the Debye-Hückel approximation.

Manning and Zimm[37] utilized the Mayer's cluster theory of ionic solutions as the starting point to calculate the thermodynamic properties of polyelectrolyte solutions. They successfully showed that the use of the Debye-Hückel screened coulomb potential between charged sites on the polymer is an adequate first approximation.

Manning38) developed a limiting law which predicts the counter-ion condensation to polymer phase at a charge density higher than a critical value, which is described as,

$$N\lambda = 1 - 1/N\xi \qquad (2)$$

where λ is the number of condensed counter-ions per fixed charge, N valence of the counter-ion and ξ a parameter which shows a line charge density of the polymer. When N=1, counter-ion condensation takes place at $\xi>1$, according to the theory.

The limiting law has been extensively applied to polyelectrolyte systems39-42) due to its simplicity and semiquantitative agreements with the experimental results, while the structure model for polyion - a straight wire with charged beads uniformly distributed along its length - has been critically discussed, e.g., Stigter43) has pointed out the model is an unrealistic postulation.

Oosawa44) obtained similar results as Manning's, i.e., a discontinuous counter-ion condensation, although the former author utilized the Poisson-Boltzmann equation and adopted a two phase model for each of the cylindrical and sphere models.

On the other hand, efforts were made by Katchalsky and Lifson45) to calculate the activity coefficients of univalent ions in the presence of a flexible polyelectrolyte by taking into account the expansion of the polymer chain due to the electrostatic interaction. The theory, however, was found to be largely a failure, i.e., it predicted equality of counter-ion and co-ion activity coefficients and overestimated the polymer dimension by close to a factor of ten. Since this failure, the mathematical difficulties in performing the correct average over polymer configurations of electrostatic interactions, have become realized and theories have evolved into two distinct species; one deals only with the expansion avoiding a precise description of interactions between polyelectrolytes and small ions using parameters such as binding constants or effective dielectric constants. The other, based on some structural model, tries to obtain knowledge about the thermodynamic behavior of small ions around a polyelectrolyte. An example of the former is the Fixman's fuzzy sphere model 46) which used an effective dielectric constant. Manning theory and Oosawa's treatment, which is based on two phase approximations, are typical of the latter.

Recently Bailey 47) has proposed a theory of polyelectrolyte expansion which assumes the Debye-Hückel screened coulomb potential and counter-ion condensation for the electrostatic interaction, and obtained semiquantitative agreement between the theory and experiment.

Odijk et al. 48) have presented an excluded volume theory of polyelectrolytes assuming that the polyion can be viewed as a worm-like chain bearing charges which interact according to the screened coulomb potential and are compensated by the counter-ion condensation (Manning theory).

Combinations of the excluded volume theories with the concept of counter-ion condensation, described above as examples, have been tried and obtained partially successful results.

(iii) The pioneering theory of the helix-coil transition in polypeptides was proposed by Zimm and Bragg$^{49)}$, followed by some theoreticians. These early theories are essentially equivalent to one another and based on statistical mechanical treatments of a one dimentional cooperative system. Most of them$^{49-52)}$, however, did not explicitly take into account the interaction of polypeptide and solvent, and were not able to explain the thermal inverse transition. Improvements of these theories were made by Peller$^{53)}$, Gibbs et al.$^{54)}$, Bixon et al.$^{55)}$and Birshtein et al.$^{56)}$, considering solvent effects.

The theories mainly concern the thermal or solvent induced helix-coil transition of nonionic polypeptides. A theory on pH induced transition of charged polypeptides was developed by Zimm and Rice$^{1)}$, who started from the Grand Partition Function. The theory was successfully compared with Wada's data on poly(glutamic acid)$^{2)}$.

Nagasawa et al.$^{3)}$and several researchers$^{4-7)}$, based upon the statistical mechanical treatment of Zimm and Rice, analysed the pH titration data of poly(glutamic acid) in aqueous NaCl solutions and estimated thermodynamic values and characteristic parameters of the transition, viz., the equilibrium constant of helix growth, s, and cooperativity parameter, σ.

Another method to obtain σ was presented by Ptitsyn and coworkers$^{8,9)}$, who expressed the statistical dimension of polypeptide in helix-coil transition region as the following equation,

$$\langle R^2\rangle = (1-\theta)\langle R^2\rangle_c + 2Nb_h^2\theta^{3/2}/\sqrt{\sigma(1-\theta)} \tag{3}$$

where $\langle R^2\rangle$ and $\langle R^2\rangle_c$ are mean square end-to-end distances of polymer chains in the transition region and random coil conformation, respectively, N the degree of polymerization, b_h helical segment length per monomer unit and θ helical content. This eq. was applied to pH induced transitions of poly(L-glutamic acid)10) and poly(L-lysine)57).

A statistical treatment of the dimension in the transition region was discussed in detail by Nagai51). Yamakawa et al.58) have recently approached the same subject with a wormlike chain model.

The dependence of the helix-coil transition of DNA on ionic strength has been interpreted by Record et al.59-62) and Manning63,64) in terms of Manning's condensation theory, which is different from the limiting law previously mentioned. Manning has successfully obtained eq.(2) by using a two phase model similar to Oosawa's and keeping his structure model intact.

Gruenwedel and coworkers65-67) have studied salt effects on the denaturation of DNA by calorimetric investigations of the transition enthalpy. Taking into account binding of water molecules as well as small ions, the authors evaluated the numbers of water and small ions released with the helix-coil transition. Larger values, however, for the counter-ion release than predicted by Manning theory, were reported in these investigations.

As can be seen in the above review, theories originally proposed to analyse the interaction and conformation of simple polyelectrolytes, have been applied to charged biopolymers. Thus in order to understand the charge induced helix-coil transition of PLG, it is a prerequisite to study the behavior of the polymer in random coil conformation to which theories for simple polyelectrolytes may be applied. For these reasons, the present study includes experiments for PLG in random coil conformation.

This thesis is composed of three kinds of experimental study.

1) Chain dimensions of sodium poly(L-glutamate)(PLGNa) in random coil and partially helical conformations are estimated by the viscosity measurements of the polymer in aq. NaCl solutions with various ionic strength and charge densities. Stockmayer-Fixman equation(eq.(1)) is used to evaluate the unperturbed dimension and the excluded volume effect of PLGNa chain. The cooperativity parameter σ of the transition is estimated by the method of Ptitsyn and coworkers (eq.(3)), where the results obtained for random coil PLGNa are taken into account. (Chapter II)

2) The hydration behaviors of PLGNa are studied by making use of compressibility data obtained from the density and ultrasonic velocity measurements of aqueous PLGNa-NaCl solutions. Knowledge of hydration to the polymer chain must be of some use for understanding interactions of polymer charges and counter-ions and dependence of the helix-coil transition on ionic strength particularly in higher concentration region of added salts, although few researches on hydration behaviors of polyelectrolytes have been referred in the above review. (Chapter III)

3) Effects of ionic species and the concentration of added salts

on the helix-coil transition of PLGNa are followed by CD measurements. With respect to the ionic strength dependence of the transition, counter-ion condensation is taken into account, based on the formulation of Manning theory which has been applied to the helix-coil transition of DNA. (Chapter IV)

REFERENCES

1) B. H. Zimm and S. A. Rice, J. Mol. Phys., 3, 391 (1960)

2) A. Wada, ibid., 3, 409 (1960)

3) M. Nagasawa and A. Holtzer, J. Amer. Chem. Soc., 86, 531 (1964)

4) R. L. Snipp, W. G. Miller and R. E. Nylund, ibid., 87, 3547 (1965)

5) D. S. Olander and A. Holtzer, ibid., 90, 4549 (1968)

6) A. Warashina and A. Ikegami, Biopolymers, 11, 529 (1972)

7) H. Kanehiro, J. Komiyama, O. Morikiyo and T. Iijima, ibid., 15, 1005 (1976)

8) O. B. Ptitsyn and A. M. Skvortsov, Biofizika, 10, 909 (1965)

9) O. B. Ptitsyn, T. V. Barskaya, I. A. Bolotina and I. A. Illarionova, ibid., 12, 386 (1967)

10) V. E. Bychkova, O. B. Ptitsyn and T. V. Barskaya, Biopolymers, 10, 2161 (1971)

11) M. Morcellet and C. Loucheux, Polymer, 16, 401 (1975)

12) H. Noguchi and J. T. Yang, Biopolymers, 1, 359 (1963)

13) W. H. Stockmayer and M. Fixman, J. Polym. Sci. Part C, 1, 137 (1963)

14) J. S. Tan and S. P. Gasper, J. Polym. Sci.: Polym. Phys. Ed., 12, 1785 (1974)

15) idem., ibid., 13, 1705 (1975)

16) M. Morcellet and C. Loucheux, Biopolymers, 15, 1857 (1976)

17) I. Noda, T. Tsuge and M. Nagasawa, J. Phys. Chem., 74, 710 (1970)

18) P. J. Flory and J. E. Osterheld, ibid., 58, 653 (1954)

REFERENCES (continued 1)

19) N. Ohno, K. Nitta, S. Makino and S. Sugai, J. Polym. Sci.: Polym. Phys. Ed., 11, 413 (1973)

20) P. Debye and A. M. Bueche, J. Chem. Phys., 16, 573 (1948)

21) J. G. Kirkwood and J. Riseman, ibid., 16, 565 (1948)

22) P. J. Flory and T. G. Fox, Jr., J. Amer. Chem. Soc., 73, 1904 (1951)

23) H. Eisenberg, J. Chem. Phys., 44, 137 (1966)

24) A. Takahashi, T. Kato and M. Nagasawa, J. Phys. Chem., 71, 2001 (1967)

25) Z. Alexandrowicz, J. Chem. Phys., 47, 4377 (1967)

26) M. Nagasawa and I. Kagawa, J. Polym. Sci., 13, 43 (1954)

27) J. J. Hermans and J. Th. G. Overbeek, Rec. Trav. Chim., 67, 761 (1948)

28) P. J. Flory, J. Chem. Phys., 21, 162 (1953)

29) S. A. Rice and F. E. Harris, J. Phys. Chem., 58, 733 (1954)

30) U. P. Strauss, D. Woodside and P. Wineman, ibid., 61, 1353 (1957)

31) U. P. Strauss and Y. P. Leung, J. Amer. Chem. Soc., 87, 1476 (1965)

32) P. D. Ross and U. P. Strauss, ibid., 82, 1311 (1960)

33) J. Hen and U. P. Strauss, J. Phys. Chem., 78, 1013 (1974)

34) R. M. Fuoss, A. Katchalsky and S. Lifson, Proc. Natl. Acad. Sci. U. S., 37, 579 (1951)

35) T. Alfley, P. Berg and H. Morawetz, J. Polym. Sci., 7, 543 (1951)

REFERENCES (continued 2)

36) D. Stigter, J. Colloid Interf. Sci., 53, 296 (1975)

37) G. S. Manning and B. H. Zimm, J. Chem. Phys., 43, 4250 (1965)

38) G. S. Manning, ibid., 51, 924 (1969)

39) G. S. Manning, Biopolymers, 11, 937 (1972)

40) N. D. Marky and G. S. Manning, ibid., 14, 1407 (1975)

41) N. Ise and T. Okubo, Macromolecules, 11, 439 (1978)

42) M. Kowblansky, M. Tomasula and P. Ander, J. Phys. Chem., 82, 1491 (1978)

43) D. Stigter, ibid., 82, 1603 (1978)

44) F. Oosawa, Polyelectrolytes, Marcel Dekker, New York, 1971

45) A. Katchalsky and S. Lifson, J. Polym. Sci., 11, 409 (1953)

46) M. Fixman, J. Chem. Phys., 41, 3772 (1964)

47) J. M. Bailey, Macromolecules, 10, 725 (1977)

48) T. Odijk and A. C. Houwaart, J. Polym. Sci.: Polym. Phys. Ed., 16, 627 (1978)

49) B. H. Zimm and J. K. Bragg, J. Chem. Phys., 31, 526 (1959)

50) J. A. Schellman, J. Phys. Chem., 62, 1485 (1958)

51) K. Nagai, J. Chem. Phys., 34, 887 (1961)

52) S. Lifson and A. Roig, ibid., 34, 1963 (1961)

53) L. Peller, J. Phys. Chem., 63, 1194 (1959)

54) J. H. Gibbs and E. A. Dimarzio, ibid., 30, 271 (1959)

55) M. Bixon and S. Lifson, Biopolymers, 4, 815 (1966)

56) T. M. Birshtein and O. B. Ptitsyn, Conformations of Macromolecules, Wiley Interscience, New York, 1966

57) T. V. Barskaya and O. B. Ptitsyn, Biopolymers, 10, 2181 (1971)

REFERENCES (continued 3)

58) H. Yamakawa and M. Fujii, J. Chem. Phys., 64, 5222 (1976)

59) M. T. Record, Jr., Biopolymers, 14, 2137 (1975)

60) M. T. Record, Jr., T. M. Lohman and P. D. Haseth, J. Mol. Biol., 107, 145 (1976)

61) M. T. Record, Jr., C. P. Woodbury and T. M. Lohman, Biopolymers, 15, 893 (1976)

62) M. T. Record, Jr., C. F. Anderson and T. M. Lohman, Q. Rev. Biophys., II, 103 (1978)

63) G. S. Manning, Biopolymers, 15, 1333 (1976)

64) G. S. Manning, Q. Rev. Biophys., II, 179 (1978)

65) D. W. Gruenwedel, C. H. Hsu and D. S. Lu, Biopolymers, 10, 47 (1971)

66) D. W. Gruenwedel, Biochim. Biophys. Acta, 340, 16 (1974)

67) idem., ibid., 395, 246 (1975)

CHAPTER II

Viscometry of PLGNa in Aqueous Solutions

ABSTRACT

Viscosity measurements of PLGNa with different molecular weights in aq. NaCl solutions have been performed to estimate the unperturbed dimension using Stockmayer-Fixman plot. It is found that the unperturbed dimension decreases with the charge density but is independent of NaCl concentration. While the expansion factor, α_η^3, shows an increasing trend with decreasing charge density. These results are interpreted to manifest that charges on the polymer affect both of the long-range and the short-range interactions of PLGNa chain.

The cooperativity parameter σ of the helix-coil transition of PLGNa has been estimated from the viscometric data by Ptitsyn's method with modifications. The increasing σ with decreasing charge density of the polymer is descussed in terms of the dependence of the unperturbed dimension on the charge density.

The viscometry of PLGNa in aq. organic solvent mixtures has shown that σ is not a simple function of the dielectric constant of solvent.

Introduction

The conformation of polyelectrolytes in aqueous salt solutions has been extensively studied by many workers. The dimension of the polymer chain, i.e., the unperturbed mean square end-to-end distance $\langle R^2 \rangle_0$ and the excluded volume effect are important points to study in such an investigation. These quantities have been obtained from viscosity or light scattering measurements$^{1)}$.

Theories of excluded volume effect were developed first on nonionic polymer and then applied to the polyelectrolyte solution that contains added salts such as NaCl, because the salts help the polymer in taking random coil conformation by suppressing the electrostatic repulsion among the charged groups on the polymer.

α_η, the hydrodynamic expansion factor, was simply written by Stockmayer and Fixman$^{2)}$ as

$$\alpha_\eta^3 = 1 + 1.55z \tag{1}$$

Here the parameter z has the usual meaning in the perturbation theories of the expansion factor. Taking this into account, Stockmayer and Fixman presented the relation,

$$\{\eta\}/N^{1/2} = K_0 + 0.51\Phi_0 B \cdot N^{1/2} \tag{2}$$

Here the relation is written in terms of the intrinsic viscosity in l/basemol $\{\eta\}$, the degree of polymerization N, a parameter related to the second virial coefficient B and the Flory constant Φ_0 equal to 2.87×10^{20}. K_0 is related to the unperturbed effective segment length b_0 as

$$K_o = \Phi_o b_o^3 \tag{3}$$

Eq.(2) and the analogues have been used to obtain the unperturbed dimension of various polymers in solution as mentioned in Chapter I.

Charged poly(amino acid) is an important subject to be studied from these points of views, since the charge density can alter not only the dimension but also the regular conformations, e.g., α-helix and β-sheet. Poly(L-glutamic acid) is known to take partly helix conformation below degree of neutralization i = 0.7 at room temperature. Hence knowledge of the dimension in the region of i higher than 0.7 will be necessary to understand the charge induced coil-helix transition accompanied with remarkable change in the dimension.

In this chapter, we discuss the viscosity of PLGNa in aq. solution under various charge densities and NaCl concentrations, in terms of Stockmayer-Fixman relation to elucidate the behaviors of the unperturbed dimension and the excluded volume effect, and of Ptitsyn's method described in Chapter I to estimate the cooperativity parameter σ of the helix-coil transition.

Experimental

Materials

PLGNa with different molecular weights were obtained following the procedure of Koiwa et al.3). Poly(γ-methyl-L-glutamate) was obtained by the polymerization of γ-methyl-L-glutamate NCA (Kyowa Hakko Co.) in 1,2-dichloroethane by using N,N-dimethyl ethylenediamine as initiator. Hydrolysis of the polymer was executed by stirring a mixture containing the polymerized solution, methanol, 2-propanol and water in 2:2:2:1 in volume and NaOH in 1.3 equivalent to the polymer. It has been reported4) that the above procedure gives PLGNa with relatively narrow molecular weight distribution. In fact we found 1.19 as Mw/Mn for S-1 sample by the fractionation using DEAE-cellulose column5). Impurities and the low molecular weight fraction of the polymer were eliminated by ultrafiltration of the polymer solution with a UP-20 filter (Toyo Roshi Co.), which is impermeable to polymers with $Mw > 10^4$. The polymer was recovered by freeze-drying. Molecular weights of these polymers were determined by the intrinsic viscosity at 25°C in 0.2 M NaCl solution through6)

$$[\eta]\ (\mathrm{dl/g}) = 5.13 \times 10^{-3} (Mw/Mo)^{0.85} \qquad (4)$$

where Mo is the molecular weight of the monomer residue. Table 1 gives the results.

Analytical grade ethylene glycol, isopropanol, t-butanol and dioxane were used as cosolvents in some experiments. Analytical grade NaCl and hydrochloric acid, and water which was distilled after the deionization, were used to prepare the solutions.

Apparatus and Methods

Viscosity measurements were made with an Ubbelohde viscometer with which the flow time of water 110.3 sec.. PLGNa solution was diluted with appropriate salt solutions of which pH were adjusted within 0.01.

Helix content of PLGNa was determined by measuring the molar ellipticity by a Jasco J 20 automatic recording spectropolarimeter through the relation[7)]

$$\theta = -[\Theta]_{222}/40{,}000 \qquad (5)$$

where θ is helix content and $[\Theta]_{222}$ is the molar ellipticity at 222 nm. All measurements were performed at 25 ± 0.1°C.

Results

Fig.1 shows the Stockmayer-Fixman plot for PLGNa with the degree of neutralization, i, = 1.00 ~ 0.70 in aqueous NaCl solutions with C_s = 1.0 ~ 0.02 M. The straight lines in the plot were drawn by the least square method. In Table 2, K_0 and B values obtained by these plots are shown. It is found that K_0 decreases with decreasing i, while it has no systematic dependence on C_s. Fig.2 shows the same kind plot for PLGNa having i in 0.60 ~ 0.30, where random coil to helix transition of the polymer takes place. Viscosity of PLGNa with i = 0.50 ~ 0.30 in 30 volume percent aq. dioxane is shown in Fig.3 in terms of eq.(2). These figures show that $\{\eta\}/N^{1/2}$ vs. $N^{1/2}$ plots are still linear at lower i and give the smaller K_0 with decreasing i. Eventually, PLGNa with i = 0.30 in 0.1 M NaCl solution and those with i = 0.40 and 0.30 in aq. dioxane give linear relations leading to negative K_0 values on the extrapolation. Under these conditions, PLGNa has the helix content shown in Table 3. It is noted that PLGNa with i = 0.70 contains ca. 2 % helix fraction. The polymer chain with such a small amount of helix may be assumed to behave as a random coil.

Fig.4 and Table 4 show the results of viscosity and CD measurements for PLGNa in aq. organic solvent mixtures.

Table 1 M and D.P. of PLGNa

	S-1	S-2	S-3	S-4
M x 10^4	14.7	10.6	7.23	6.12
D.P.	971	703	478	405

M : Molecular weight, D.P. : Degree of polymerization

Table 3 Helix content of PLGNa(S-1)

i	0.1 M NaCl	0.1 M NaCl - 30vol.% dioxane
0.60	0.184	
0.50	0.354	0.649
0.45	0.474	
0.40	0.603	0.825
0.35	0.663	
0.30	0.758	0.906

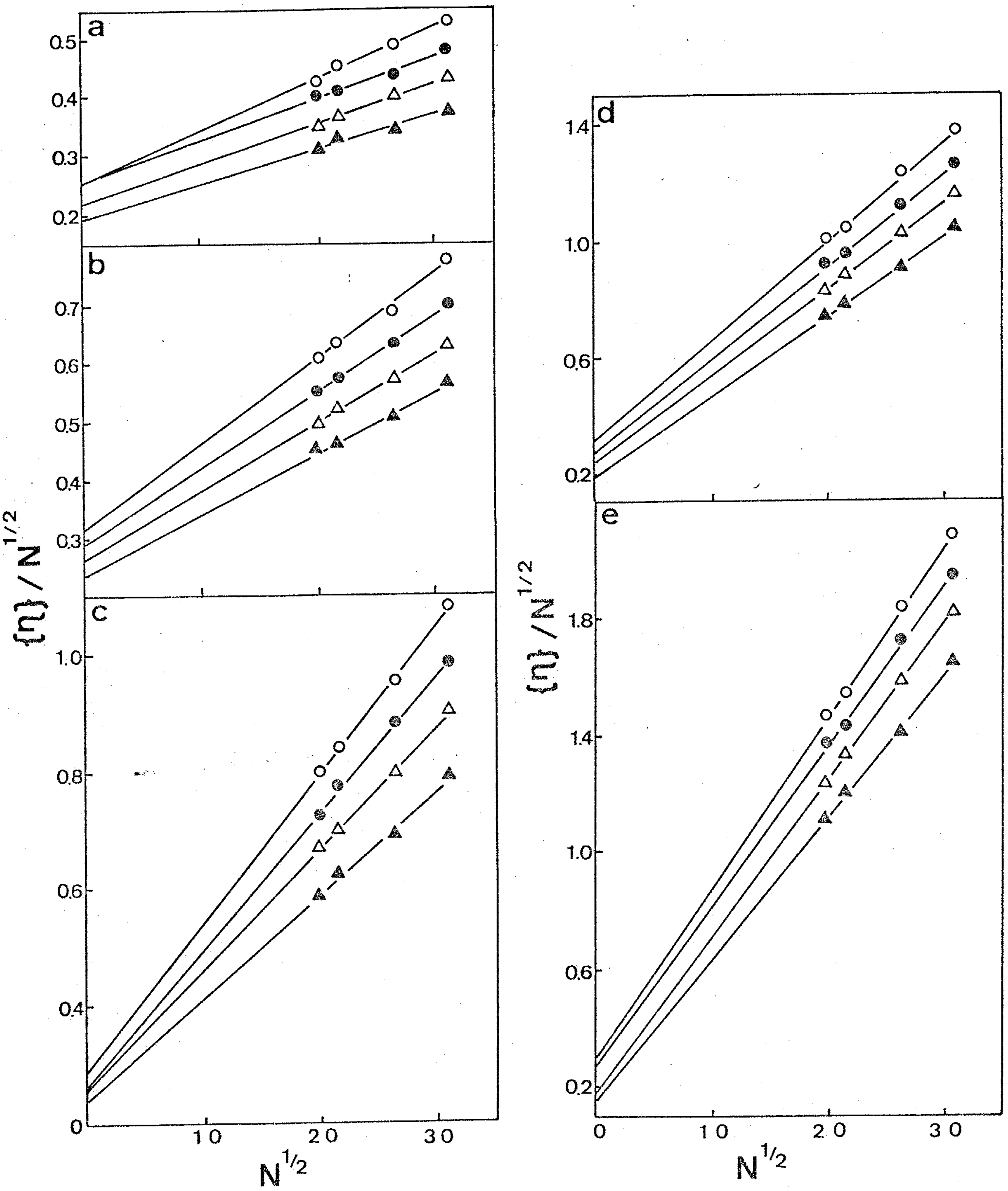

Fig.1 Stockmayer-Fixman plot for PLGNa in aq. NaCl solution

a. C_s = 1.00 M, b. 0.25 M, c. 0.10 M, d. 0.05 M, e. 0.02 M

(○) i = 1.00 ; (●) 0.90 ; (△) 0.80 ; (▲) 0.70

Table 2 $\{\eta\}$, K_0 and B of PLGNa

2-1 PLGNa-NaCl

C_s (M)	i	$\{\eta\}$ (1/basemol)				K_0	$B \times 10^{23}$
		S-1	S-2	S-3	S-4		
1.00	1.00	16.5	12.9	9.82	8.59	0.251	6.09
	0.90	14.9	11.7	8.97	8.06	0.254	4.92
	0.80	13.4	10.6	8.00	7.10	0.213	4.77
	0.70	11.7	9.04	7.22	6.21	0.196	4.02
0.25	1.00	23.8	18.0	13.7	12.2	0.316	9.69
	0.90	21.5	16.6	12.5	11.0	0.286	8.80
	0.80	19.2	15.1	11.2	9.82	0.260	7.88
	0.70	17.2	13.2	9.94	8.95	0.225	7.15
0.10	1.00	33.5	25.3	18.3	16.0	0.283	17.3
	0.90	30.5	23.2	16.9	14.5	0.252	16.0
	0.80	27.8	21.0	15.3	13.4	0.246	14.2
	0.70	24.4	18.1	13.5	11.8	0.233	11.9
	0.60	19.9	14.9	11.0	9.88	0.175	10.1
	0.50	16.0	12.2	8.89	7.56	0.134	8.33
	0.45	15.6	11.6	8.00	7.00	0.062	9.63
	0.40	15.8	11.8	8.16	6.69	0.030	10.5
	0.35	16.2	11.6	7.90	6.88	0.011	11.1
	0.30	16.9	12.1	7.89	-	-0.068	13.5
0.05	1.00	42.5	32.6	22.9	20.1	0.315	23.1
	0.90	39.3	29.6	20.9	18.5	0.267	21.8
	0.80	36.0	27.1	19.3	16.6	0.228	20.4
	0.70	32.6	24.0	17.2	15.0	0.191	18.6

2-1 continued

C_s(M)	i	$\{\eta\}$ (l/basemol) S-1	S-2	S-3	S-4	K_0	B x 10^{23}
0.02	1.00	64.8	48.4	33.6	29.4	0.297	39.2
	0.90	60.4	45.4	31.3	27.4	0.277	36.6
	0.80	56.3	41.9	29.0	24.6	0.187	35.6
	0.70	51.0	37.1	26.3	22.3	0.164	32.2

2-2 PLGNa-0.1M NaCl-30vol.% dioxane

i	$\{\eta\}$ (l/basemol) S-1	S-2	S-3	S-4	K_0	B x 10^{23}
0.50	17.5	13.9	9.79	8.54	0.102	10.9
0.40	24.0	17.4	10.9	9.75	-0.036	17.8
0.30	30.0	20.7	12.7	10.8	-0.270	27.0

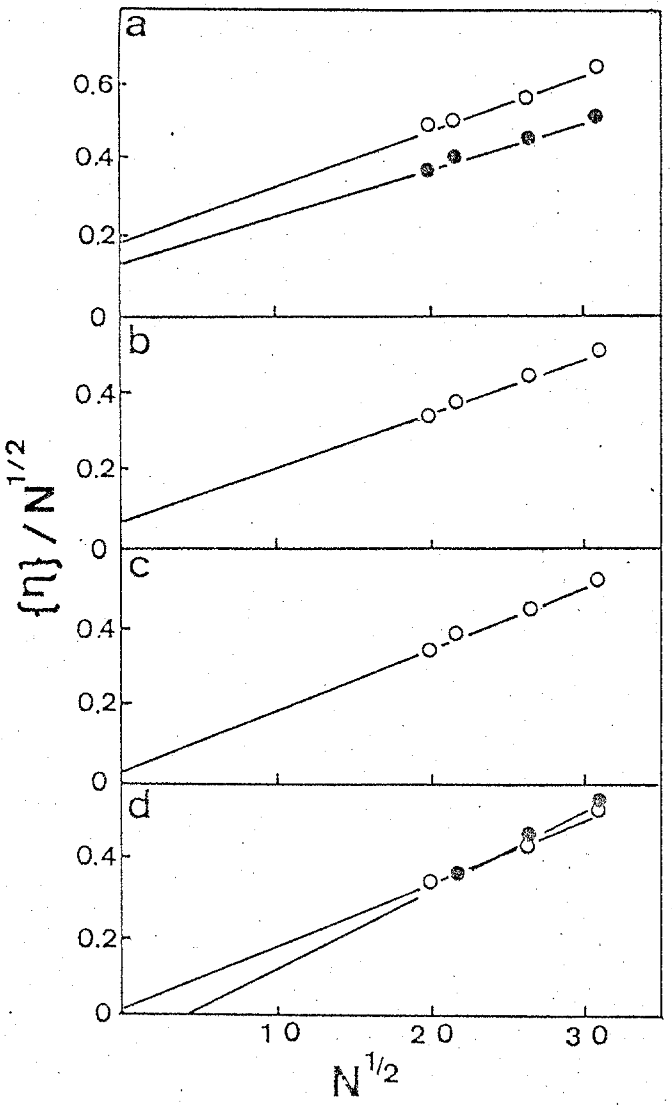

Fig.2 Stockmayer-Fixman plot for PLGNa in aq. 0.1M NaCl soln.: a. (○) i = 0.60 (●) i = 0.50, b. i = 0.45, c. i = 0.40 d. (○) i = 0.35, (●) i = 0.30

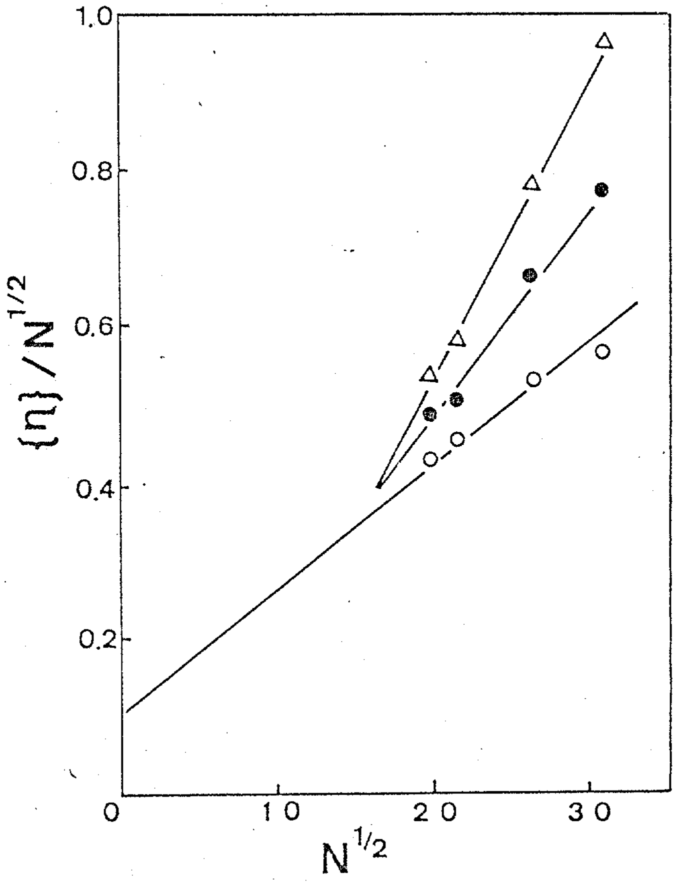

Fig.3 Stockmayer-Fixman plot for PLGNa in 0.1M NaCl-30vol.% dioxane aq. soln. (○) i = 0.50, (●) 0.40, (△) 0.30

Table 4 {η} and θ of PLGNa(S-2) in aq. 0.05M NaCl-20vol.% organic solvent mixtures

	Dioxane		t-BuOH		iso-PrOH		Ethylene glycol	
i	{η}	θ	{η}	θ	{η}	θ	{η}	θ
1.00	24.0		25.5		26.6		29.3	
0.90	22.1		24.2		24.8		27.6	
0.80	20.5		22.6		23.0		25.8	
0.75	19.7		21.1	0.023	21.7	0.044	23.9	
0.70	18.1	0.047	19.6	0.140	19.6	0.133	22.5	0.028
0.65	17.0	0.145	18.7	0.224	18.1	0.196	20.7	0.103
0.60	15.8	0.271	18.2	0.338	16.9	0.346	18.7	0.240
0.55	15.0	0.452	18.0	0.504	16.9	0.504	17.1	0.380
0.50	15.1	0.560	18.6	0.625	17.1	0.620	16.3	0.548
0.40	17.1	0.793	21.6	0.830	19.6	0.835	17.7	0.784
0.30	19.4	0.886	23.6	0.919	21.6	0.917	18.4	0.877
0.20	19.3	0.914	25.2	0.956	22.7	0.963	17.6	0.905

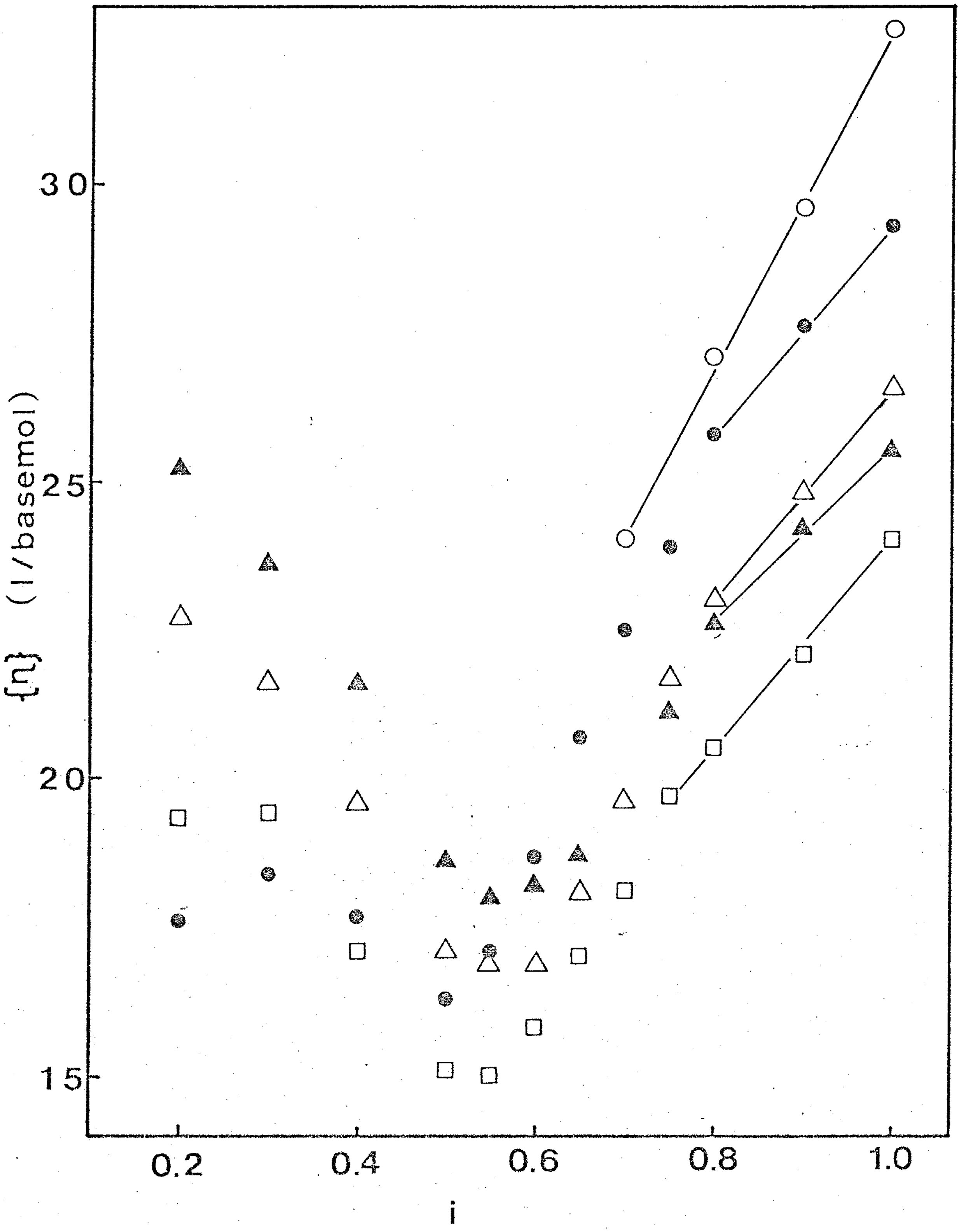

Fig.4 Dependence of {η} on i for PLGNa in aq. 0.05M NaCl-20vol.% organic solvent mixtures : (○) aqueous solution ; (●) ethylene glycol ; (△) isopropanol ; (▲) t-butanol ; (□) dioxane

Discussion

1. Unperturbed Dimension and Excluded Volume Effect of PLGNa

Equation (2) indicates that intrinsic viscosity of a linear polymer is contributed by two terms ; one is related to the short-range interaction in the polymer bonds and the other to the long-range interaction. We discuss here how the change in the charge density affects each of the two.

Nagasawa and coworkers[8)] have shown for the first time that K_0 values for Na poly(acrylate) as obtained by the extrapolation of the Stockmayer-Fixman plot decrease with decreasing i, indicating the unperturbed dimension depends on the charge density. K_0 values obtained here for PLGNa having i = 1.00 ~ 0.70 reveal that this is the case for this polymer too under the ionic strength investigated. In Fig.5, $\{\eta\}$ of PLGNa(S-1) having i = 1.00 ~ 0.70 were plotted against $C_s^{-1/2}$ to find $\{\eta\}$ at $C_s = \infty$ from the intercepts of the linear extrapolations. These values represent the viscosities of this polymer under the condition that the long-range electrostatic interaction is eliminated and hence the short-range and a formally nonelectrostatic long-range interactions are in action. They decrease with decreasing i, which also shows that the short-range interaction is under the influence of the charge density.

Due to the long extrapolation in Fig.1, K_0 values under different salt concentrations show a scatter in which no systematic trend is found.(Discussion in this respect will be made in Chapter V.) Averaging the K_0 values for C_s = 1.0 ~ 0.02 M gives 0.303,

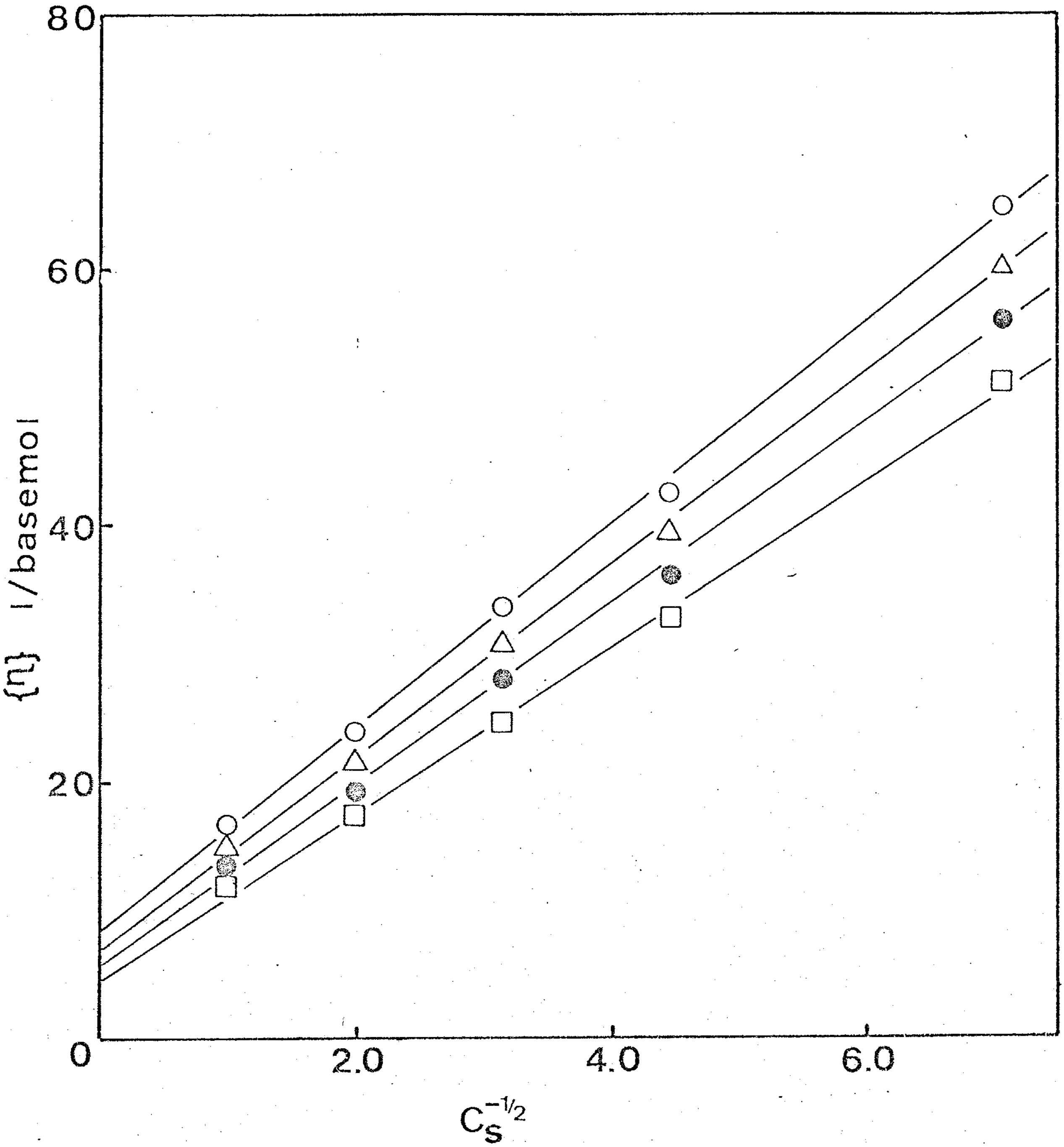

Fig.5 Dependence of {η} on $C_s^{-1/2}$ for PLGNa(S-1) in aq. NaCl solution : (○) i = 1.00 ; (△) 0.90 ; (●) 0.80 ; (□) 0.70

0.267, 0.227 and 0.202 for i = 1.00, 0.90, 0.80 and 0.70, respectively, within ca. 10 percent deviations. b_0 values calculated from these K_0 values through eq.(3) are given in Table 5, which show a decreasing trend from 10.2 Å to 8.9 Å with decreasing i from 1.00 to 0.70. Morcellet and Loucheux$^{9)}$ have obtained 8.15 Å for b_0 value of PLGNa having i = 1.0 in 0.133 M NaCl - 33 vol.% dioxane, and discussed that the increased counter-ion binding for PLGNa with the addition of dioxane could result in the reduced chain dimension. However their b_0 value smaller than ours should be attributed to the use of low molecular weight PLGNa rather than the enhanced degree of counter-ion binding in aq. organic solvent, because the application of eq.(2) to PLGNa of which molecular weight is lower than 6×10^4 gives smaller values as K_0 or b_0 than actual values.

The expansion factors, α_η^3, which were calculated by

$$\alpha_\eta^3 = \{\eta\}/\{\eta\}_0 \tag{6}$$

are shown in Table 6. Here $\{\eta\}_0$ is the intrinsic viscosity of unperturbed polymer chain and can be obtained through the relation $\{\eta\}_0 = K_0 N^{1/2}$. It is found in Table 6 that α_η^3 shows a decreasing trend with increasing i, which may be closely related with the positive dependence of K_0 on i. In other words, the effect of the increased charge density is taken into the short-range interaction rather than into the the long-range one, resulting in the smaller α_η. This point will be discussed in Chapter V once again.

α_η^3 are plotted against $C_s^{-1/2}$ in Fig.6 to show the dependence of the long-range electrostatic interaction on the ionic strength.

Table 5 Dependence of b_0 on i and comparison between $\{\eta\}_{Cs\to\infty}$ and $\{\eta\}_0$. (b_0 values were calculated by eq.(3) using mean values of K_0.)

i	$b_0 \times 10^8$ cm	$\{\eta\}_{Cs\to\infty}$ a)	$\{\eta\}_0$ a)
1.00	10.2	8.06	9.44
0.90	9.7	6.73	8.33
0.80	9.3	5.42	7.07
0.70	8.9	4.38	6.29

a) Values for S-1 sample

Table 6 α_η^3 of PLGNa(S-1) in aq. NaCl solution

	C_s (M)				
i	1.00	0.25	0.10	0.05	0.02
1.00	1.74	2.52	3.55	4.50	6.87
0.90	1.78	2.58	3.66	4.72	7.25
0.80	1.89	2.72	3.94	5.08	7.97
0.70	1.86	2.74	3.87	5.18	8.11

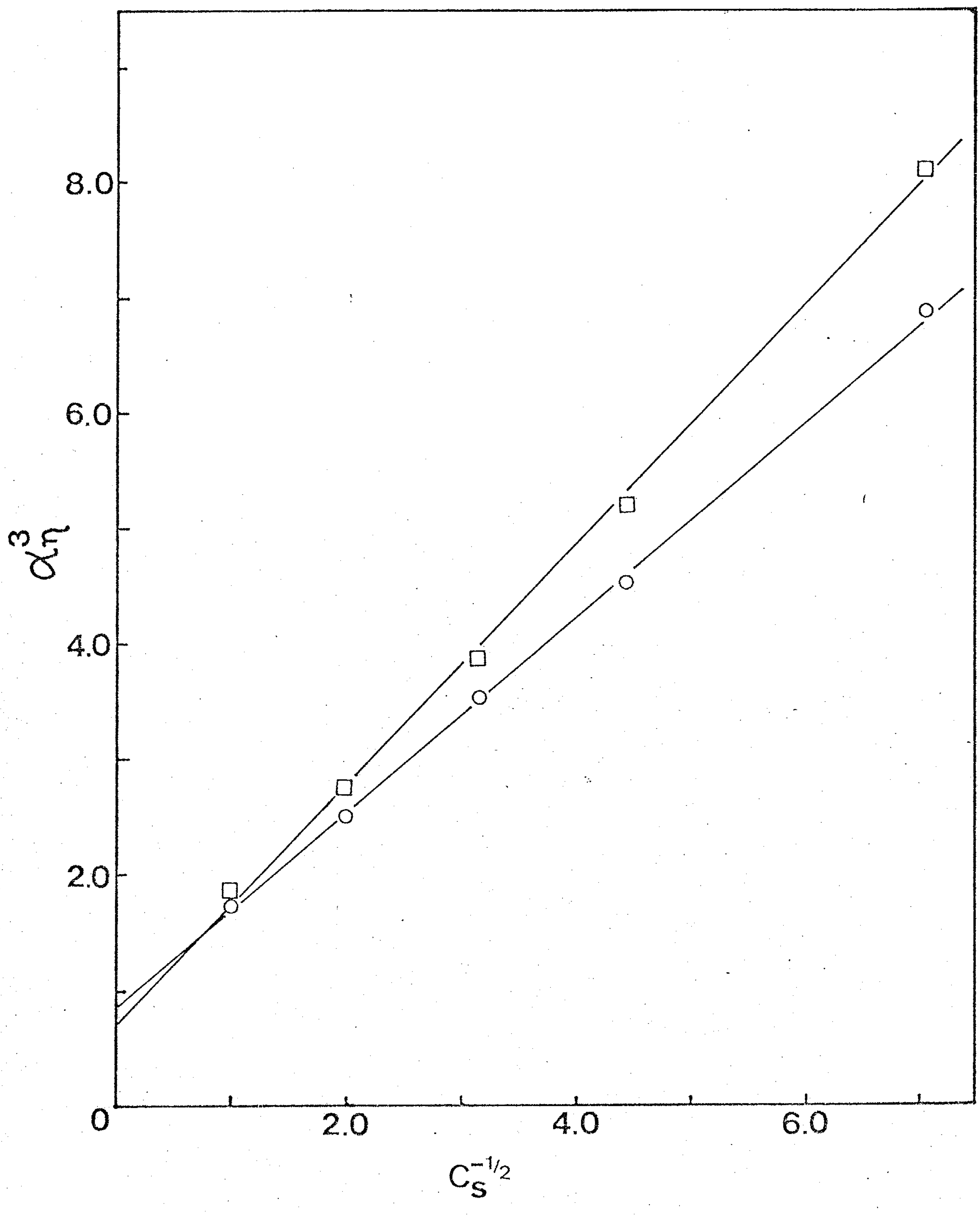

Fig.6 Dependence of α_η^3 on $C_s^{-1/2}$ for PLGNa(S-1) in aq. NaCl solution : (○) i = 1.00 ; (□) i = 0.70

The linear dependence explains that of $\{\eta\}$ on $C_s^{-1/2}$ found in Fig.5, since $\{\eta\}_\circ$ is insensitive to the salt concentration. Fig.6 indicates that α_η^3 extrapolated to $C_s = \infty$ should fall to the values smaller than unity, implying that the excluded volume effect of PLGNa segments is negative for the hypothetical elimination of the long-range electrostatic interaction. Comparison of $\{\eta\}_{Cs\to\infty}$ and $\{\eta\}_\circ$ in Table 5 gives an equivalent result, i.e., $\{\eta\}_{Cs\to\infty} < \{\eta\}_\circ$. Since B is related with the excluded volume of the polymer segment, it can be used as a measure of the excluded volume effect. The plots of B against $C_s^{-1/2}$ shown in Fig.7 should be linearly extrapolated to negative values at $C_s^{-1/2} = 0$ disregarding the deviated points at $C_s = 1.0$ M. A negative B at $C_s = \infty$ also means that the nonelectrostatic long-range interaction is attractive one, though the origin is not clear. (These results will be also reexamined in Chapter V.)

With the decrease in i, PLGNa forms partial helix. The chain becomes more extended, giving rise to a deviation from a random coil toward a rigid rod. Table 2 shows that PLGNa having i = 0.30 in 0.1 M NaCl gives a negative $K_\circ$ value if eq.(2) is applied to the viscosity data. Addition of 30 vol.% dioxane to the solvent, which induces an increase in the helix content, exaggerates the negative $K_\circ$ values as shown in Table 2. Table 7 shows Mark-Sakurada-Houwink parameter $\bar{a}$ for the systems investigated. This value begins to increase when i is decreased below 0.50 and becomes larger than unity. Parameter a takes a value between 0.5 and 1.0 according to the expansive deviation from the Gaussian distribution of the polymer segments, and 2.0 when the polymer is a rigid rod.

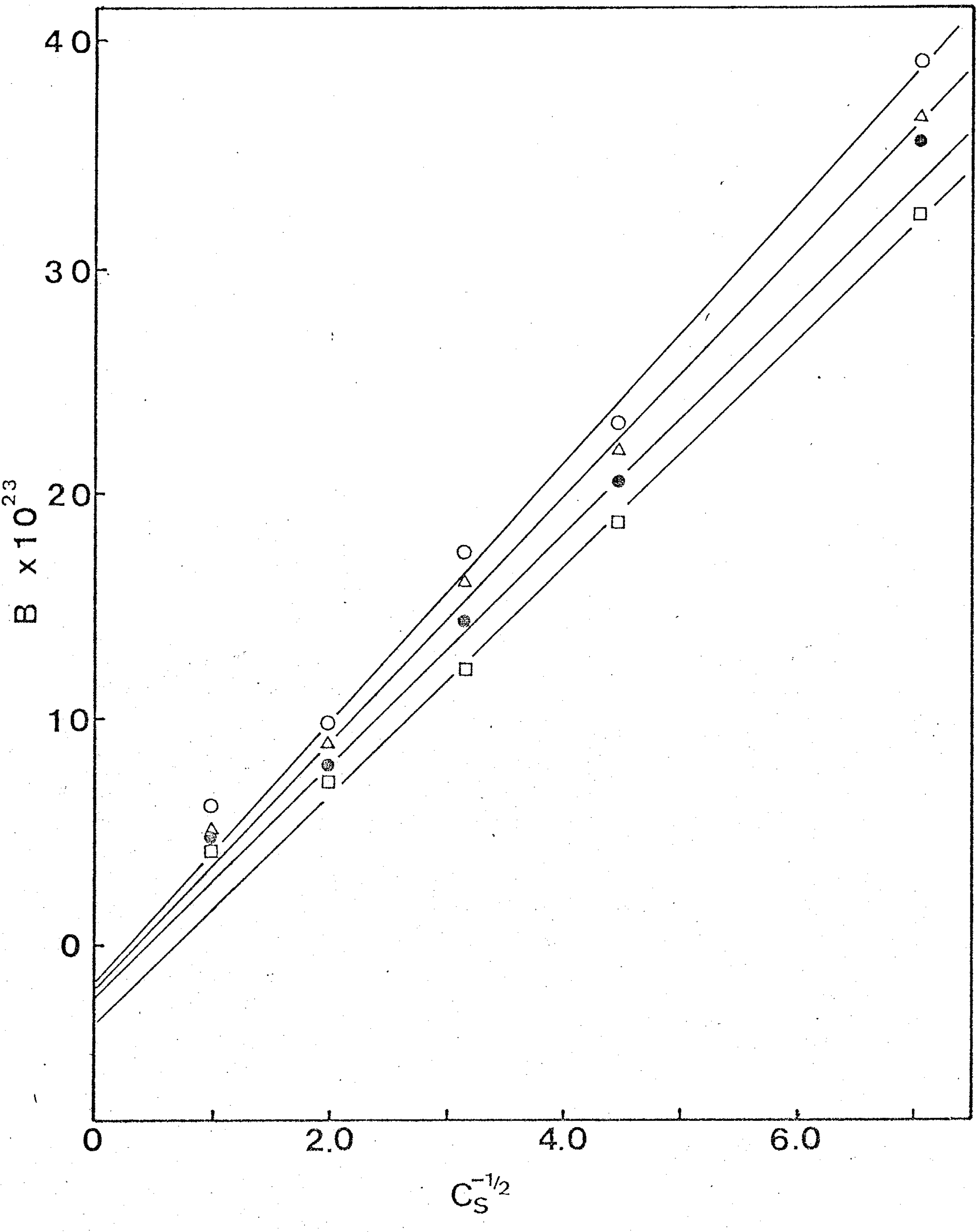

Fig.7 Dependence of B on $C_s^{-1/2}$ for PLGNa in aq. NaCl soln.
(○) i = 1.00 ; (△) 0.90 ; (○) 0.80 ; (□) 0.70

Table 7 Mark-Sakurada-Houwink parameter a of PLGNa

			C_s (M)			
i	1.00	0.25	0.10	0.05	0.02	0.1M NaCl-30vol.% dioxane
1.00	0.739	0.760	0.843	0.866	0.914	
0.90	0.700	0.764	0.851	0.874	0.915	
0.80	0.722	0.768	0.839	0.883	0.940	
0.70	0.703	0.750	0.825	0.889	0.937	
0.60			0.805			
0.50			0.850			0.887
0.45			0.924			
0.40			0.971			1.04
0.35			0.983			
0.30			1.08			1.19

Therefore, the increasing trend of a with decreasing i can be interpreted as being caused by the decreasing flexibility of the polymer chain due to the increase of the helix content. In fact, negative K_0 has a correspondence to a larger than unity, as found in Tables 2 and 7. The polymer chain having such a low flexibility cannot be assumed as a random coil, that Stockmayer-Fixman plot is inapplicable to poly(amino acid) in, even partially, helical conformation.

2. Estimation of σ from Viscometric Data of PLGNa

The helix-coil transition of polypeptides is characterized by two equilibrium constants s and σ ; s applies to the growth of the helical part in the polymer chain and σ to the initiation and is called " cooperativity parameter ". The smaller σ, the sharper becomes the transition and eventually " all or none " type.

Methods of determining σ have been proposed by many researchers[10-12]. Ptitsyn et al.[13] developed a method using viscometric data and applied it to the helix-coil transition of PLGNa[14,15] and poly(L-lysine)(PLL)[16]. They introduced eq.(7) to express $\langle R^2\rangle$, the mean square end-to-end distance of a helix-containing polypeptide chain, as a function of σ and θ, the helix content.

$$\langle R^2\rangle = (1-\theta)\langle R^2\rangle_c + 2Nb_h^2\theta^{3/2}/\sqrt{\sigma(1-\theta)} \qquad (7)$$

where $\langle R^2\rangle_c$ is the mean square end-to-end distance of the random coil polymer, N the degree of polymerization and b_h the helical segment length per monomer unit. Eq.(8) obtained by the rearrangement of eq.(7) was used to evaluate σ from the slope of the plot of $f(\theta)\alpha_c^2/(1-\theta)$ against $(\theta/1-\theta)^{3/2}$. Here α_c is the expansion factor for the random coil polymer and b_0 is the unperturbed segment length.

$$f(\theta) \equiv \langle R^2\rangle/\langle R^2\rangle_c = 1 - \theta + 2b_h^2\theta^{3/2}/\alpha_c^2 b_0^2\sqrt{\sigma(1-\theta)} \quad (8)$$

$\langle R^2\rangle/\langle R^2\rangle_c$ and α_c^2 were obtained by equating these to $(\{\eta\}/\{\eta\}_c)^{2/3}$ and $(\{\eta\}_c/\{\eta\}_0)^{2/3}$, respectively. While $\{\eta\}_{Cs\to\infty}$, the intrinsic viscosity extrapolated to infinite concentration of added electrolyte, was used for $\{\eta\}_0$ under theta conditions, this is not appropriate here because $\{\eta\}_0$ is greater than $\{\eta\}_{Cs\to\infty}$ for PLGNa in aq. NaCl solution as described in the preceding section.

There are two points to be modified in Ptitsyn's method. σ values for PLGNa in aq. and aq. organic solvents containing NaCl are estimated as the following.

The first problem in Ptitsyn's method is the use of $\{\eta\}_c$ in the alkaline region to calculate $\langle R^2\rangle_c$. This is inappropriate since the intrinsic viscosity of PLGNa changes with the charge density of the polymer as shown in Figs.4 and 8. The dependence of $\{\eta\}$ on the degree of neutralization i should be taken into account because the decrease in i gives rise to the coil-helix transition. $\{\eta\}$ of PLGNa decreases linearly with i in the random coil region indicated by solid lines in the figures, and the deviation from the linear plots should be attributed to the conformational change of the polymer. Hypothetical $\{\eta\}_c$ must be estimated, therefore, in the transition region. Here we obtain $\{\eta\}_c$ by assuming a linear dependence in the entire range, even in the transition region. This assumption may be, at least to a certain extent, supported by the fact that the linear part extends to

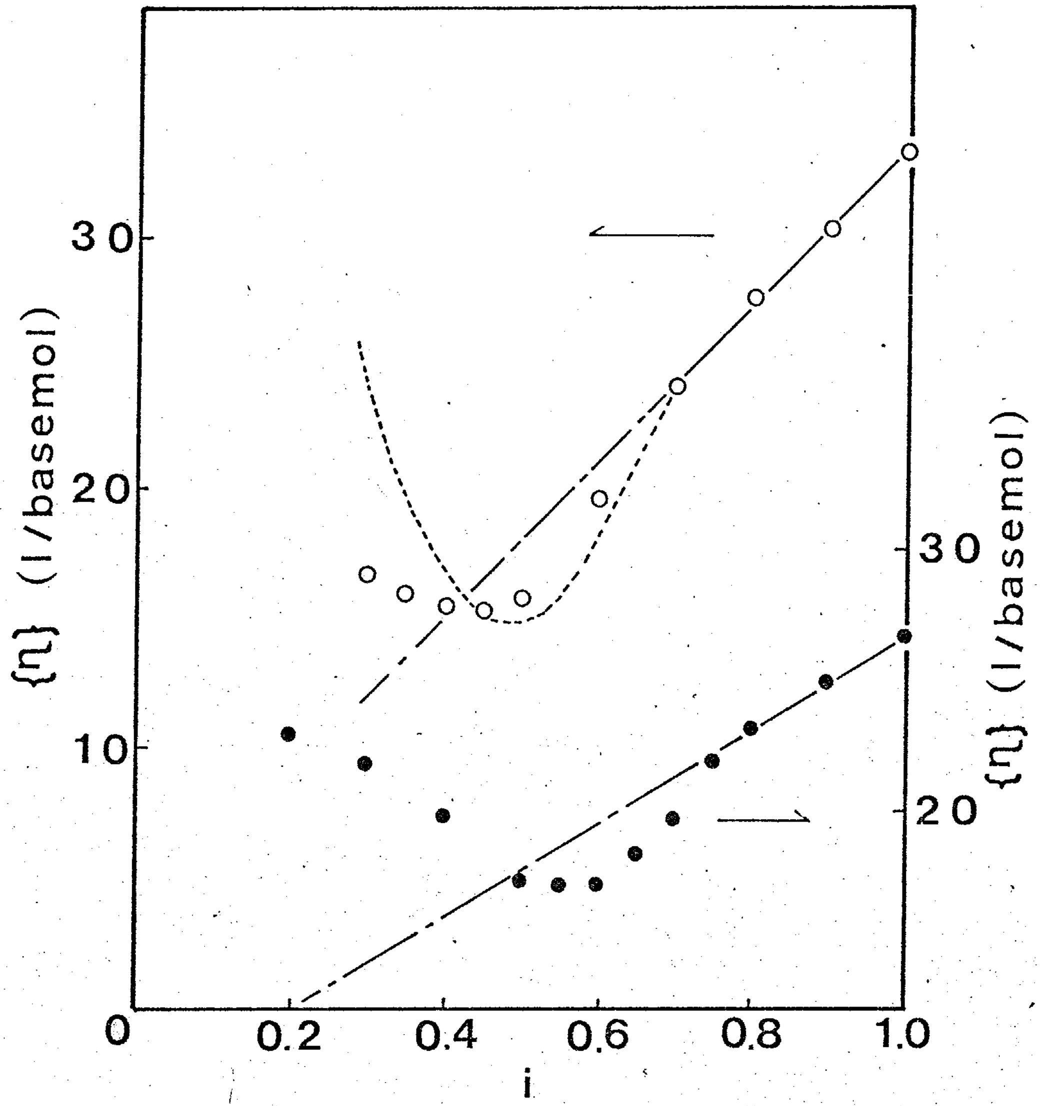

Fig.8 Plot of {η} vs. i for PLGNa solution : (○) PLGNa(S-1) - 0.10M NaCl ; (●) PLGNa(S-2) - 0.05M - 20vol.% isopropanol

—— - —— - —— : hypothetical $\{\eta\}_c$

---------------- : hypothetical {η} calculated with $\sigma = 1 \times 10^{-3}$

$i = 0.6$ if the transition region for PLGNa in aq. 0.1 M NaCl solution is lowered to below $i = 0.6$ by raising the temperature to 50°C. (Fig.9)

The second problem concerns the use of eq.(8) to obtain σ. Since α_C and b_0 change with i, σ cannot be estimated by the plot of $f(\theta)\alpha_C^2/(1-\theta)$ against $(\theta/1-\theta)^{3/2}$, but evaluated directly from eq.(7) using the relation $[\eta] = \Phi_0 \langle R^2\rangle^{3/2}/N$. The values of σ thus obtained for PLGNa in 0.1 M NaCl and 0.05 M NaCl-20 vol.% isopropanol are shown in Table 8. $\sigma = 2.5 \times 10^{-3}$ for PLGNa$(M \doteqdot 9 \times 10^4)$ in 0.2 M NaCl at 22°C obtained by Bychkova et al.[15] is favorably compared with our $\sigma = 2.5 \times 10^{-4} \sim 1.4 \times 10^{-3}$ considering the higher molecular weight of our sample. σ obtained as $2.0 \times 10^{-4} \sim 1.0 \times 10^{-3}$ for PLGNa in 0.05 M NaCl-20 vol.% isopropanol is also interpreted in the same way.

Table 8 shows that in both solvent media σ increases with decreasing i, even in the region $0.1<\theta<0.6$ where eq.(7) should be valid. Such a dependence of σ on i can be interpreted as being consistent with the results obtained in the above section. The unperturbed segment length b_0 of PLGNa decreases with decreasing i, which means that the short-range interaction is under the influence of the charge density. Therefore, it is inferred that the decrease of i would favorably initiate the helix formation through the decrease of the short-range interaction. In fact Zimm-Rice and Warashina et al. have statistically treated the charge-induced helix-coil transition of PLGNa in aq. NaCl solution by taking into consideration the contribution of electrostatic interaction to the cooperativity parameter. In chapter IV, the helix-coil tran-

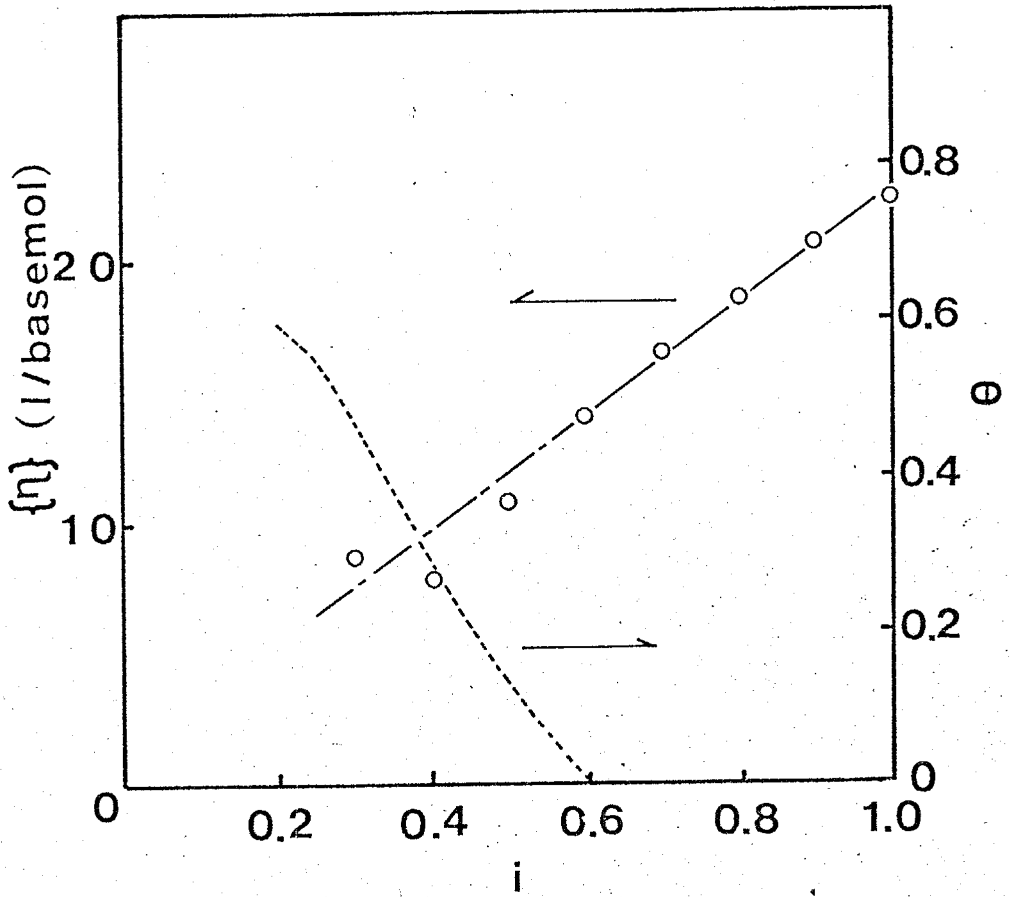

Fig.9 Plot of {η} and θ vs. i for PLGNa(S-2) in aq. 0.10M NaCl solution at 50°C

Table 8 The cooperativity parameter σ calculated by eq.(7)

	PLGNa(S-1) in 0.1M NaCl		PLGNa(S-2) in 0.05M NaCl-20vol.% isopropanol	
i	θ	$\sigma \times 10^3$	θ	$\sigma \times 10^3$
0.75			0.04	0.05
0.70			0.13	0.22
0.65			0.20	0.34
0.60	0.18	0.28	0.35	0.57
0.55			0.50	0.86
0.50	0.35	0.78	0.62	1.3
0.45	0.47	1.0		
0.40	0.60	1.4	0.84	3.6
0.35	0.66	1.7		
0.30	0.76	2.4	0.92	9.8

Table 9 σ calculated by eq.(7) for PLGNa in various solvents

	$\sigma \times 10^3$			
solvent	$\theta = 0.1$	$\theta = 0.6$	mean	dielectric constant
0.1M NaCl[a)]	0.20	1.4	0.53	78.5
0.05M NaCl-20vol.% E.G.[b)]	0.48	1.4	0.82	72.2
0.05M NaCl-20vol.% iso-PrOH[b)]	0.20	1.1	0.47	67.2
0.05M NaCl-20vol.% t-BuOH[b)]	0.14	1.0	0.37	65.2
0.05M NaCl-20vol.% Dioxane[b)]	0.20	1.3	0.51	60.8

a)PLGNa S-1, b)PLGNa S-2

sition of PLGNa in aq. NaCl solution will be analysed with a model based on the dependence of σ on the charge density.

Table 9 shows σ values estimated by eq.(7) for PLGNa in various solvents. It is found from the table that σ has no major dependence on the dielectric constant of the solvent. Since the random coil configuration is greatly stabilized by the dipole-dipole interaction of the adjacent peptide groups$^{19)}$, it is expected that the higher the dielectric constant of the solvent is, the larger σ becomes. But this is not the case. The other factors, for example, preferential solvation to the polymer of the organic component, must be taken into account to explain the system specific σ.

3. Comparison of the Viscosity Behavior of PLGNa in Aqueous and Aqueous Organic Solvents

As shown in Fig.8, hypothetical $\{\eta\}$ values for PLGNa in 0.1 M NaCl, calculated by eq.(7) with constant σ, give a sharper rise than actual one below $i = 0.45 \sim 0.50$, which is similar to those in aq. organic solvents. However, the increase of σ with decreasing i cannot be explained by the slight increase of $\{\eta\}$ of PLGNa in aq. NaCl solution below $i = 0.45$, because σ in aq. organic solvents is similarly dependent on i (Table 8). Explanations for such difference in the $\{\eta\}$ dependence on i between the two systems are based on the larger σ and the incompleteness of the transition in the aqueous solution. The main cause, however, may be the larger values of $\{\eta\}_c$ and the steeper slope of the $\{\eta\}_c$ dependence on i in aq. NaCl solution, since the dimension of PLGNa in the helix-coil transition region is given by the sum of the contributions of random coil and helical parts as shown in eq.(7). The larger the decrease of $\{\eta\}_c$ with decreasing i results in seemingly smaller contribution of the helical part. In fact the i dependence of $\{\eta\}$ of PLGNa shown in Figs.4 and 8 may be reasonably explained by the above considerations. It is, however, very difficult to ascertain the causes of the decreasing $\{\eta\}$ in the coil region with decreasing dielectric constant of the solvent. Ptitsyn et al.$^{14)}$ and Morcellet et al.$^{9)}$ ascribed this decreased $\{\eta\}_c$ in aq. organic solvent to the enhanced degree of counter-ion binding. According to Manning theory, effective charge density of PLGNa decreases with decreasing the dielectric constant D. However the dependence of α_η on D is differently predicted by theories ; Fixman$^{20)}$ expressed $\alpha_{\eta el}^3$, expansion factor due to electrostatic interaction, as being proportional to $\alpha/b_0\sqrt{C_s D}$ and many other theoreticians$^{21)}$ predicted $\alpha_{\eta el}$ could be a function of $\alpha^2/C_s b_0^{3/2}$. Here α is degree of dissociation of charged groups. As the experimental fact is that α_η^3 depends on $C_s^{-1/2}$, if we assume $D^{-1/2}$ dependence of $\alpha_{\eta el}^3$, a decreasing trend of $\{\eta\}_c$ with decreasing D can be obtained. The detail discussion will be given in Chapter V, because it is a prerequisite to discuss Manning theory as applied to these systems.

In summary, viscometry of PLGNa in aq. and aq. organic solvents containing NaCl has been performed. It is shown with Stockmayer-Fixman plot that the short-range interaction is influenced by charge density but not the long-range one in the random coil region, and with a modified Ptitsyn's method that σ increases with decreasing i, which is consistent with the i dependence of K_0 or b_0.

REFERENCES

1) ref. 14 ~ 19, 23 ~ 25 in Chapter I

2) W. H. Stockmayer and M. Fixman, J. Polym. Sci. Part C, 1, 137 (1963)

3) Y. Koiwa and Y. Fujimoto, the 22th Kobunshi Toronkai, pII, 31 (1973)

4) K. Hiramatsu, Seni Gakkai Nenji Taikai, 189 (1971)

5) H. Kanehiro, J. Komiyama and T. Iijima, Nihon Kagaku Kaishi, in press

6) R. J. Hawkins and A. Holtzer, Macromolecules, 5, 294 (1972)

7) G. Holzwarth and P. Doty, J. Amer. Chem. Soc., 87, 218 (1965)

8) I. Noda, T. Tsuge and M. Nagasawa, J. Phys. Chem., 74, 710 (1970)

9) M. Morcellet and C. Loucheux, Biopolymers, 15, 1857 (1976)

10) B. H. Zimm, P. Doty and K. Iso, Proc. Natl. Acad. Sci. U. S., 45, 1601 (1959)

11) J. Applequist, J. Chem. Phys., 38, 934 (1963)

12) Y. Hayashi, A. Teramoto, K. Kawahara and H. Fujita, Biopolymers, 8, 403 (1969)

13) O. B. Ptitsyn and A. M. Skvortsov, Biofizika, 10, 909 (1965)

14) O. B. Ptitsyn, T. V. Barskaya, I. A. Bolotina and N. G. Illarionova, Biofizika, 12, 386 (1967)

15) V. E. Bychkova, O. B. Ptitsyn and T. V. Barskaya, Biopolymers, 10, 2161 (1971)

16) T. V. Barskaya and O. B. Ptitsyn, Biopolymers, 10, 2181 (1971)

17) B. H. Zimm and S. A. Rice, J. Mol. Phys., 3, 391 (1960)

REFERENCES (continued)

18) A. Warashina and A. Ikegami, Biopolymers, 11, 529 (1972)

19) D. A. Brant and P. J. Flory, J. Amer. Chem. Soc., 87, 2791 (1965)

20) M. Fixman, J. Chem. Phys., 41, 3772 (1964)

21) ref. 25, 27 and 45 in Chapter I

CHAPTER III

Hydration Behavior of PLGNa in Aqueous NaCl Solution

ABSTRACT

Density and ultrasonic velocity measurements for PLGNa in aq. NaCl solution have been performed with varying the degree of neutralization, i, and the salt concentration, C_s. Apparent molar compressibility of the polymer, ϕ_p, is calculated from these data. The i dependence of ϕ_p shows that apparent hydration number of charged group of the polymer is about 7.

The similar experiments have been carried out for PAANa. The results show that counter-ion condensation for the system does not give any significant change in the hydration around the charged groups.

The number of water molecules released with the helix formation of PLGNa is estimated by assuming that the compressibility change due to the coil-helix transition is a linear function of helix content, which has been justified for the transition of PLLHBr induced by addition of $NaClO_4$ based upon the compressibility data.

Introduction

Hydration of biological macromolecules is one of the most important factors determining their conformational states such as denaturation of protein and helix-coil transitions of DNA and polypeptides. Many researchers$^{1-4)}$ have interpreted the thermodynamic data on the helix-coil transition of DNA by taking account of a change in the hydration accompanying the conformational transition. Synthetic polypeptides such as poly(glutamic acid) or poly-lysine, however, are little investigated from this point of view.

Hydration of polyelectrolytes has been extensively studied using various methods. Gekko and Noguchi$^{5)}$ studied the hydration of dextran derivatives using ultrasonic velocity method. Conway et al.$^{6)}$ discussed the hydration of polyethyleneimine from the partial molar volume, $\overline{V}°$, and the apparent molar compressibility of the polyelectrolyte, ϕ_k°, with the assumed simple additivity of $\overline{V}°$ and ϕ_k°.

In this chapter, the hydration of PLGNa in aq. NaCl solution was estimated for a range of the degree of neutralization, i. It is well known that the decrease of pH or i brings about the conformational transition from coil to helix for PLGNa. But under ordinary conditions in respect to temperature and salt concentration in the aqueous solution, PLGNa assumes random coil conformation in higher region of i, 0.7 ~ 1.0, where the polymer is a simple polyelectrolyte. Therefore, estimation of the hydration around the charged group in this region would give a base to elucidate the hydration change in the transition region.

The density and the ultrasonic velocity of PLGNa in aq. NaCl solution were measured to obtain the adiabatic compressibility. A method to estimate hydration numbers of low molecular-weight compounds in aqueous solution was proposed by Passynsky[7)]. Application of this method to polyelectrolyte was done by Conway et al.[6)]. When one aims to obtain hydration number from compressibility data, apparent molar compressibility, ϕ, is more convenient than adiabatic compressibility, β, directly calculated from density, d, and sound velocity, u, through the relation, $\beta = 1/u^2d$. Apparent molar compressibility of a polymer is obtained as[6)]

$$\phi_p = 10^3(\beta d_w - \beta_w d)/C_p d_w + \beta_w Mo/d_w \qquad (1)$$

Suffix p and w represent polymer and bulk water, respectively. Mo is molecular weight of the monomer unit and C_p is the polymer concentration in basemol/l. ϕ_p for a polyelectrolyte can be divided into some contributions as follows ;

$$\phi_p = \phi_i + \phi_{hy} = \phi_i + \phi_{hy'} + \phi_{el} \qquad (2)$$

where ϕ_i is the intrinsic molar compressibility of the polymer residue which contains the contribution from void volume, and ϕ_{hy} represents the contribution from the hydrated water onto the polymer, which is given as a sum of the contribution from the electrostrict water around the charged groups, ϕ_{el}, and the others, $\phi_{hy'}$. A residue of PLG contains polar groups(CO, NH, COOH) and nonpolar groups(CH_2CH_2, CH). Water molecules hydrated around the two groups have different molar compressibilities, ϕ_{wpo} and ϕ_{wnp}, respectively. Therefore, $\phi_{hy'}$ in eq.(2) is given as

$$\phi_{hy'} = n_{po}(\phi_{wpo} - \phi_w) + n_{np}(\phi_{wnp} - \phi_w) \qquad (3)$$

where n and ϕ_w mean hydration number of each group and molar compressibility of bulk water, respectively. Compressibility of electrostrict water for simple- and poly-electrolytes has been supposed to be negligible compared with that of bulk water. Then ϕ_{el} in eq.(2) is related with the charge fraction of the polymer, α(which is equal to i except when i is very low) as

$$\phi_{el} = - n_{el}\phi_w\alpha \qquad (4)$$

If ϕ_i and $\phi_{hy'}$ are not affected by changing α, the number of electrostrictly hydrated water molecules n_{el} can be estimated from

$$-\phi_p/\phi_w = \text{constant} + n_{el}\alpha \qquad (5)$$

The slope of the linear plot of $-\phi_p/\phi_w$ against α gives n_{el}.

The above formalism applies to PLGNa in random coil conformation. When $\alpha < 0.7$, contributions of coil-helix transition must be taken into account. Thus the apparent molar compressibility of helix-containing PLGNa, $\phi_{p\theta}$, is expressed as

$$\phi_{p\theta} = (1-\theta)\phi_{ic} + \theta\phi_{ih} + \phi_{hy''}(\theta) - n_{el}\phi_w\alpha \qquad (6)$$

Here θ is helix content and suffix c and h mean random coil and helical conformations, respectively. $\phi_{hy''}(\theta)$ corresponds to $\phi_{hy'}$ of the polymer containing partial helix. It is also assumed here that n_{el} does not depend on the conformation.

Experimental

Materials

PLGNa used in this study was kindly supplied by Kyowa Hakko Co.. Poly(acrylic acid)(PAA) and poly(L-lysine hydrobromide) (PLLHBr) were used for comparing with and interpreting results obtained for PLGNa. The former was supplied from Nohon Junyaku Co. and the latter was purchased from Protein Research Foundation. Molecular weights of these polymers were determined by viscometry ; PLGNa = 8.4×10^4, PAANa = 9.9×10^4, PLLHBr = 2.9×10^5. All polymer samples were ultrafiltrated through Ultra Filter UP 20 (Toyo Roshi) to eliminate low molecular-weight substances, and then collected by freeze-drying. Stock solutions were made by dissolving these polymer in distilled water and the concentrations were determined by weight. α of PLGNa and PAANa were changed by adding appropriate aliquats of 0.1N HCl.

Apparatus and Methods

The densities were measured with a Precision Density Meter DMA-02 C(Anton Paar, Graz, Austria) which was calibrated by mercury (Merck Suprapur grade) and distilled water. The accuracy was $\pm 2 \times 10^{-6}$ g/cm^3. The ultrasonic velocities were measured at 5MHz with a sing around ultrasonic velocity meter(Chōonpa Kogyo) which was calibrated by distilled water and the accuracy was ± 2 cm/sec. Helix content of PLGNa and PLLHBr was estimated by CD measurements. The detail is described in Chapter II. Counter-ion activity of PAANa was measured with a Micro Processor Ionanalyser 901(Orion

Research) with a sodium ion specific electrode Model 94-11A.

The density and sound velocity measurements were done at 25 ± 0.005°C and the other measurements at 25 ± 0.05°C.

Results and Discussion

The values of d, u and β of aq. PLGNa-NaCl solutions are listed in Table 1. Apparent molar compressibility ϕ_p of PLGNa was calculated by eq.(1) using these values. Fig.1 shows that dependence of ϕ_p on C_p can be neglected within the experimental error. Therefore, ϕ_p obtained in the region of C_p = 6~7 x 10^{-2}basemol/l is used in the following analysis.

Hydration numbers of simple electrolytes have been estimated from the compressibility data assuming that the compressibility of the electrolytes is negligible. An assumption like that, however, should not be accepted in this case, that is, ϕ_i of polyelectrolytes take some positive values$^{8)}$. Therefore it must be made certain whether ϕ_i is independent of α or not, to accept the slope of the plot of eq.(5) as n_{el}. Plots of $-\phi_p/\phi_w$ vs. C_s(concentration of added salt in mol/l) for PLGNa in aq. NaCl solutions are shown in Fig.2. The linear relation between $-\phi_p/\phi_w$ and C_s, even at C_s = 0 in Fig.2 implies that change in the polymer dimension has no explicit influence on the ϕ_p value, or in other words, ϕ_i does not depend on the polymer dimension, because at C_s = 0 the polymer chain is extremely extended as can be seen from viscometry. Therefore it is inferred that the influence of the dimension change due to the change of α is not incorporated in eq.(2).

Fig.3 shows the plot of eq.(5) for PLGNa in aq. NaCl solutions. In the α region where PLGNa takes random coil conformation(α = 1.00 ~0.70), $-\phi_p/\phi_w$ linearly depends on α, as expected. Values of the slopes, viz., apparent hydration numbers around the charged groups of PLGNa(COO^-Na^+), are given in Table 2.

Table 1 d, u and β of aq. PLGNa-NaCl solution

i	d g/cm^3	u m/sec	C_p x 10^2basemol/l	β x 10^{11}cm^2/dyne
C_s = 0.1 M				
1.00	1.006628	1510.73	7.0742	4.3527
0.90	1.006050	1509.91	6.6153	4.3599
0.80	1.005522	1509.15	6.1994	4.3666
0.70	1.005863	1509.33	6.9988	4.3641
0.60	1.005335	1508.56	6.5368	4.3708
solvent	1.001149	1504.37		4.4136
0.55	1.005088	1508.06	6.3322	4.3748
0.50	1.004848	1507.66	6.1323	4.3782
0.45	1.004627	1507.30	5.9477	4.3813
solvent	1.001171	1504.42		4.4132
C_s = 0.2 M				
1.00	1.010554	1516.68	6.9428	4.3018
0.90	1.010136	1516.00	6.7047	4.3075
0.80	1.009761	1515.41	6.4850	4.3125
0.70	1.009411	1514.81	6.2808	4.3173
solvent	1.005217	1510.46		4.3604
0.60	1.009426	1514.81	6.6717	4.3173
0.55	1.009226	1514.36	6.5622	4.3207
0.50	1.009034	1513.95	6.4434	4.3239
0.45	1.008858	1513.68	6.3385	4.3262
solvent	1.005208	1510.59		4.3596

Table 1 continued

i	d g/cm^3	u m/sec	$C_p \times 10^2$ basemol/l	$\beta \times 10^{11}$ cm^2/dyne
C_s = 0.4 M				
1.00	1.018658	1529.10	7.0808	4.1986
0.90	1.018310	1528.55	6.9473	4.2030
0.80	1.017982	1528.035	6.8195	4.2072
0.70	1.017689	1527.48	6.7182	4.2115
solvent	1.013277	1522.96		4.2550
0.60	1.017415	1526.93	6.6022	4.2157
0.55	1.017254	1526.51	6.5486	4.2186
0.50	1.017098	1526.19	6.4812	4.2211
0.45	1.016953	1525.86	6.4342	4.2235
solvent	1.013251	1522.91		4.2553
C_s = 0.5 M				
1.00	1.022307	1534.73	6.7033	4.1529
0.90	1.022015	1534.22	6.6177	4.1569
0.80	1.021724	1533.75	6.5343	4.1606
0.70	1.021465	1533.19	6.4451	4.1647
solvent	1.017267	1528.82		4.2058
0.60	1.021206	1532.49	6.3650	4.1696
0.55	1.021061	1532.12	6.3254	4.1722
0.50	1.020916	1531.84	6.2780	4.1743
0.45	1.020787	1531.61	6.2292	4.1761
solvent	1.017280	1528.68		4.2065

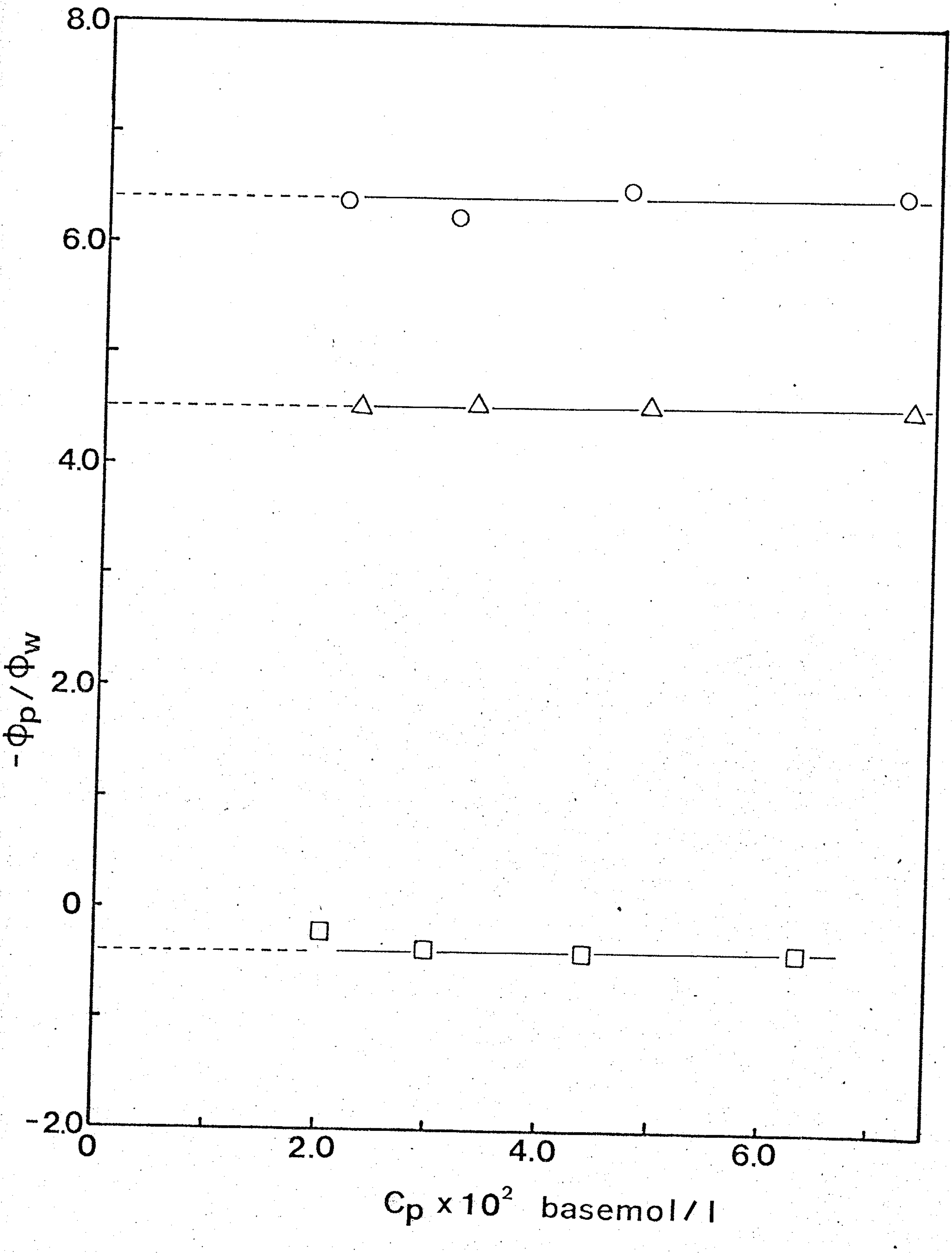

Fig.1 Dependence of ϕ_p on C_p : (○) PLGNa-0.07M NaCl, α = 1.0 (△) PLGNa-0.07M NaCl, α = 0.7 ; (□) PLLHBr-0.9254M $NaClO_4$, α = 1.0

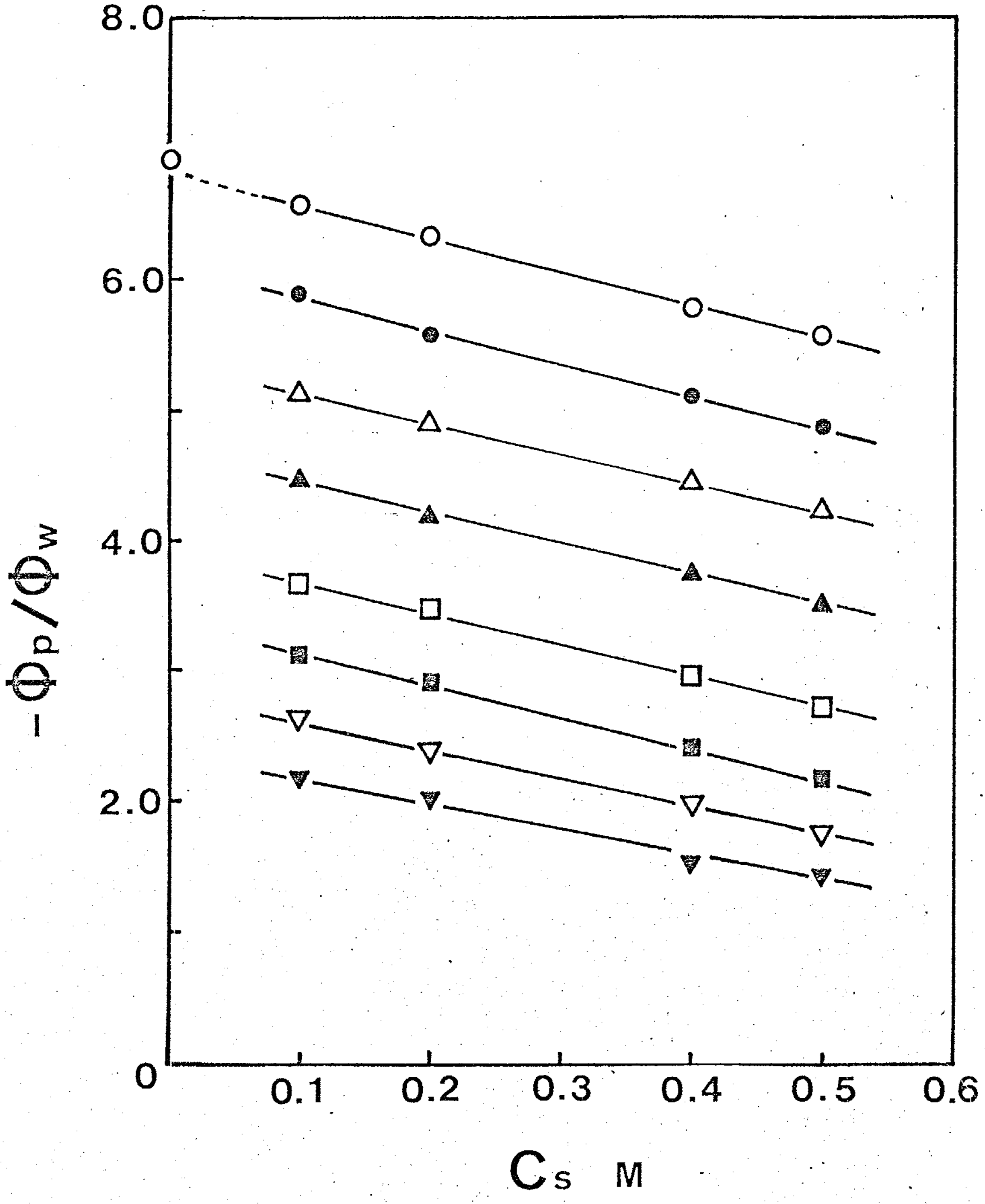

Fig.2 Plots of $-\phi_p/\phi_w$ against C_s for PLGNa-NaCl α = 1.00, 0.90, 0.80, 0.70, 0.60, 0.55, 0.50, 0.45 from top to bottom

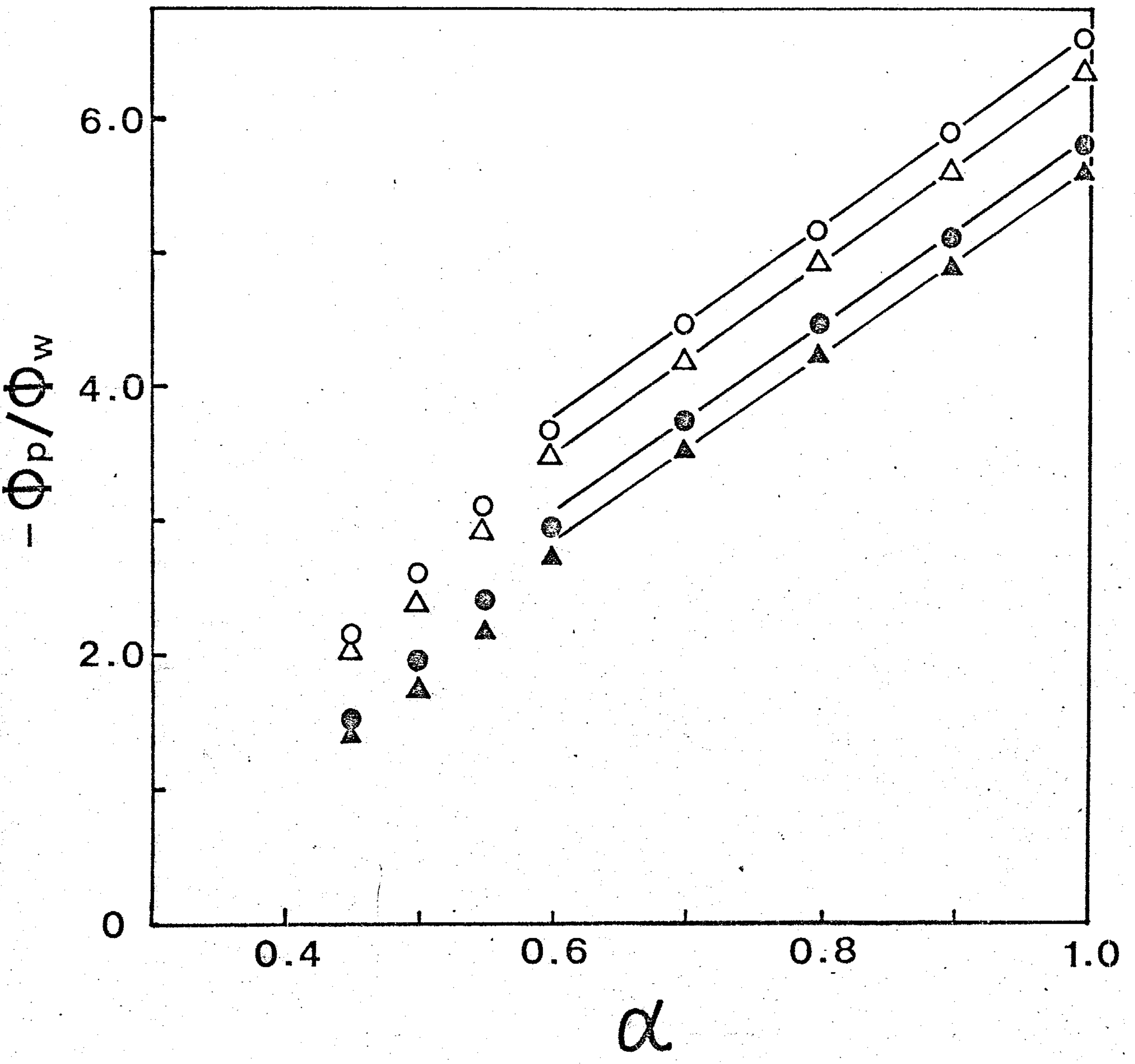

Fig. 3 Plots of $-\phi_p/\phi_w$ against α for PLGNa-NaCl

(○) C_s = 0.1M ; (△) 0.2M ; (●) 0.4M ; (▲) 0.5M

Table 2 Apparent hydration number, n_{el}, around charged group(COO^-Na^+) of PLGNa and PAANa

C_s M	α	n_{el} PLGNa	n_{el} PAANa
0.1	1.0 - 0.7	7.0	5.2
	0.7 - 0.4		7.2
	0.4 - 0.1		7.8
0.2	1.0 - 0.7	7.1	5.2
	0.7 - 0.4		6.8
	0.4 - 0.1		
0.4	1.0 - 0.7	6.8	5.4
	0.7 - 0.4		6.4
	0.4 - 0.1		7.2
0.5	1.0 - 0.7	6.8	4.9
	0.7 - 0.4		6.4
	0.4 - 0.1		7.2

Deviation from the linear plot of $-\phi_p/\phi_w$ vs. α are observed below $\alpha = 0.70$ for each C_s. The deviation may originate from the coil-helix transition, which occurs below $\alpha = 0.70$ under the condition in this study. It must be reminded, however, that Manning theory predicts that counter-ion condensation takes place at $\alpha > 0.505$ for PLGNa. And we should remind that there is a world-wide controversy for the hydration state of the "bound" counter-ion ; some people strongly argue for the dehydrative counter-ion binding and many other people stand against this opinion with an idea that the primary hydration of counter-ion in the "bound" state is essentially intact. Therefore it sould be once examined if the values of n_{el} obtained from the slopes of the plots in Fig.3, correspond to those of counter-ion condensed charged group(COO^-Na^+), and if the deviation from the linear plot below $\alpha = 0.70$ is to be ascribed partly to the difference between n_{el}'s of counter-ion condensed and non-condensed charged groups. The hydration state of counter-ion, Na^+, is discussed referring to the apparent molar compressibility of PAANa in aq. NaCl solutions obtained from the density and sound velocity measurements. PAANa does not give any conformational transition like coil-helix transition with varying α. The results are summarized in Table 3. Fig.4 shows the plot of eq.(5) for PAANa in aq. NaCl solutions. A clear break at $\alpha = 0.70$ and a relatively small change in the slope at $\alpha = 0.40$ are found for each C_s. As the counter-ion condensation of PAANa is expected to take place at $\alpha > 0.35$ according to Manning theory, the break found at $\alpha = 0.40$ rather than the clear one at $\alpha = 0.70$ is attributed to the counter-ion condensation.

Table 3 d, u and β of aq. PAANa-NaCl solution

3 - 1 $C_s = 0.1$ M

i	d g/cm^3	u m/sec	$C_p \times 10^2$ basemol/l	$\beta \times 10^{11}$ cm^2/dyne
1.00	1.005071	1508.83	6.8112	4.3704
0.90	1.004592	1508.24	6.3682	4.3759
0.80	1.00417	1507.79	5.9890	4.3804
0.70	1.003802	1507.43	5.6529	4.3841
solvent	1.001154	1504.42		4.4133
0.60	1.003898	1507.43	6.3548	4.3837
0.50	1.003512	1506.89	5.9665	4.3885
0.40	1.003163	1506.44	5.6281	4.3926
0.30	1.003617	1506.62	7.7585	4.3896
solvent	1.001147	1504.46		4.4131
0.20	1.003178	1506.08	7.1979	4.3947
0.10	1.002787	1505.49	6.7150	4.3998
0.00	1.002501	1504.87	6.2927	4.4047
solvent	1.001145	1504.51		4.4128

Table 3 - 2 $C_s = 0.2$ M

i	d g/cm^3	u m/sec	C_p x 10^{2}basemol/l	β x 10^{11}cm^2/dyne
1.00	1.009093	1514.95	6.8111	4.3179
0.90	1.008729	1514.45	6.5822	4.3223
0.80	1.008390	1514.13	6.3760	4.3256
0.70	1.008074	1513.81	6.1769	4.3288
solvent	1.005215	1510.68		4.3591
0.60	1.008027	1513.68	6.5679	4.3297
0.50	1.007720	1513.18	6.3562	4.3339
0.40	1.007416	1512.81	6.1672	4.3373
0.30	1.007117	1512.45	5.9733	4.3407
solvent	1.005211	1510.73		4.3588
0.20	1.006840	1511.95	5.8073	4.3447
0.10	1.006593	1511.41	5.6409	4.3489
0.00	1.006400	1511.04	5.4834	4.3519
solvent	1.005223	1510.68		4.3591

Table 3 - 3 $C_s = 0.4$ M

i	d g/cm^3	u m/sec	$C_p \times 10^2$ basemol/l	$\beta \times 10^{11}$ cm^2/dyne
1.00	1.017070	1527.16	6.8062	4.2158
0.90	1.01678	1526.79	6.6909	4.2191
0.80	1.016512	1526.42	6.5858	4.2222
0.70	1.016227	1526.09	6.4693	4.2252
solvent	1.013266	1522.91		4.2553
0.60	1.015942	1525.77	6.3720	4.2282
0.50	1.015666	1525.22	6.2658	4.2324
0.40	1.015413	1524.99	6.1754	4.2347
0.30	1.01516	1524.57	6.0781	4.2381
0.20	1.01493	1524.20	5.9942	4.2411
0.10	1.01470	1523.69	5.9004	4.2449
solvent	1.013255	1522.96		4.2551

Table 3 - 4 C_s = 0.5 M

i	d g/cm^3	u m/sec	C_p x 10^2basemol/l	β x 10^{11}cm^2/dyne
1.00	1.020947	1533.05	6.6468	4.1676
0.90	1.020680	1532.68	6.5534	4.1707
0.80	1.020438	1532.49	6.4882	4.1727
0.70	1.020169	1532.17	6.3928	4.1756
solvent	1.017265	1528.96		4.2051
0.60	1.019876	1531.84	6.3109	4.1785
0.50	1.019628	1531.38	6.2293	4.1821
0.40	1.019382	1531.01	6.1540	4.1851
0.30	1.019135	1530.59	6.0726	4.1884
solvent	1.017252	1529.01		4.2049
0.20	1.018896	1530.22	6.0064	4.1915
0.10	1.018671	1529.70	5.9361	4.1952
0.05	1.018583	1529.61	5.8970	4.1961
solvent	1.017252	1529.01		4.2049

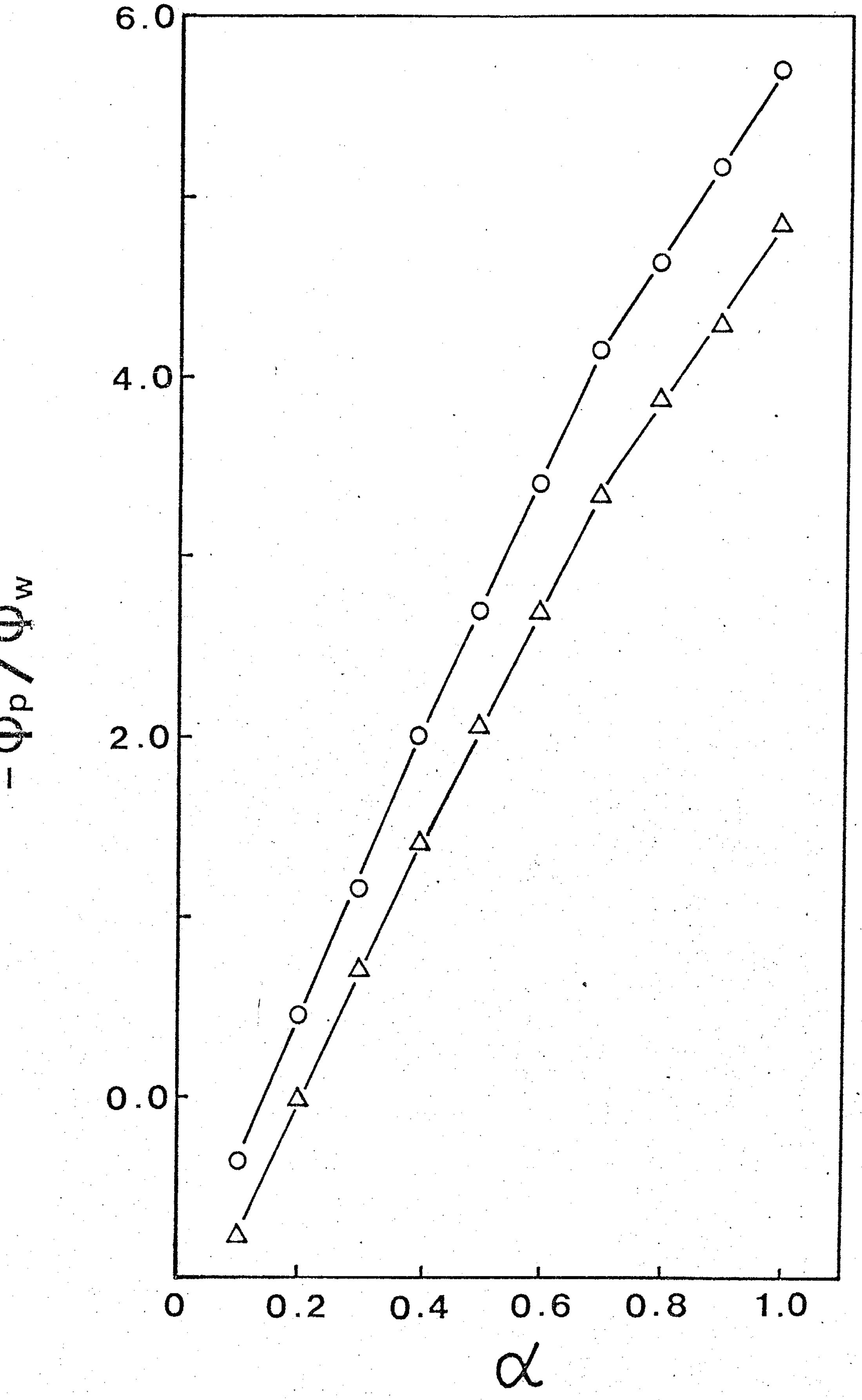

Fig.4 Plots of $-\phi_p/\phi_w$ against α for PAANa-NaCl

(○) C_s = 0.1M ; (△) C_s = 0.5M

Wall et al.$^{9)}$ reported that the charge fraction of PAANa slightly decreases with decreasing α from 1.0 to 0.4, followed by sharp decrease. However they obtained this result by transference experiments. In other words, they studied the property of PAANa in an electric field. We have performed counter-ion activity measurements with a Na^+ selective electrode to make certain whether any change in the activity exists between $\alpha = 0.70$ and 0.60 or not, because the behavior of Na^+ around PAA main chain in an electric field may be different from that under ordinary conditions. The result is given in Table 4. The values in the third and the last columns were calculated by assuming simple additivity between the activities of Na^+ from the polyelectrolyte and NaCl. Experiments were done in the region of α from 1.00 to 0.50, due to hindrance of H^+ to the electrode in the lower region of α. The counter-ion activity coefficient monotonously increases with decreasing α. This suggests that at least at $\alpha \geq 0.60$ for PAANa, counter-ion condensation takes place. In fact counter-ion activities per polymer basemol shown in the last column of Table 4, are nearly constant with varying α. From these results alone, it is not concluded that the small change in n_{el} at $\alpha = 0.40$ for PAANa is caused from counter-ion condensation, but it can be said that the difference of n_{el}'s, if any, for condensed and non-condensed Na^+ should be small. Manning$^{10)}$ has obtained the same results as his limiting law on counter-ion condensation by using two phase model which assumes that counter-ion moves freely in the condensed phase, with hydration shell intact. The present discussion seems to support the validity of the assumption for PAANa and perhaps for PLGNa.

Table 4 Counter-ion activity of PAANa in aq. 0.01M NaCl solution

α	C_p x 10^3basemol/l	Counter-ion Activity Coeff.	Counter-ion Activity/C_p
1.0	11.5	0.23	0.23
0.9	10.4	0.26	0.23
0.8	9.38	0.30	0.24
0.7	8.58	0.34	0.24
0.6	7.90	0.37	0.22
0.5	7.32	0.45	0.23

The break at $\alpha = 0.70$ in the plot of eq.(5) for PAANa must be due to other reasons, one of which may be "collapse" of the water structure around the polymer skeleton which is stable in higher charge density. Based on this inferrence, the break at $\alpha = 0.70$ for PAANa should be resulted from the change of ϕ_{hy}, rather than ϕ_{el} in eq.(2). This means that the hydration number n_{el} obtained from the plot of eq.(5) for PLGNa is mere an apparent value which contains some contribution from a possible dependency of ϕ_{hy}, on α.

Values of n_{el} obtained from linear parts of the plots in Fig.3 and Fig.4 are summarized in Table 2. n_{el} for PLGNa is about 7 for each C_s, while for PAANa it is about 5 in the region of $\alpha = 0.70 \sim 1.00$. If hydration numbers of Na^+ from PLGNa and PAANa are not different from that of Na^+ in bulk phase, electrostrictly hydrated water molecules around COO^- group will be about 2.5 mole for PLGNa and only about 0.5 mole for PAANa, because 4.5 is obtained as the hydration number of Na^+ in aq. simple electrolyte solution by the compressibility data. The smaller hydration number of carboxyl anion for PAANa than PLGNa has the same origin as the break in the slope at $\alpha = 0.70$ for PAANa, that is, the higher charge density and the shorter side chain of PAANa which produce the more stable hydration structure around the polymer.(Here it should be reminded that n_{el} represents the number of water molecules liberated when the charged group is protonated.) Ise and Okubo[11)] have estimated hydration numbers due to electrostriction for charged groups(COO^-) of PAANa and PLGNa from the partial molar volume measurements. The value of 3 obtained by them for these polymers can be compared with our result ; 2.5 for PLGNa and 0.5 for PAANa.

Apparent molar compressibility for helix-containing polymer is expressed by eq.(6). Contribution of helix formation to compressibility is given as,

$$\phi_p - \phi_{p\theta} = (\phi_{ic} - \phi_{ih})\theta + \phi_{hy'} - \phi_{hy''}(\theta) \qquad (7)$$

where it is also assumed that ϕ_p of PLGNa in hypothetical random coil conformation linearly decreases with α even in the transition region. If $\phi_{hy''}(\theta)$ is a linear function of θ, contribution of helix formation to the compressibility would be obtained from the slope of the plot of $\phi_p - \phi_{p\theta}$ vs. θ. For the coil-helix transition of PLGNa induced by decreasing α, $\phi_{hy'}$ may also change with the helix formation. The validity of eq.(7) is examined by applying it to a system in which the coil-helix transition is induced without affecting $\phi_{hy'}$. The coil-helix transition of PLL induced by addition of ClO_4^- ion is one of the cases. Ebert et al.[12) explained the salt induced transition as caused by the super helix constructed by ClO_4^- ions intervening just between two adjacent ε-NH_3^+ groups in the helical conformation, which is an optimum condition for screening electrostatic repulsion force among charged groups. The fact that ClO_4^- ion is an effective structure breaker of water allows the anion to be accessible to charged groups of PLL. Therefore the binding of ClO_4^- ion to the polymer contributes to $\phi_{hy''}(\theta)$ but not to $\phi_{hy'}$. Density and ultrasonic velocity measurements for PLLHBr in aq. $NaClO_4$ and NaCl solutions at $\alpha = 1.0$, were performed and the data are summarized in Table 5. Fig.5 shows plots of $-\phi_p/\phi_w$ vs. C_s and θ vs. C_s. It is seen that the dependence of the apparent molar compressibility on the concentration of $NaClO_4$,

Table 5 d, u and β of aq. PLLHBr solution (i = 1.00)

C_s M	d g/cm^3	u m/sec	C_p x 10^{2}basemol/l	β x 10^{11}cm^2/dyne
PLLHBr-NaClO$_4$				
0.0925	1.009510	1505.05	6.3914	4.3731
solvent	1.004916	1500.95		4.4171
0.1850	1.017342	1507.02	6.3926	4.3281
solvent	1.012728	1503.30		4.3694
0.2775	1.024893	1509.66	6.3949	4.2812
solvent	1.020304	1506.17		4.3204
0.4627	1.040512	1515.25	6.3832	4.1859
solvent	1.035846	1511.88		4.2235
0.7404	1.063702	1524.73	6.3751	4.0438
solvent	1.058902	1521.21		4.0810
0.9254	1.078957	1531.31	6.3863	3.9525
solvent	1.075104	1528.50		3.9813
PLLHBr-NaCl				
0.1	1.005788	1508.81	6.3945	4.3674
solvent	1.001177	1504.57		4.4123
0.3	1.013838	1521.17	6.3972	4.2626
solvent	1.009218	1516.77		4.3070
0.5	1.021927	1533.40	6.3900	4.1617
solvent	1.017299	1528.92		4.2052

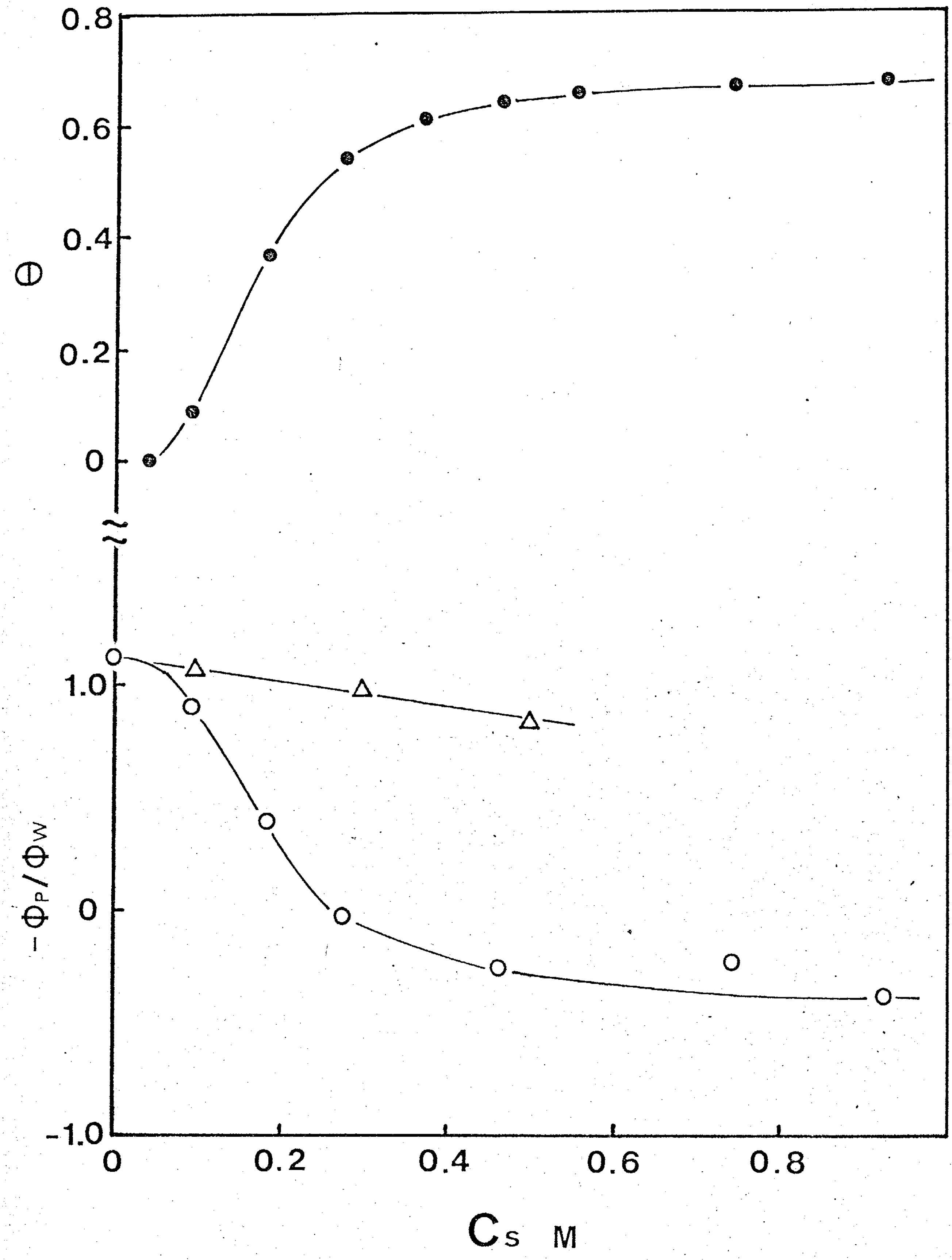

Fig. 5 Plots of θ (helical content) and $-\phi_p/\phi_w$ against C_s (conc. of added salt) : (●) PLLHBr-NaClO$_4$; (○) PLLHBr-NaClO$_4$; (△) PLLHBr-NaCl

C_s, is clearly correspondent with that of θ on C_s. ϕ_p of PLLHBr in hypothetical random coil conformation in the salt solution is necessary to apply eq.(7) to this system. ϕ_p of PLLHBr in aq. NaCl solution only slightly decreases with C_s as shown in Fig.5. Hence it is safely assumed that ϕ_p in aq. $NaClO_4$ solution would hardly depend on C_s. The constant ϕ_p gave a linear plot for PLLHBr in aq. $NaClO_4$ solution shown in Fig.6, indicating that contribution of helix formation to compressibility is additive. The interpretation along these lines can be extended to PLGNa in the transition region by assuming that ϕ_p is given by the linear extrapolation from the random coil region. Fig.6 contains the results. The plot for PLGNa shows a sigmoidal shape. The sigmoid may result from the estimation of ϕ_p of hypothetical random coil by the simple extrapolation. However a rough evaluation of the slope gives values as 0.8 ~ 1.2, which is a sum of contributions from the change of the intrinsic compressibility of the polymer and the difference in the hydration of the polymer in the two conformations. The former, $\phi_{ih}- \phi_{ic}$, is probably small negative since helical conformation is more regid than random coil conformation. The latter, $\phi_{hy''}(\theta) - \phi_{hy'}$, would be positive because water molecules whose ϕ is smaller than ϕ_w in bulk are released with the helix formation. Shiio$^{13)}$ has estimated the hydration number of sugars by assuming the adiabatic compressibility equal to that of ice, 1.8×10^{-11} cm^2/dyne. Gekko and Noguchi$^{5)}$ also have obtained the hydrogen-bonded hydration number of oligodextran based on the same assumption. If two water molecules whose ϕ_{wpo} is identical with that of ice are liberated from around one amide group in PLGNa main chain with

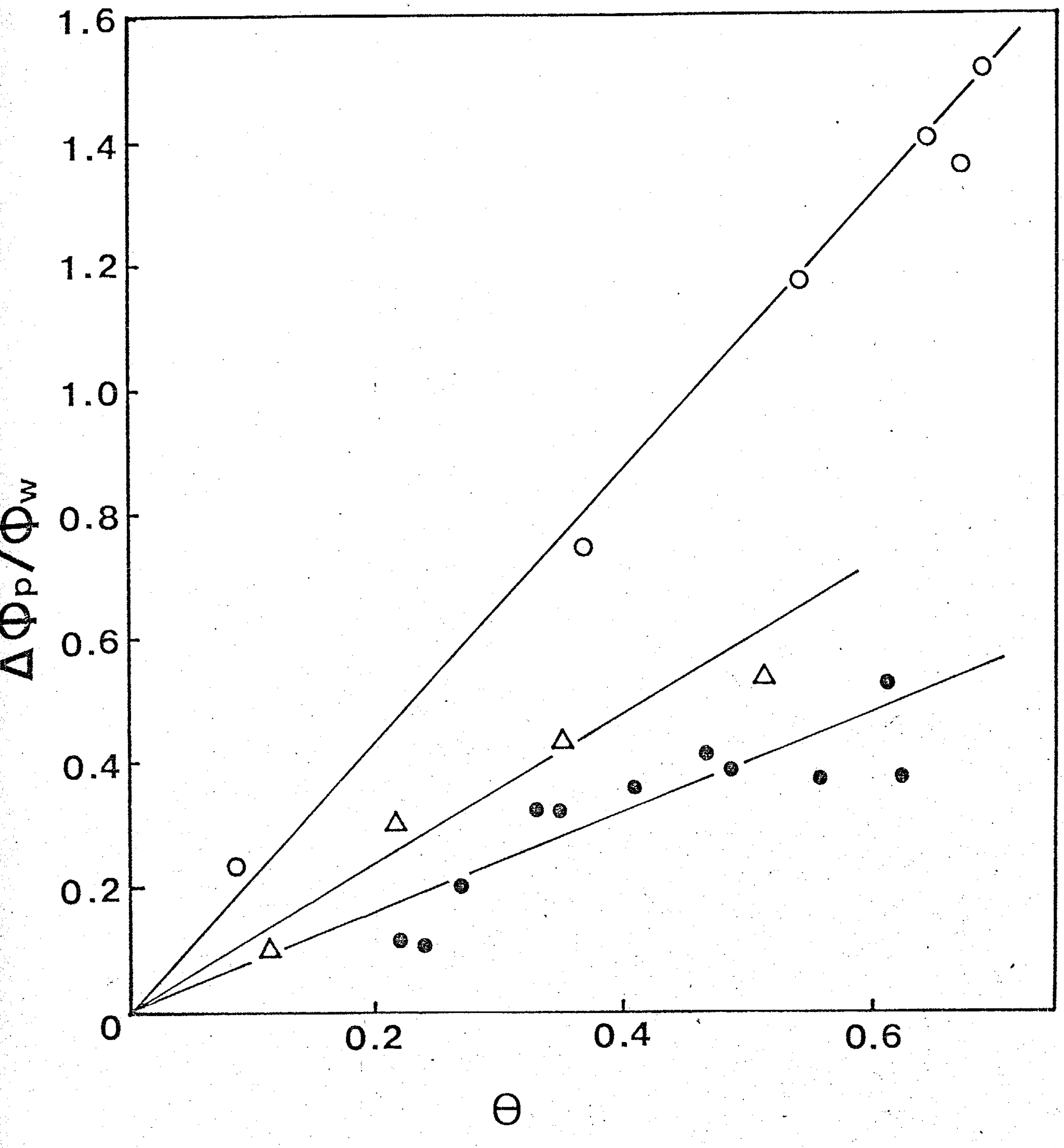

Fig.6 Plots of $\Delta\phi_p/\phi_w$ against θ : (○) PLLHBr-$NaClO_4$; (△) PLGNa-0.1M NaCl ; (●) PLGNa-0.2,0.4, and 0.5M NaCl

the helix formation, the contribution to the slope of the plot of eq.(7) will be 1.3, by which the slope obtained for PLGNa can be explained. ϕ_{wnp} of the other hydration water, if any, is nearly equal to ϕ_w in bulk phase, and hence the number cannot be known. Mori et al.[14)] have estimated the number of water molecules dehydrated upon helix formation on the basis of the preferential binding data for PLGNa and PLLHBr in aq. organic solvents, and obtained 5 as the number of nonpolar part hydration for these polymers. The activity of these water molecules in the hydrated state, however, seems not to be much different from that of bulk water unlike the case of electrostrictly hydrated water. The situation is similar in aqueous solutions, too, and one or two water molecules, at most, are thermodynamically released upon the helix formation. It follows that the influence of hydration to the coil-helix transition through the activity change is slight in dilute salt solutions, but come to be significant only in the concentrated region.

The difference between the slopes obtained for PLGNa and PLLHBr, 1.0 and 2.2, is ascribed to the difference of methods used to induce coil-helix transition. In the salt-induced transition, a contribution of the change of the hydration state due to the binding of ClO_4^- ion is also contained in the slope of the plot of eq.(7). Therefore it is difficult to compare numbers of water molecules liberated with the helix formation in the two systems. It is, however, noted that ϕ_p of PLLHBr is much smaller than that of PLGNa or PAANa. This means that ϕ_i and/or the hydration number of the former is smaller than that of the latter. Since PLL has longer side chain than PLG or PAA, the larger ϕ_i of PLL is possibly the origin of this difference. The hydration number due to electrostriction of the counter-ion, Br^-, of PLLHBr, which takes an important part in ϕ_p, is only 1.8, while that of Na^+ is 4.5. Therefore smaller hydration number of PLLHBr also contributes to the smaller ϕ_p.

In conclusion, the hydration number of PLGNa due to electrostriction was estimated to be about 7 by the compressibility data in the region of $\alpha = 0.7 \sim 1.0$, and the number is only slightly changed by counter-ion condensation, supporting Manning's assumption.

Assuming that the molar compressibility of water bound to amide group in the main chain of PLGNa is equal to that of ice, two water molecules are liberated upon the helix formation with appreciable compressibility change, and the other water molecules released at helix formation, if any, seem to have ϕ nearly equal to ϕ_w in bulk. This suggests that the influence of hydration to the coil-helix transition through the activity change can be neglected in dilute salt solution.

REFERENCES

1) D. W. Gruenwedel, C. H. Hsu and D. S. Lu, Biopolymers, 10, 47 (1971)

2) D. W. Gruenwedel, Biochim. Biophys. Acta, 340, 16 (1974)

3) idem., ibid., 395, 246 (1975)

4) B. Wolf and S. Hanlon, Biochemistry, 14, 1661 (1975)

5) K. Gekko and H. Noguchi, Macromolecules, 7, 224 (1974)

6-a) J. Lawrence and B. E. Conway, J. Phys. Chem., 75, 2353 (1971)

6-b) idem., ibid., 75, 2362 (1971)

7-a) A. C. Passynsky, Zhur. Fiz. Khim., 11, 608 (1938)

7-b) idem., ibid., 20, 981 (1946)

8) K. Gekko and H. Noguchi, J. Phys. Chem., 83, 2706 (1979)

9) J. R. Huizenga, P. F. Grieger and F. T. Wall, J. Amer. Chem. Soc., 72, 2636 (1950)

10) G. S. Manning, Q. Rev. Biophys., II, 179 (1978)

11) N. Ise and T. Okubo, Macromolecules, 2, 401 (1969)

12) Ch. Ebert and G. Ebert, Colloid Polym. Sci., 255, 1041 (1977)

13) H. Shiio, J. Amer. Chem. Soc., 80, 70 (1958)

14) T. Mori, J. Komiyama and T. Iijima, J. Chem. Soc. Faraday I, 74, 2583 (1978)

CHAPTER IV

Ionic Strength Dependence of Charge Induced Helix-Coil Transition of PLGNa in Aqueous Solution

ABSTRACT

Helix contents of PLGNa in aq. salt solutions have been obtained as functions of the degree of neutralization and salt concentration by CD measurements. The salts are LiCl, NaCl, KCl, RbCl,CsCl, $MgCl_2$, $CaCl_2$ and $BaCl_2$. The helix content of PLGNa in aq. NaCl solution increases with the salt concentration, C_s, when the degree of neutralization, i, higher than o.30, while it decreases when i is lower than 0.25. A theory which has been developed by Manning and Record et al. for the helix-coil transition of DNA, is used to interpret the results and turns out to be inadequate for transition systems with such low cooperativity as PLGNa in aq. solution. A modification of the theory based on a model polymer chain with alternating coil and helical portions, can explain the results for PLGNa in aq. NaCl solutions. The enhanced helix content for PLGNa in aq. alkaline earth metal salt solutions is attributed to the increased degree of counter-ion condensation rather than to the complex formation between the cation and charged groups on PLG.

Introduction

The charge induced helix-coil transition of PLGNa in aq. solution has been investigated by many workers$^{1)}$. Most of them, however, used the pH titration method to estimate the transition free energy of hypothetical uncharged polypeptide and much less attention was payed to the dependence of helix content on ionic strength. Systematic investigations on salt concentration effects to the conformational change of PLGNa or any other charged poly(amino acid)s can hardly be found in literature. Kanehiro$^{2)}$ studied the effects of alkali metal and tetraalkylammonium chlorides by ORD measurements and found constant helix content of PLGNa in aq. NaCl solution in the region of C_s between 0.1M and 0.5M at i = 0.4375. Larger helix content in aq. 0.1M NaCl solution than in the absence of the salt was observed, which was attributed to the increased screening effect of electrostatic interaction among the charged groups with salt concentration.

Recently, Record et al.$^{3,4)}$ have applied Manning theory to the helix-coil transition of DNA and successfully discussed the dependence of the melting temperature on added salt concentration. The helix-coil transition of PLGNa should also be treated by taking the counter-ion condensation phenomenon into account.

In this chapter, the helical content of PLGNa in aqueous solution of alkali and alkaline earth metal chloride is measured by CD and the results are discussed with emphasis on the dependence of the helix content on ionic strength. The formulation developed for DNA system by Record et al.$^{5)}$ and Manning$^{6)}$ is employed for the discussion.

Experimental

Materials

The stock solution of PLGNa in 1.776×10^{-2} basemol/l was used for CD and pH measurements. Added salts were alkali and alkaline earth metal chlorides ; LiCl, NaCl, KCl, RbCl, CsCl, $MgCl_2$, $CaCl_2$ and $BaCl_2$, which were obtained from Kanto Chem. Co. or Nakarai Chem. Ltd.(Rb and Cs salts) and Merck(Ca and Ba salts, Spurapur) as analytical grade reagents. Deionized and afterward distilled water was used throughout the experiments.

Apparatus and Methods

CD measurements were performed at several temperatures with a Jasco J 20 automatic recording spectropolarimeter. pH measurements were made with an F-7ss pH meter(Hitachi Horiba) for PLGNa aq. solution containing LiCl, NaCl, CsCl and the three alkaline earth metal chlorides at room temperature(25 ± 0.5°C).

Polymer solutions for CD and pH measurements were prepared as follows ; 5.0 ml of polymer solution containing HCl added to obtain desired degree of neutralization and 5.0 ml of aqueous salt solution are mixed. In the preparation, it is essential carefully to pipet the polymer solution under stirring with a magnetic stirrer for obtaining data with high reproducibility.

Results

Helix contents estimated by eq.(5) in Chapter II for PLGNa in aq. NaCl solutions are given in Table 1. Plot of the helix content vs. log C_s at 25°C is shown in Fig.1. Table 2 and Figs. 2-4 contain the similar data on PLGNa in aq. alkali chlorides and alkaline earth metal chlorides solutions. The helix content of PLGNa in aq. NaCl solutions increases with increasing C_s except at lower i.

Figs.5-7 show the results of pH measurements for various systems of PLGNa. Apparent pK values are plotted against α for PLGNa in 0.1M NaCl and 0.1M $MgCl_2$ in Fig.5. Figs.6 and 7 show the dependence of pH on log I, where I is ionic strength, for selected systems of PLGNa-alkali or alkaline earth metal salts. All the pH data are summarized in Table 3.

Table 1 Helix content of PLGNa in aq. NaCl solutions

1 - 1 15°C

i = 0.25		i = 0.30		i = 0.35		i = 0.40		i = 0.60	
$-\log C_s$	H.C.(%)	$-\log C_s$	H.C.(%)	$-\log C_s$	H.C.(%)	$-\log C_s$	H.C.(%)	$-\log C_s$	H.C.(%)
3.178	94.4	3.208	88.5	3.240	74.0	3.275	52.0	2.628	0.3
2.779	94.5	2.791	89.3	2.803	78.0	2.815	58.1	2.271	0.9
2.574	94.1	2.582	90.1	2.589	79.0	2.597	60.5	1.985	3.2
2.247	94.0	2.250	90.1	2.254	80.9	2.257	64.2	1.691	6.8
1.972	93.5	1.974	90.4	1.976	82.2	1.978	67.9	1.298	12.7
1.685	92.7	1.686	90.4	1.687	83.7	1.688	70.7	0.998	17.9
1.295	92.0	1.296	90.1	1.296	84.7	1.296	74.8	0.698	24.2
0.997	90.9	0.997	89.3	0.998	85.6	0.998	76.7	0.301	34.6
0.698	89.2	0.698	88.4	0.698	85.3	0.698	78.9		
0.300	82.4	0.300	85.9	0.301	83.9	0.301	79.5		

* H.C. : Helix Content

1 - 2 20°C

i = 0.25		i = 0.30		i = 0.35		i = 0.40	
-lig C_s	H.C.(%)	-log C_s	H.C.(%)	-log C_s	H.C.(%)	-log C_s	H.C.(%)
3.177	92.1	3.207	84.8	3.239	69.3	3.274	47.0
2.779	91.9	2.790	85.9	2.802	73.0	2.815	53.5
2.574	92.0	2.582	86.4	2.589	74.2	2.597	55.8
2.247	91.6	2.250	86.8	2.254	76.4	2.257	59.9
1.972	90.9	1.974	86.9	1.976	77.4	1.977	62.4
1.685	90.1	1.686	86.9	1.687	78.7	1.688	65.6
1.295	89.4	1.296	86.9	1.296	79.8	1.296	69.6
0.997	88.0	0.997	86.0	0.998	80.5	0.998	71.5
0.698	87.0	0.698	84.8	0.698	80.6	0.698	74.1
0.300	81.3	0.300	81.2	0.301	79.6	0.301	74.8

1 - 2 Continued.

i = 0.45		i = 0.50		i = 0.60	
$-\log C_s$	H.C.(%)	$-\log C_s$	H.C.(%)	$-\log C_s$	H.C.(%)
3.312	32.4	3.353	22.8	2.271	0.8
2.828	38.6	2.841	25.4	1.985	2.8
2.604	40.4	2.612	25.5	1.691	5.3
2.261	45.1	2.264	27.5	1.298	9.9
1.979	49.0	1.981	29.3	0.998	15.0
1.689	53.5	1.689	33.3	0.698	20.4
1.297	58.0	1.297	39.1	0.301	29.3
0.998	61.7	0.998	44.0		
0.698	64.9	0.698	49.4		
0.301	68.8	0.301	56.2		

1-- 3 25°C

i = 0.20		i = 0.25		i = 0.30		i = 0.35		i = 0.40	
-log C_s	H.C.(%)	-log C_s	H.C.(%)	-log C_s	H.C.(%)	-log C_s	H.C.(%)	-log C_s	H.C.(%)
3.150	91.1	3.178	87.2	3.203	78.1	3.235	60.1	3.270	36.9
2.768	90.6	2.779	87.1	2.789	79.1	2.801	64.8	2.813	44.0
2.567	90.2	2.575	87.4	2.581	79.9	2.588	66.0	2.596	46.4
2.244	89.2	2.247	87.0	2.250	80.7	2.253	68.8	2.257	51.5
1.970	88.6	1.972	86.2	1.974	81.0	1.975	70.5	1.977	55.0
1.684	86.7	1.685	85.3	1.686	80.9	1.687	72.8	1.687	58.1
		1.295	84.5	1.296	80.8	1.296	74.1	1.296	62.9
		0.997	83.4	0.997	80.4	0.998	74.7	0.998	65.3
		0.698	81.8	0.698	71.6	0.698	74.9	0.698	67.2
		0.300	75.6	0.301	77.9	0.301	75.0	0.301	68.9

1 - 3 Continued.

i = 0.45		i = 0.50		i = 0.55		i = 0.60	
$-\log C_s$	H.C.(%)	$-\log C_s$	H.C.(%)	$-\log C_s$	H.C.(%)	$-\log C_s$	H.C.(%)
3.313	15.9	3.354	4.4	2.854	1.5	2.271	0.6
2.828	23.9	2.841	8.7	2.662	2.5	1.985	2.0
2.604	26.2	2.612	10.7	2.268	5.4	1.691	4.5
2.261	31.5	2.264	15.8	1.983	7.9	1.298	7.8
1.979	36.1	1.981	19.8	1.690	11.4	0.998	11.5
1.689	40.5	1.689	23.9	1.298	17.1	0.698	16.4
1.297	46.5	1.297	30.2	0.998	21.8	0.301	23.6
0.998	51.4	0.998	35.4	0.698	27.2		
0.698	56.1	0.698	40.8	0.301	35.1		
0.301	60.1	0.301	47.6				

1 - 4 30°C

i = 0.20		i = 0.30		i = 3.50		i = 0.40	
$-\log C_s$	H.C.(%)	$-\log C_s$	H.C.(%)	$-\log C_s$	H.C.(%)	$-\log C_s$	H.C.(%)
3.145	88.0	3.203	73.5	3.235	53.3	3.282	29.9
2.765	87.1	2.789	74.3	2.801	57.3	2.817	34.7
2.566	86.6	2.581	74.5	2.588	59.4	2.598	-
2.243	85.8	2.250	75.5	2.253	61.9	2.258	41.0
1.970	85.0	1.974	75.8	1.975	63.8	1.978	43.3
1.684	84.2	1.686	76.0	1.187	65.6	1.688	47.1
1.295	82.3	1.296	76.0	1.296	67.4	1.297	51.3
0.997	80.3	0.997	74.9	0.998	68.5	0.988	54.2
0.697	78.5	0.698	74.2	0.698	68.6	0.698	57.2
0.300	75.4	0.301	72.2	0.301	68.3	0.301	57.1

1 - 4 Continued.

i = 0.45		i = 0.50		i = 0.60	
$-\log C_s$	H.C.(%)	$-\log C_s$	H.C.(%)	$-\log C_s$	H.C.(%)
3.320	13.8	3.361	3.1	2.272	0.5
2.830	17.4	2.843	5.8	1.985	1.4
2.606	19.5	2.613	7.6	1.691	2.7
2.261	23.4	2.265	10.8	1.298	5.6
1.980	26.4	1.981	13.7	0.998	8.4
1.689	31.0	1.690	17.4	0.698	12.0
1.297	36.6	1.297	23.3	0.301	18.1
0.998	40.2	0.998	27.7		
0.698	44.4	0.698	32.6		
0.301	49.0	0.301	38.9		

1 - 5 40°C

i = 0.20		i = 0.25		i = 0.30		i = 0.35	
-log C_s	H.C.(%)	-log C_s	H.C.(%)	-log C_s	H.C.(%)	-log C_s	H.C.(%)
3.157	77.3	3.185	68.0	3.215	48.7	3.247	29.7
2.770	76.9	2.782	68.6	2.793	51.8	2.805	34.9
2.569	77.1	2.576	69.2	2.583	54.1	2.591	36.9
2.244	76.0	2.248	69.5	2.251	56.7	2.254	40.4
1.971	75.2	1.973	69.2	1.974	57.8	1.976	43.0
1.684	74.0	1.685	68.9	1.686	59.0	1.687	46.3
1.295	71.7	1.295	68.4	1.296	60.7	1.296	48.8
0.997	70.2	0.997	67.3	0.997	60.6	0.998	50.7
0.697	68.6	0.698	66.0	0.698	60.7	0.698	52.2
0.300	62.5	0.300	63.0	0.301	59.1	0.301	53.0

1 - 5 Continued.

i = 0.40		i = 0.45		i = 0.50	
-log C_s	H.C.(%)	-log C_s	H.C.(%)	-log C_s	H.C.(%)
3.282	14.4	3.320	6.8	3.361	2.8
2.817	19.0	2.830	10.0	2.843	4.3
2.598	21.4	2.606	11.6	2.613	5.2
2.258	25.5	2.261	14.4	2.265	7.0
1.978	28.9	1.980	17.1	1.981	8.8
1.688	32.8	1.689	20.6	1.690	11.6
1.297	37.3	1.297	24.9	1.297	15.1
0.998	39.8	0.998	28.3	0.998	18.2
0.698	43.2	0.698	31.9	0.698	21.9
0.301	46.5	0.301	36.6	0.301	27.3

1 - 6 50°C

i = 0.20		i = 0.25		i = 0.30	
$-\log C_s$	H.C.(%)	$-\log C_s$	H.C.(%)	$-\log C_s$	H.C.(%)
3.157	66.8	3.185	54.4	3.215	36.7
2.770	66.5	2.782	55.0	2.793	39.0
2.569	66.4	2.576	55.9	2.583	40.5
2.244	65.5	2.248	57.3	2.251	42.8
1.971	64.9	1.973	57.4	1.974	44.2
1.684	62.9	1.685	56.4	1.686	45.9
1.295	61.5	1.295	55.6	1.296	46.5
0.997	59.5	0.997	55.2	0.997	47.3
0.697	56.8	0.698	53.5	0.698	47.1
0.300	53.3	0.300	50.4	0.301	45.9

i = 0.35		i = 0.40		i = 0.45	
$-\log C_s$	H.C.(%)	$-\log C_s$	H.C.(%)	$-\log C_s$	H.C.(%)
3.247	20.4	3.282	11.1	3.320	6.0
2.805	24.5	2.817	13.6	2.830	7.7
2.591	26.2	2.598	15.2	2.606	8.9
2.254	28.9	2.258	17.9	2.261	10.9
1.976	31.4	1.978	20.5	1.980	12.6
1.687	34.0	1.688	23.1	1.689	14.8
1.296	36.5	1.297	26.4	1.297	17.9
0.998	38.2	0.998	29.1	0.998	20.5
0.698	39.2	0.698	30.6	0.698	23.3
0.301	39.8	0.301	34.1	0.301	26.5

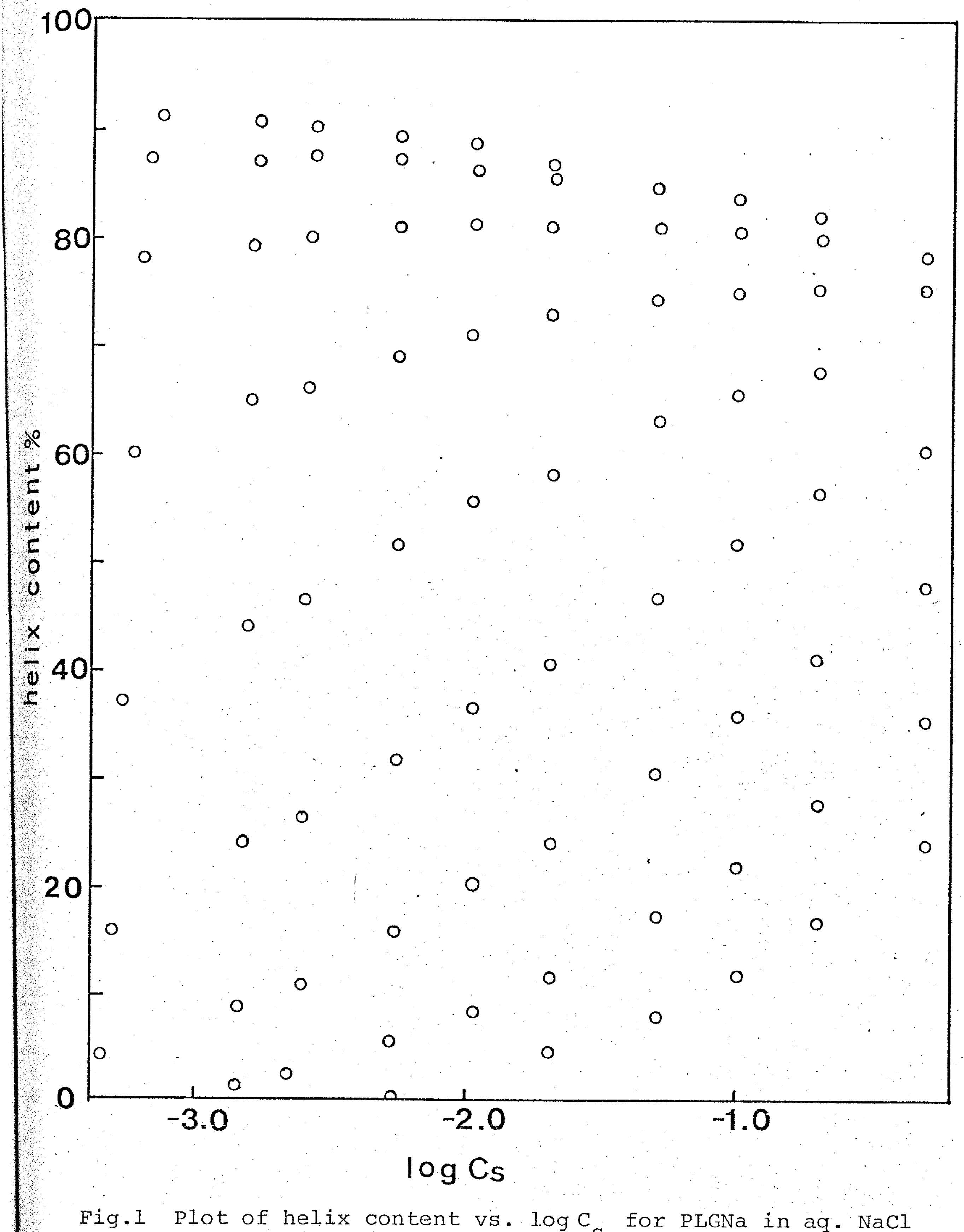

Fig.1 Plot of helix content vs. log C_s for PLGNa in aq. NaCl solutions at 25°C : i = 0.20, 0.25, 0.30, 0.35, 0.40, 0.45, 0.50 0.55, 0.60 from top to bottom.

Table 2 Helix content of PLGNa in aq. alkali and alkaline earth metal chlorides solutions at 25°C

2 - 1 LiCl

i = 0.35		i = 0.40		i = 0.45	
$-\log C_s^*$	H.C.(%)	$-\log C_s^*$	H.C.(%)	$-\log C_s^*$	H.C.(%)
3.239	59.2	3.273	34.7	3.311	16.3
2.802	64.9	2.814	43.4	2.827	22.9
2.589	66.4	2.596	47.1	2.604	26.7
2.254	68.3	2.257	52.0	2.261	31.1
1.976	70.8	1.977	54.3	1.979	35.7
1.687	72.7	1.687	58.4	1.689	40.7
1.296	74.8	1.296	62.9	1.297	46.5
0.998	74.9	0.998	64.3	0.998	49.8
0.698	74.8	0.698	66.1	0.698	52.9
0.301	72.9	0.301	65.7	0.301	53.3

2 - 2 KCl

i = 0.40	
$-\log C_s^*$	H.C.(%)
3.273	34.9
2.814	44.7
2.596	47.3
2.257	50.7
1.977	54.7
1.687	58.4
1.296	63.0
0.998	64.7
0.698	66.1
0.301	67.0

* NaCl produced by the titration of PLGNa is contained in C_s.

2 - 3 RbCl

i = 0.35		i = 0.40		i = 0.45	
$-\log C_s^*$	H.C.(%)	$-\log C_s^*$	H.C.(%)	$-\log C_s^*$	H.C.(%)
3.239	64.4	3.273	36.4	3.311	18.8
2.849	65.9	2.863	43.8	2.877	23.7
2.647	65.4	2.656	45.6	2.665	27.0
2.322	68.8	2.326	51.3	2.330	31.5
2.048	71.2	2.050	54.8		
1.761	72.3	1.762	58.5	1.763	40.7
1.372	73.8	1.372	62.7	1.373	46.9
1.074	74.8	1.074	64.2	1.074	50.4
0.774	75.0	0.774	66.3	0.774	53.7
0.377	73.5	0.377	66.9	0.377	56.6

2 - 4 CsCl

i = 0.35		i = 0.40		i = 0.45	
$-\log C_s^*$	H.C.(%)	$-\log C_s^*$	H.C.(%)	$-\log C_s^*$	H.C.(%)
3.239	59.9	3.273	35.6	3.311	15.0
2.802	62.9	2.814	43.0	2.827	23.4
2.589	65.6	2.596	46.2	2.604	26.9
2.254	68.2	2.257	51.8	2.261	31.0
1.976	70.5	1.977	55.2	1.979	36.1
1.687	71.3	1.687	58.1	1.689	40.7
1.296	72.4	1.296	61.2	1.297	45.4
0.998	72.2	0.998	62.1	0.998	47.3
0.698	71.0	0.698	62.0	0.698	47.8
0.301	65.6	0.301	56.6	0.301	43.8

* NaCl produced by the titration of PLGNa is contained in C_s.

2 - 5 $MgCl_2$

$-\log C_s^*$	Helix Content (%) i = 0.35	i = 0.40	i = 0.45	i = 0.50	i = 0.60	i = 0.70	i = 0.80
2.950	78.6	72.0	64.7	54.6	29.3	10.0	0.9
2.649	78.0	72.0	64.2	55.2	30.7	11.4	1.4
2.251	76.9	71.1	64.4	55.3	32.2	12.4	2.3
1.950	76.4	70.8	64.3	56.0	33.1	14.0	2.9
1.649	75.7	70.2	64.0	56.0	34.5	14.6	3.6
1.251	74.7	69.5	64.6	57.2	36.1	16.4	4.6
0.950	74.1	70.1	65.0	57.9	38.0	18.5	5.8
0.649	72.3	68.8	65.0	59.1	40.2	20.5	7.5
0.251	69.2	67.1	63.8	59.6	43.5	24.5	10.6

* Concentration of $MgCl_2$

2 - 6 $CaCl_2$

$-\log C_s^*$	H.C.(%) i = 0.50	H.C.(%) i = 0.60
3.078	56.2	34.5
2.777	57.1	35.8
2.379	56.2	36.5
2.078	56.0	37.1
1.777	55.1	38.0
1.380	55.4	38.5
1.078	53.4	37.5

* Concentration of $CaCl_2$

2 - 7 $BaCl_2$

$-\log C_s^*$	H.C.(%) i = 0.60
3.008	25.4
2.707	26.3
2.309	27.1
2.008	28.9
1.707	30.2

* Concentration of $BaCl_2$

2 - 8 $MgCl_2$-NaCl (i = 0.50)

	Helix Content (%)		
$-\log C_s^*$	9.66×10^{-5}M $MgCl_2$	2.42×10^{-4}M $MgCl_2$	3.86×10^{-4}M $MgCl_2$
3.352	33.6	48.2	51.7
3.000	32.0	45.5	49.5
2.699	30.3	42.7	47.1
2.300	29.2	38.4	42.3
2.000	28.7	35.0	38.8
1.699	28.7	32.9	34.9
1.301	32.2	34.5	34.5
1.000	37.1	36.8	37.8
0.699	41.7	41.4	42.3
0.301	48.9	48.5	48.2

* Concentration of NaCl

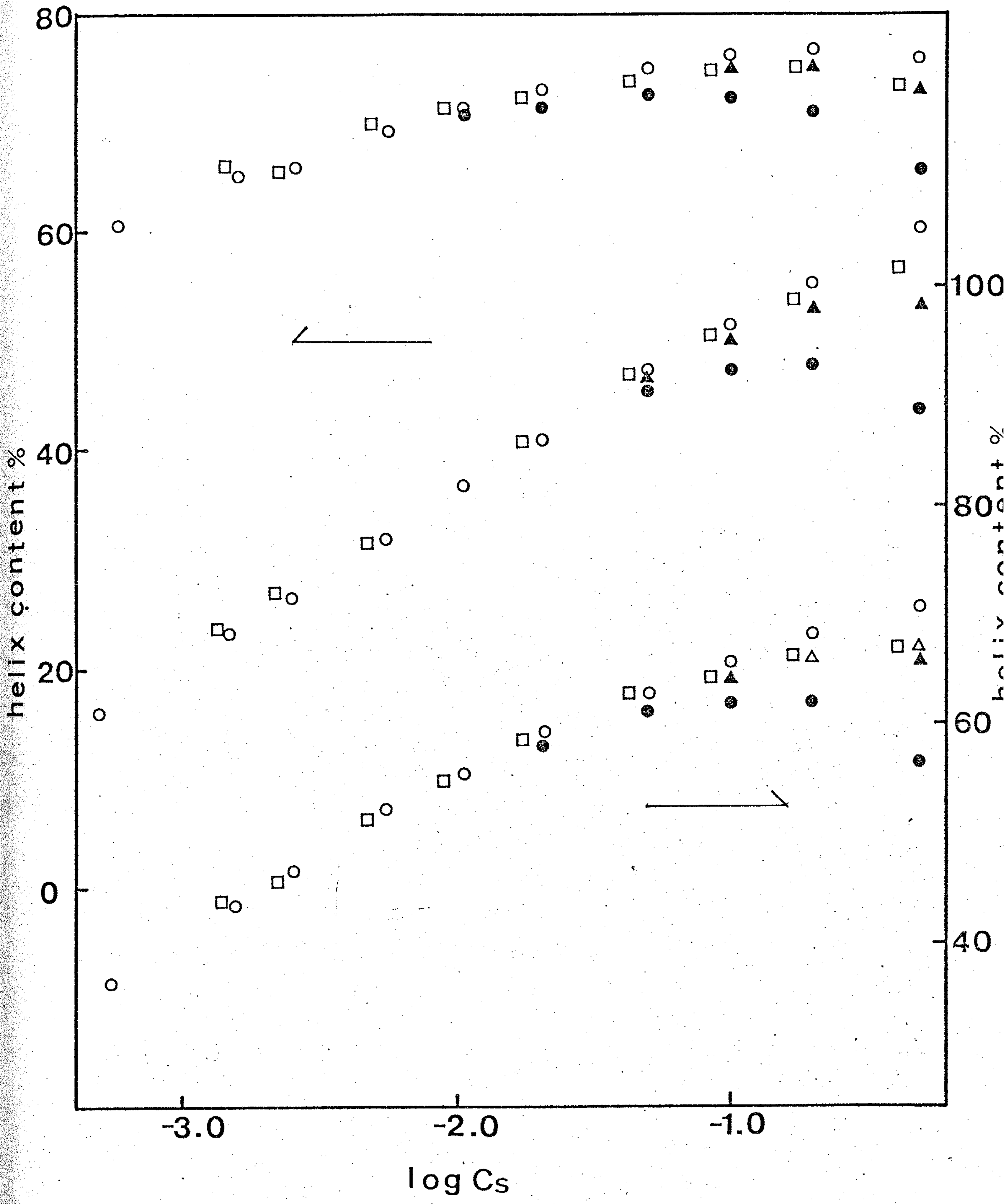

Fig.2 Plot of helix content vs. log C_s for PLGNa in aq. alkali metal chloride solutions : i = 0.35, 0.45, 0.40 from top to bottom (▲) LiCl ; (○) NaCl ; (△) KCl ; (□) RbCl ; (●) CsCl.

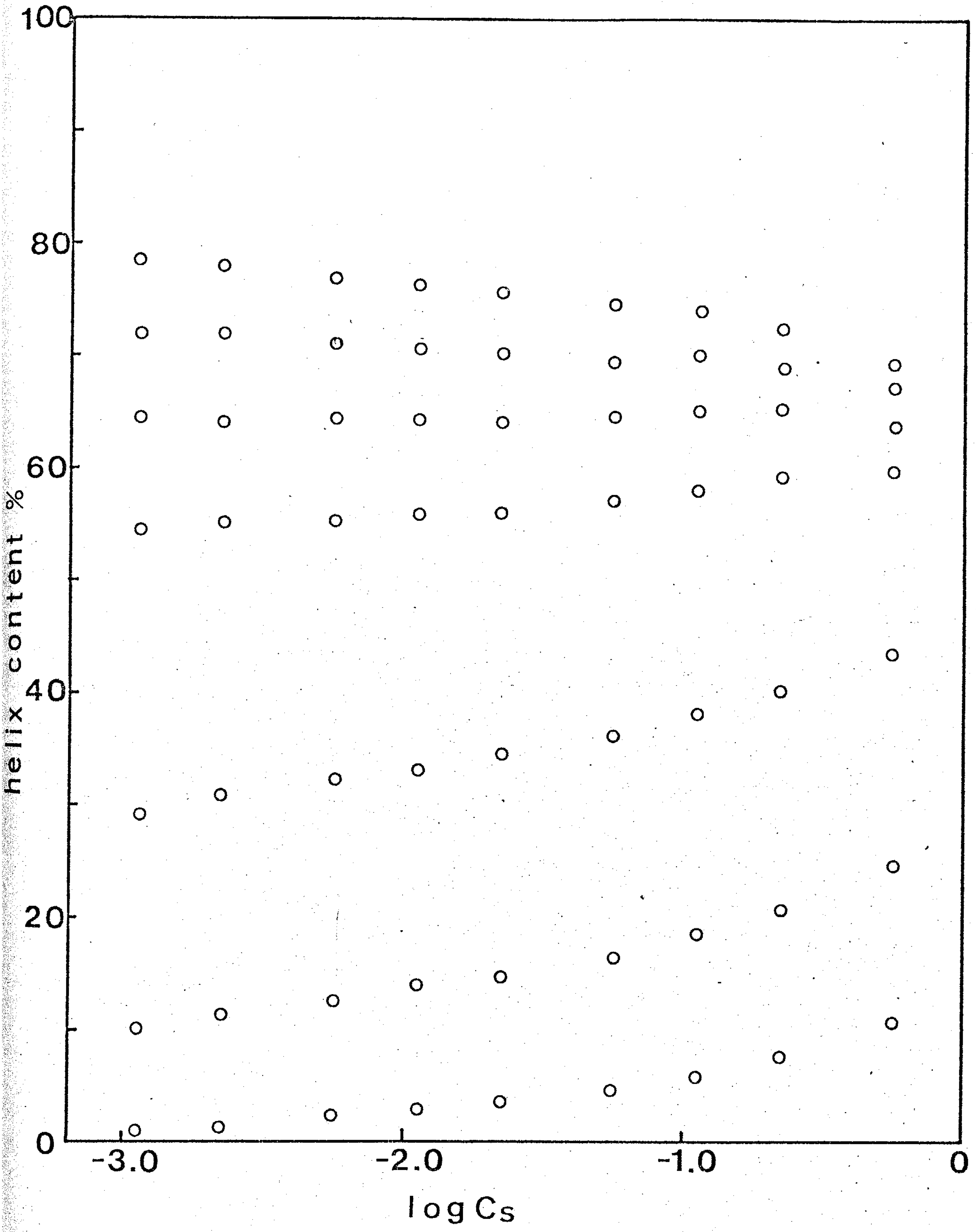

Fig.3 Plot of helix content vs. log C_s for PLGNa in aq. $MgCl_2$ solutions : i = 0.35, 0.40, 0.45, 0.50, 0.60, 0.70, 0.80 from top to bottom.

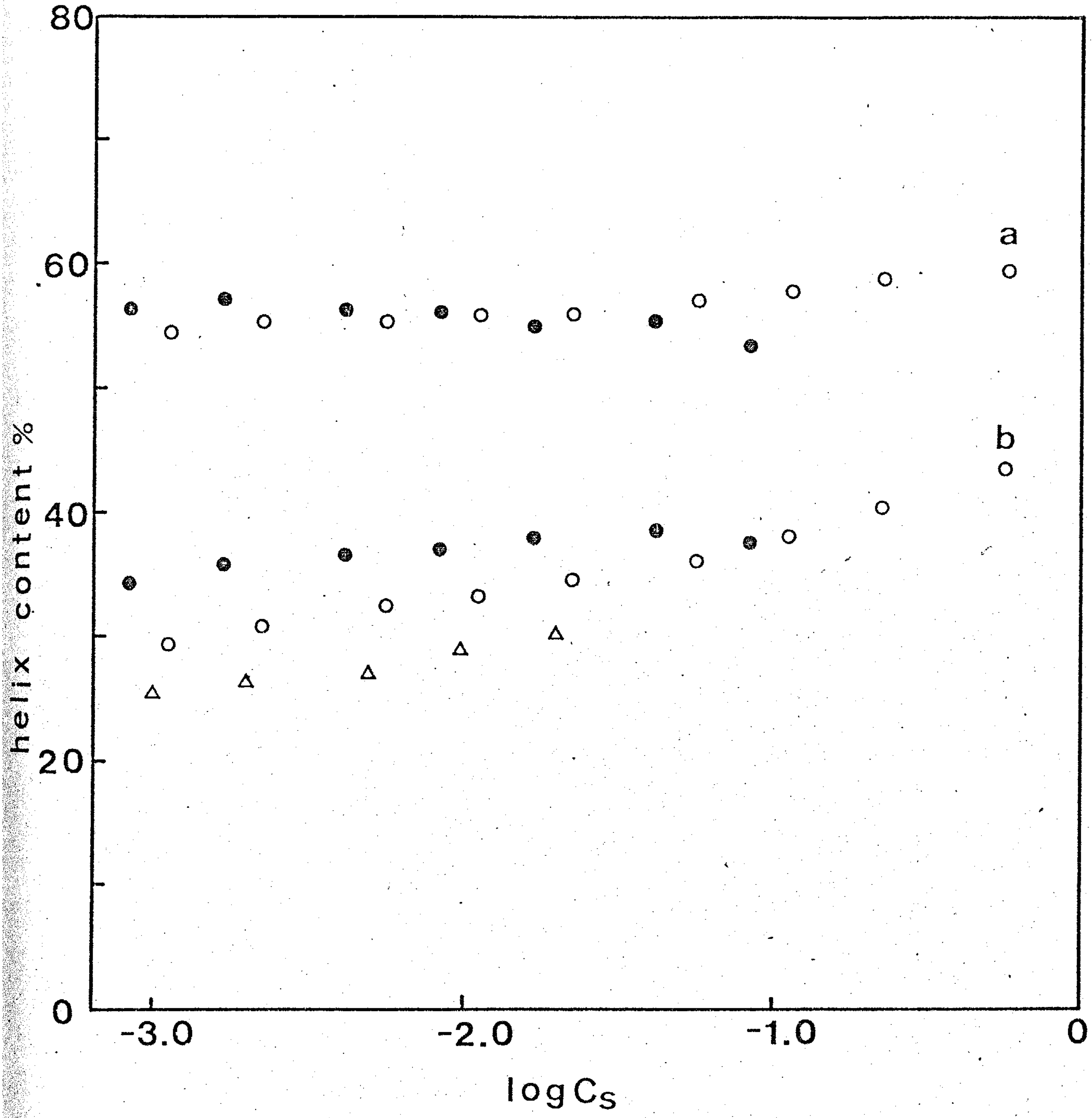

Fig.4 Plot of helix content vs. log C_s for PLGNa in aq. alkaline earth metal chloride solutions : a. i = 0.50, b. i = 0.60 (○) $MgCl_2$; (●) $CaCl_2$; (△) $BaCl_2$.

Table 3 pH values of PLGNa in aq. salt salutions

3 - 1 NaCl

i = 0.20		i = 0.25		i = 0.30	
-log I	pH	-log I	pH	-log I	pH
3.15	5.16	3.18	5.46	3.21	5.74
2.77	5.01	2.78	5.33	2.79	5.54
2.57	4.93	2.57	5.22	2.58	5.43
2.24	4.79	2.25	5.06	2.25	5.25
1.97	4.68	1.97	4.92	1.98	5.10
1.68	4.58	1.68	4.80	1.69	4.97
1.29	4.49	1.30	4.65	1.30	4.80
1.00	4.38	1.00	4.53	1.00	4.655
0.70	4.30	0.70	4.42	0.70	4.52
0.30	4.18	0.30	4.27	0.30	4.36

i = 0.35		i = 0.40		i = 0.45	
-log I	pH	-log I	pH	-log I	pH
3.24	5.91	3.27	6.06	3.31	6.23
2.80	5.70	2.81	5.85	2.83	6.01
2.59	5.59	2.60	5.75	2.60	5.88
2.25	5.42	2.26	5.58	2.26	5.70
1.98	5.28	1.98	5.44	1.98	5.55
1.69	5.14	1.69	5.30	1.69	5.41
1.30	4.96	1.30	5.11	1.30	5.22
1.00	4.815	1.00	4.965	1.00	5.07
0.70	4.67	0.70	4.81	0.70	4.92
0.30	4.48	0.30	4.61	0.30	4.71

3 - 2 LiCl (i = 0.45)

-log I	pH
2.83	5.95
2.60	5.83
2.26	5.66
1.98	5.50
1.69	5.36
1.30	5.16
1.00	5.01
0.70	4.85
0.30	4.64

3 - 3 CsCl (i = 0.45)

-log I	pH
2.83	6.02
2.60	5.89
2.26	5.71
1.98	5.58
1.69	5.44
1.30	5.27
1.00	5.16
0.70	5.06
0.30	4.97

3 - 4 $MgCl_2$

i = 0.313		i = 0.40		i = 0.45		i = 0.50		i = 0.60	
-log I	pH	-log I	pH	-log I	pH	-log I	pH	-log I	pH
2.48	5.10	2.48	5.19	2.49	5.30	2.49	5.35	2.50	5.51
2.21	5.00	2.21	5.09	2.21	5.18	2.21	5.24	2.22	5.395
1.83	4.885	1.83	4.98	1.83	5.06	1.83	5.12	1.83	5.275
1.53	4.805	1.53	4.88	1.53	4.975	1.53	5.03	1.53	5.19
1.23	4.715	1.23	4.80	1.23	4.88	1.23	4.94	1.23	5.09
0.84	4.585	0.84	4.67	0.84	4.74	0.84	4.80	0.84	4.95
0.54	4.47	0.54	4.54	0.54	4.625	0.54	4.67	0.54	4.82
0.24	4.32	0.24	4.40	0.24	4.475	0.24	4.51	0.24	4.66
-0.16	4.06	-0.16	4.14	-0.16	4.21	-0.16	4.25	-0.16	4.40

3 - 5 $CaCl_2$ (i = 0.45)

-log I	pH
2.49	5.26
2.22	5.15
1.84	5.02
1.54	4.93
1.24	4.84
0.85	4.70
0.54	4.59
0.24	4.445
-0.15	4.19

3 - 6 $BaCl_2$ (i = 0.45)

-log I	pH
2.47	5.31
2.19	5.21
1.81	5.09
1.51	5.01
1.22	4.92
0.82	4.78
0.52	4.67
0.22	4.53
-0.18	4.31

3 - 7 $MgCl_2$-NaCl (i = 0.50)

9.66×10^{-5}M $MgCl_2$		2.42×10^{-4}M $MgCl_2$		3.86×10^{-4}M $MgCl_2$	
-log I	pH	-log I	pH	-log I	pH
3.13	5.90	2.93	5.37	2.80	5.455
2.76	5.76	2.66	5.45	2.58	5.445
2.56	5.73	2.50	5.45	2.44	5.445
2.24	5.62	2.21	5.43	2.18	5.435
1.97	5.53	1.95	5.38	1.94	5.40
1.68	5.44	1.67	5.33	1.67	5.355
1.29	5.29	1.29	5.24	1.29	5.26
1.00	5.155	0.99	5.13	0.99	5.14
0.70	5.01	0.70	4.995	0.70	5.00
0.30	4.80	0.30	4.785	0.30	4.795

3 - 8 0.1M NaCl ($C_p = 3.49\times10^{-2}$ basemol/l)

α	pH	pK = pH - log α/1-α
1.00	7.11	
0.90	6.11	5.16
0.80	5.70	5.10
0.75	5.55	5.07
0.70	5.40	5.03
0.65	5.28	5.01
0.60	5.16	4.98
0.55	5.05	4.96
0.50	4.94	4.94
0.45	4.82	4.91
0.40	4.70	4.88
0.35	4.54	4.81
0.30	4.39	4.76
0.25	4.24	4.72

3 - 9 0.1M $MgCl_2$ ($C_p = 3.49\times10^{-2}$ basemol/l)

α	pH	pK = pH - log α/1-α
1.00	6.44	
0.95	5.68	4.40
0.90	5.385	4.43
0.85	5.19	4.44
0.80	5.04	4.44
0.75	4.92	4.44
0.70	4.81	4.44
0.65	4.71	4.44
0.60	4.62	4.44
0.55	4.53	4.44
0.50	4.44	4.44
0.45	4.35	4.44
0.40	4.25	4.43
0.35	4.14	4.41
0.30	4.035	4.40

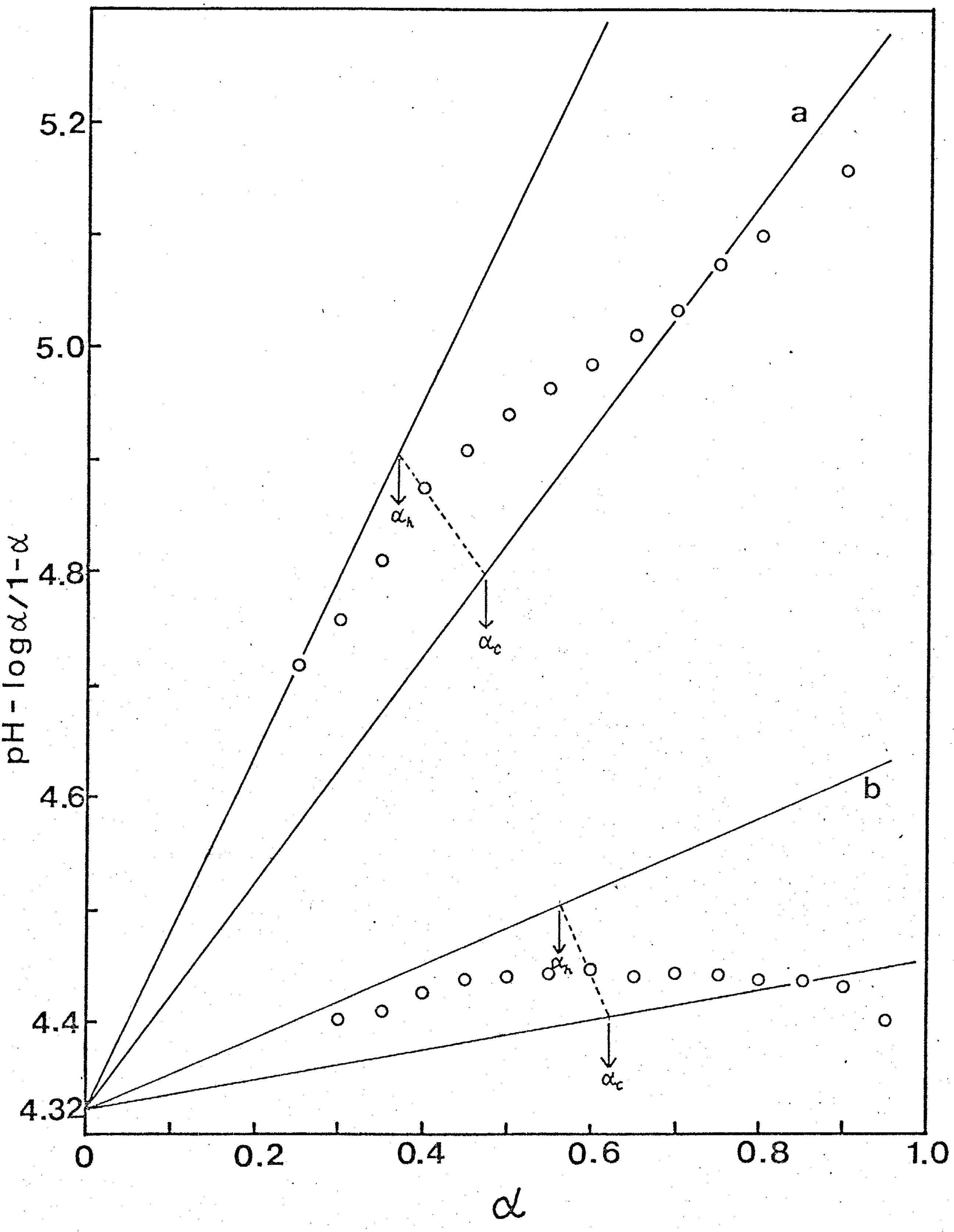

Fig.5 Titration curves of PLGNa in aq. salt solutions : a. 0.1M NaCl, b. 0.1M $MgCl_2$, C_p = 3.49 x 10^{-2}basemol/l for both systems.

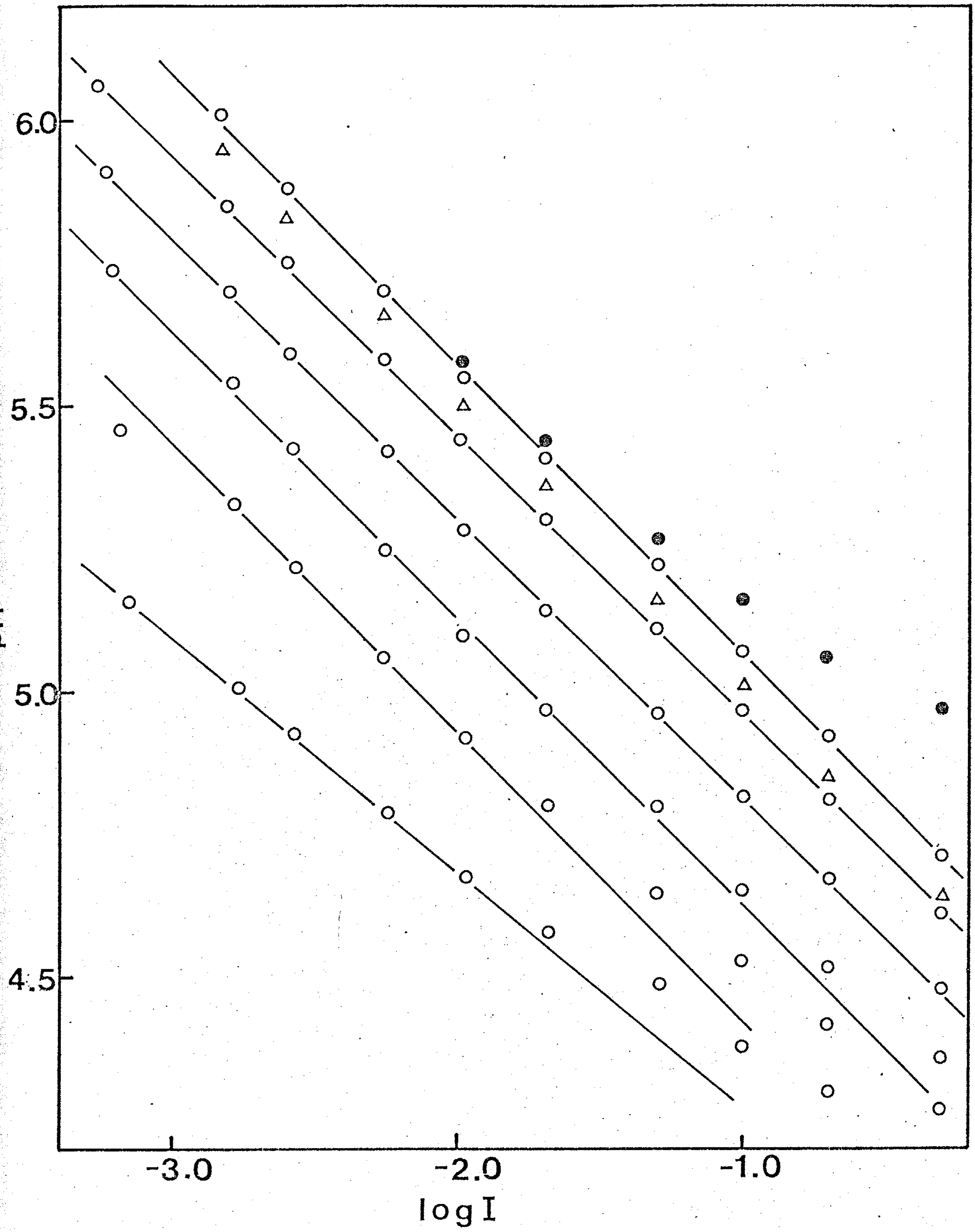

Fig.6 Dependence of pH on log I for PLGNa in aq. alkali metal chloride solutions : (○) NaCl, i = 0.45, 0.40, 0.35, 0.30, 0.25 0.20 from top to bottom ; (●) CsCl, i = 0.45 ; (△) LiCl, i = 0.45.

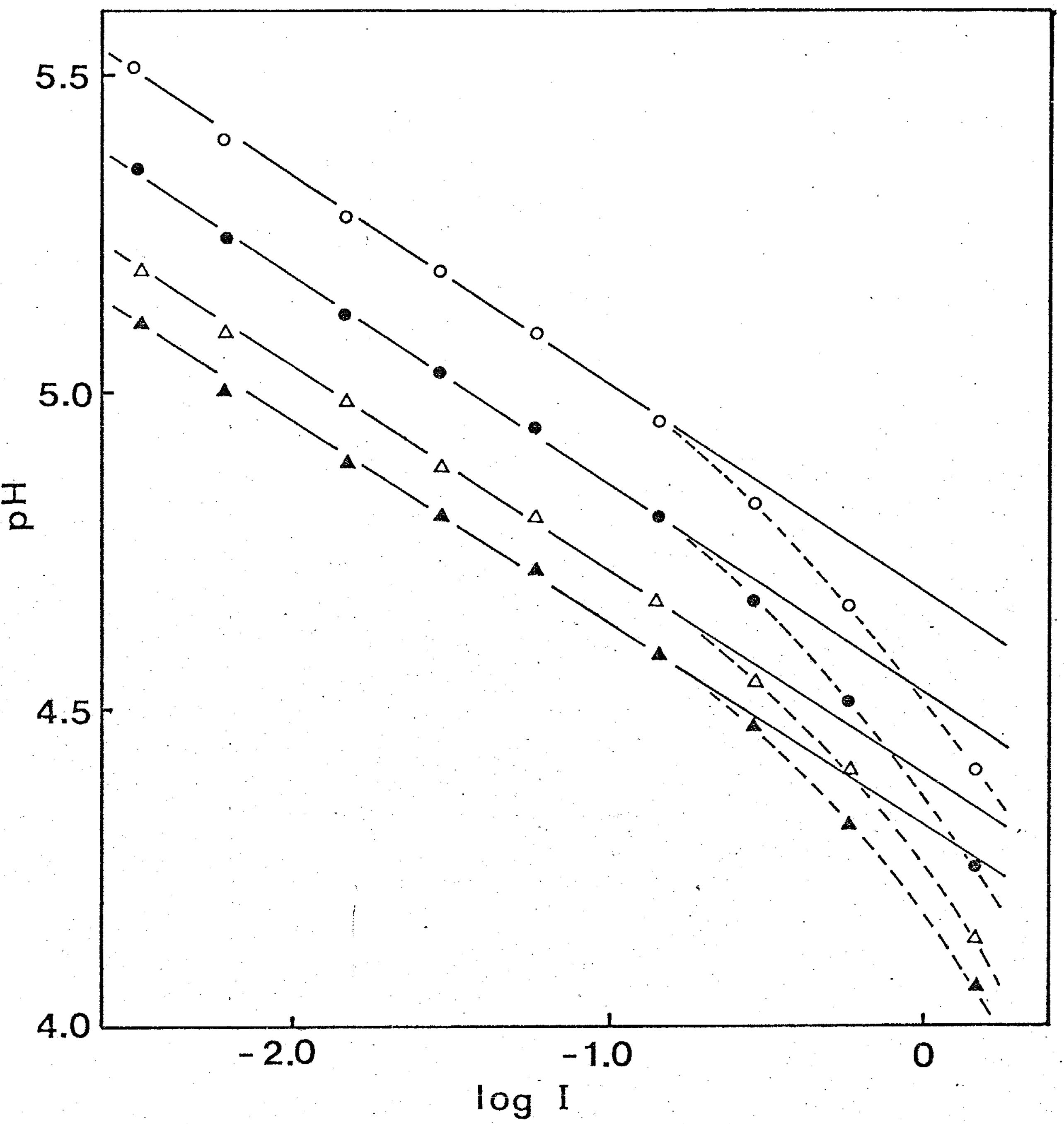

Fig.7 Dependence of pH on log I for PLGNa in aq. $MgCl_2$ solutions : (○) i = 0.60 ; (●) i = 0.50 ; (△) i = 0.40 ; (▲) i = 0.313.

Discussion

1. Theory

Salt effects on the conformation of biological polymers have been extensively studied with attention to DNA helix-coil transition ; Record et al.$^{5)}$ and Manning$^{6)}$ applied Manning's counter-ion condensation theory to the helix-coil transition. Here the important points in their theoretical derivation are followed and some extention is made to discuss the characteristic feature of the polypeptide helix formation.

Suppose a linear polyion dissolved in a solvent containing a simple salt under the condition $I \gg C_p$, where I is the ionic strength and C_p is the equivalent concentration of the polyion. A parameter proportional to the axial charge density of the linear polyion, ξ, is defined as

$$\xi = e^2/DkTb \tag{1}$$

where e is the protonic charge, D the bulk dielectric constant of solvent, k Boltzmann constant, T the Kelvin temperature and b the avarage axial charge spacing.

Electrostatic free energy per charged group, g_{el}, is

$$g_{el} = -(1-N\lambda_N)^2 \xi \ln(1-e^{-\kappa b}) \tag{2}$$

Contribution of the mixing of free counter-ions, condensed counter-ions and solvent molecules, g_{mix}, is given as

$$g_{mix} = \lambda_N \ln(10^3 \lambda_N V_p^{-1}/C_N) \tag{3}$$

where $g_i = G_i/n_pRT$ (G_i; a contribution to free energy of the system, n_p; the total number of moles of charged groups on the polyion), N is the valence of counter-ion, λ_N the number of associated counter-ions per fixed charge, κ the Debye-Hückel screening parameter and V_p in cm^3/mole of fixed charge is the volume of the region surrounding the polyion within which counter-ion are condensed. Eq.(3) is obtained by omitting terms independent of λ_N. To obtain the actual equilibrium state, that is, a state of incomplete dissociation and incomplete binding, minimization of the sum g_{el} + g_{mix} with respect to λ_N must be performed. The result is

$$1 + \ln(10^3\lambda_N V_p^{-1}/C_N) = -2N\xi(1-N\lambda_N)\ln(1-e^{-\kappa b}) \qquad (4)$$

In the limit $C_N \to 0$, a term $-\ln C_N$ in each side of eq.(4) diverges to infinity. Therefore, under such a condition, the following equation must be satisfied to cancel the terms.

$$N\lambda_N = 1 - (N\xi)^{-1} \qquad (5)$$

Taking into account the above, Record et al.[5)] have treated the helix-coil transition of DNA as follows ;

$$\mathrm{COIL} + \Delta n\ M^+ \overset{K}{\rightleftarrows} \mathrm{HELIX} \qquad (6)$$

where COIL and HELIX represent cooperative units in coil and helix conformations, respectively, and Δn the stoichiometric amount of counter-ion condensation per cooperative unit of the transition, M^+ concentration of the monovalent counter-ion. From eq.(5),

$$\Delta n = N_u(\xi_c^{-1} - \xi_h^{-1}) \qquad (7)$$

where N_u is the number of charged groups contained in a cooperative unit, and c and h represent coil and helix conformations, respectively. Then, the equilibrium constant of the coil-helix transition observed, K_{obs}, and K in eq.(6) can be related as

$$\ln K_{obs} = \ln K + \ln \gamma_c/\gamma_h + N_u(\xi_c^{-1} - \xi_h^{-1}) \ln a_+ \qquad (8)$$

As the activity coefficient γ of a cooperative unit can be obtained from G_{el}, viz.,

$$\ln \gamma = G_{el}/RT = -\xi^{-1} \ln(1-e^{-\kappa b}) \qquad (9)$$

from eq.(8) and eq.(9),

$$d \ln K_{obs}/d \ln a_\pm = N_u(\xi_c^{-1} - \xi_h^{-1})/2 \qquad (10)$$

where it is assumed that in the limit a_+(activity of the cation) $\rightarrow 0$, $a_+ \simeq a_\pm$ and $\ln(1-e^{-\kappa b}) \simeq \ln \kappa b$. Therefore, if an equilibrium as described by eq.(6) holds also for the coil-helix transition of charged polypeptides such as PLGNa and PLL, the plot of $\ln \theta/1-\theta$ vs. $\ln a_\pm$ should be analysed with eq.(10). It is, however, to be noted that the formulation from eq.(7) to eq.(10) is derived for DNA under neutral pH where titration effects are unimportant. As i, the degree of neutralization, of PLGNa in the present study is smaller than unity, the difference of α, the degree of dissociation of carboxyl groups, in random coil parts and helix parts must be taken into account. These two α being represented by α_c and α_h, respectively, eq.(10) is modified as[4)]

$$d \ln(\theta/1-\theta)/d \ln C_s = N_u\{(\xi_c^{-1} - \xi_h^{-1})/2 - (\alpha_c - \alpha_h)\}$$
$$\text{for } \alpha_c \xi_c > 1,\ \alpha_h \xi_h > 1$$

$$= N_u(\alpha_h - \xi_h^{-1}/2 - \alpha_c^2\xi_c/2)$$
$$\text{for } \alpha_c\xi_c \leq 1,\ \alpha_h\xi_h > 1 \qquad (11)$$
$$= N_u(\alpha_h^2\xi_h - \alpha_c^2\xi_c)/2$$
$$\text{for } \alpha_c\xi_c \leq 1,\ \alpha_h\xi_h \leq 1$$

where $\ln C_s$ is used instead of $\ln a_+$ or $\ln a_\pm$ because the difference in $\ln C_s$ and $\ln a_\pm$ for NaCl becomes appreciable only in higher C_s region over 0.1 M.

2. Interpretation of the results on PLGNa in aq. NaCl soln. by means of eq.(11)

Fig.8 shows $\ln(\theta/1-\theta)$ vs. $\ln C_s$ plot for PLGNa in aq. NaCl solution at 25°C, where values of θ measured at constant i were corrected to those at constant α by taking into account the dependence of α on C_s with the following relationship,

$$\alpha = i + C_{H^+}/C_p \qquad (12)$$

where C_{H^+} and C_p are equivalent concentrations of proton and polyion, respectively. C_{H^+} was calculated using the pH data for PLGNa in aq. NaCl solution in Table 3. It can be seen from Fig.8 that the plots of $\ln(\theta/1-\theta)$ vs. $\ln C_s$ are similar to those of helix content vs. $\log C_s$ in Fig.1. The linear parts of the plots extend to higher C_s region with increasing α. Values of the slopes, the left-hand side of eq.(11), are summarized in Table 4 together with those obtained without the correction by eq.(12). It is clear that corrected values are only moderately larger than the uncorrected ones, and the slopes show a decreasing trend with decreasing α. α or i at which the slope takes a value near naught is 0.25 in

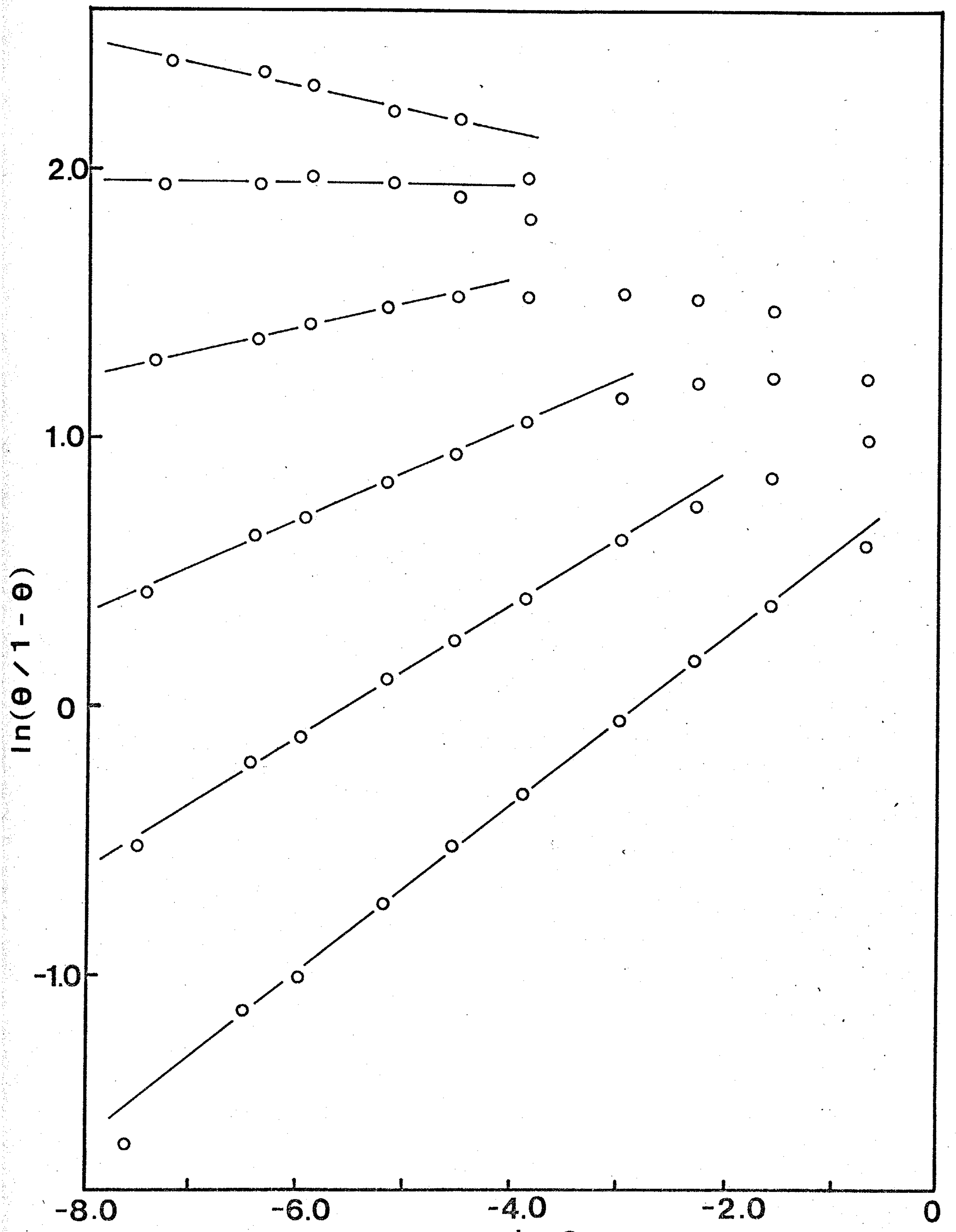

Fig.8 Plot of ln(θ/1-θ) vs. ln C_s for PLGNa in aq. NaCl solutions at 25°C : α = 0.20, 0.25, 0.30, 0.35, 0.40, 0.45 from top to bottom.

Table 4 Slopes of linear parts in $\ln(\theta/1-\theta)$ vs. $\ln C_s$ plots

4 - 1 PLGNa-NaCl

			Slope			
i (α)	15°C	20°C	25°C	30°C	40°C	50°C
0.20			-0.078(-0.088)	-0.090	0.0	0.0
0.25	0.0	0.0	0.0 (0.0)		0.036	0.054
0.30	0.070	0.086	0.074(0.089)	0.047	0.146	0.115
0.35	0.160	0.157	0.147(0.174)	0.132	0.184	0.180
0.40	0.220	0.196	0.222(0.248)	0.198	0.268	0.243
0.45		0.228	0.289(0.313)	0.273	0.294	0.254
0.50		0.293	0.348	0.322	0.326	
0.55			0.421			

4 - 2 PLGNa-$MgCl_2$(25°C)

i	Slope
0.35	-0.055
0.40	-0.032
0.45	0.0
0.50	0.032
0.60	0.077
0.70	0.147
0.80	0.315

the temperature region below 30°C while 0.20 at 40 and 50°C. This difference may be caused by certain reasons. One is the increasing trend of α with raising temperature.

Eqs.(2), (3) and (8) indicate that the dependence of helix content on C_s is determined by a balance of contributions from g_{el} and g_{mix} in random coil and helix conformations. This can be true when C_s is so low that the contribution from specific interactions between alkali salts and the polymer can safely be negrected. Therefore eq.(11) is applied to the dependence of helix content on C_s in lower C_s region investigated. Table 5 shows value of the slopes calculated with eq.(11). α_c, α_h and σ needed for the calculation were obtained from Fig.5 in this chapter and Table 8 in Chapter II. (N_u was estimated through the relation $N_u = 1/\sqrt{\sigma}$) These values were obtained based on the data for PLGNa in aq. 0.1 M NaCl solution. The use of the values thus obtained may be justified for the examination on the α dependence of the slope in lowe C_s region, because increasing or decreasing tendency of $\alpha_c - \alpha_h$ and σ with increasing α would not be affected by decreasing C_s to $10^{-2} \sim 10^{-3}$ M. Eq.(11) predicts positive slopes even in the region of α where counter-ion condensation does not take place in either conformation, because ξ_h is much larger than ξ_c for PLGNa in water at 25°C, i.e., the values are 4.76 and 1.98, respectively. The discrepancy between the dependencies of the slope on α predicte by Manning theory and obtained experimentally, should be attributed to the inappropriate application of the formulation derived for DNA systems to the helix-coil transition of PLGNa rather than defects of the theory itself, since counter-ion condensation phe-

Table 5 Calculated values of $d\ln(\theta/1-\theta)/d\ln C_s$ with eq.(11)

α	$d\ln(\theta/1-\theta)/d\ln C_s$ expl.	$d\ln(\theta/1-\theta)/d\ln C_s$ calcd.	θ^a	α_c	α_h	$\sigma \times 10^3$
0.20	-0.09		0.91	0.25	0.195	
0.25	0.0		0.875	0.31	0.24	
0.30	0.09	0.94	0.785	0.36	0.28	2.4
0.35	0.17	1.4	0.625	0.40	0.32	1.7
0.40	0.25	1.1	0.41	0.44	0.34	1.4
0.45	0.31	1.5	0.205	0.47	0.37	1.0
0.50	0.35^b	1.2	0.075	0.51	0.395	0.78

a ; Values at $C_s = 10^{-3}$M, b ; Value at $i = 0.50$

nomenon has been observed in many systems containing various polyelectrolytes[7]. In fact Manning theory has given a semiquantitative explanation for the helix-coil transition of DNA.

3. Extension of Manning theory to alternating helix-coil chain of PLGNa

The most significant difference between the helix-coil transitions of DNA and PLGNa would be the one in the cooperativity in these transitions. The size of the cooperative unit of the former transition is larger than, typically, one hundred, while in the latter case, the size is at most about thirty.

By assuming the Debye-Hückel screened coulomb potential between fixed charges on a polyion, Manning derived eq.(2) as the first term in Mayer's cluster theory for ionic solutions. Manning[8] obtained the following equation as the contribution of ring diagrams which begin and end on different charged sites, $F_{rp}^{(2)}$, as

$$F_{rp}^{(2)}/C_p = -\xi \sum_{j=1}^{\nu-1} (1-j/\nu)\exp(-\kappa jb)/j \qquad (13)$$

where ν is the number of fixed charges on each polyion. In the limit $\nu \to \infty$, j/ν may be neglected, then,

$$F_{rp}^{(2)}/C_p = -\xi \sum_{j=1}^{\infty} \exp(-\kappa jb)/j = \xi \ln(1-e^{-\kappa b}) \qquad (14).$$

The contribution of ring diagrams which begin and end on the same charged site on the polyion, $F_{rp}^{(1)}$, is given as

$$F_{rp}^{(1)}/C_p = \xi\kappa/2 \qquad (15)$$

which can be neglected in the limit $C_s \to 0$, compared with $F_{rp}^{(2)}/C_p$.

Infinity as the upper limit of the summation in eq.(13) may lead to a serious mistake when the equation is applied to the helix-coil transition for which cooperative unit is short, as found in PLGNa. End effects must be taken into account. As each helical part lies between random coil parts in the transition region of PLGNa, a fixed charge in the helical part may interact with charges on coil parts adjacent to the helical part. The use of eq.(14) for a perfect coil and a perfect helical polymer chains would not be appropriate, either, because C_s used in practice is higher than $10^{-3} \sim 10^{-4}$ M where κ^{-1} and ν take finite values.

Here we estimate g_{el} based on the models illustrated in Fig.9. To begin with, we treat a polyion with uniform axial charge spacing. (Model 1 in Fig.9) The interactions between fixed charges via screened coulomb potential assumed in Manning theory are employed but are cutted off at a distance from the particular charge where the condition $\kappa nb \simeq 1$ is satisfied. This cutting-off may be justified because the contribution of electrostatic free energy from the region of $\kappa nb \simeq 1$ to the whole g_{el} must be very small at sufficiently low C_s, typically 10^{-3} M. Then, g_{el} can be obtained by summing up the electrostatic energy as the following equation,

$$g_{el} = (1-\lambda_1)^2 \xi \sum_{j=1}^{n} \exp(-\kappa jb)/j \qquad (16)$$

$$n \simeq 1/\kappa b$$

where n is an integer, λ_1 stands for the univalent counter-ion such as Na^+. Now, we can obtain λ_1 by carrying out minimization of $g_{el} + g_{mix}$ with respect to λ_1,

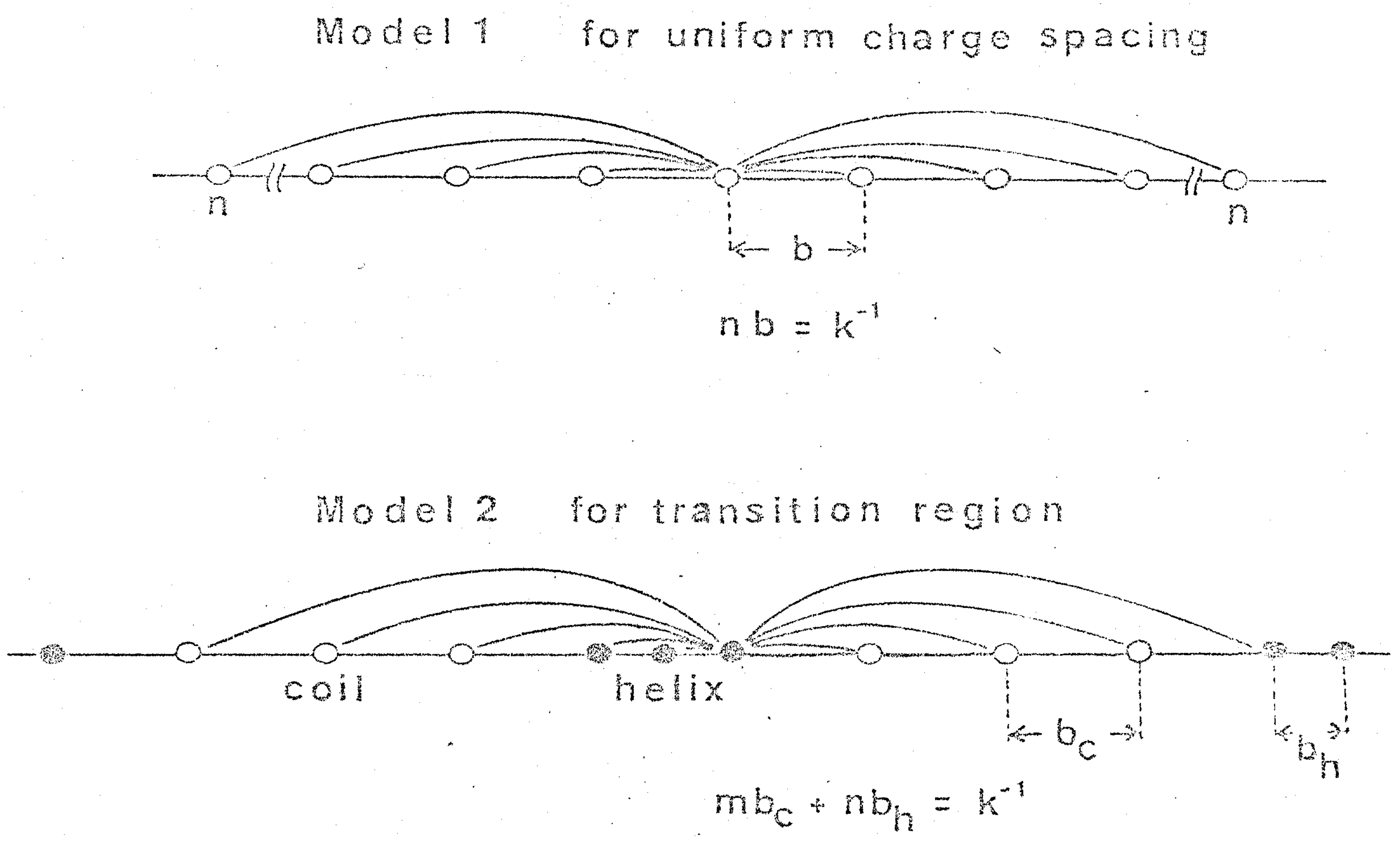

Fig.9 Models for electrostatic interaction between charged groups in a polypeptide chain.

$$1 + \ln \lambda_1 10^3 V_p^{-1}/C_s = -2\xi(1-\lambda_1)\Sigma \qquad (17)$$

where C_s is the concentration of added salt such as NaCl and Σ represents $\sum_{j=1}^{n} \exp(-\kappa jb)/j$. In the above equation, terms dependent on $\ln C_s$ must be canceled because degree of counter-ion condensation does not dependent on C_s in the lower region($< 10^{-2} \sim 10^{-3}$M). Then, λ_1 is given as

$$\lambda_1 = 1 - 1/2(\xi\, \Delta\Sigma/\Delta\ln C_s) \qquad (18)$$

This equation is different from eq.(5) with $N = 1$ only in a term $\Delta\Sigma/\Delta\ln C_s$ instead of 1/2. The dependence of Σ on $\ln C_s$, $\Delta\Sigma/\Delta\ln C_s$, was calculated simply by dividing the difference of Σ by that of $\ln C_s$ for each pair of C_s shown in Table 6. The difference between λ_1 estimated using eq.(18) and that by Manning theory(eq.(5)) becomes larger with increasing C_s, as can be seen from Table 6. The increasing discrepancy may be due to the fact that the Debye-Hückel screened potential used is valid only at lower limit of C_s investigated in the present study. It is rather worth while to notice the fairly good agreement between the values of λ_1 obtained by the two methods in the lower C_s region. This means that the use of infinity as ν does not lead any serious error in estimating λ_1 in such region of C_s. But it may not be true in the transition region. In the following, g_{el} of charges in the transition region is estimated based upon Model 2 in Fig.9.

Expressions used for summing up the electrostatic energy between charges on 1) the same coil(helix) part and 2) different

Table 6 Σ and λ_1 calculated by eq.(16) and eq.(18) respectively.

6 - 1. Random coil conformation

a. $\alpha = 1.0$, $b_c = 3.6 \times 10^{-8}$cm , λ_1(Manning) = 0.495

C_s (M)	n	Σ	$\Delta\Sigma/\Delta\ln C_s$	λ_1
5.0×10^{-4}	38	3.432		
			} 0.486	0.480
1.0×10^{-3}	27	3.095		
			} 0.486	0.480
2.0×10^{-3}	19	2.758		
			} 0.480	0.474
5.0×10^{-3}	12	2.318		
			} 0.494	0.489
1.0×10^{-2}	8	1.976		
			} 0.426	0.470
2.0×10^{-2}	6	1.976		
			} 0.418	0.396
5.0×10^{-2}	4	1.298		
			} 0.382	0.339
1.0×10^{-1}	3	1.033		
			} 0.390	0.352
2.0×10^{-1}	2	0.763		
			} 0.361	0.300
5.0×10^{-1}	1	0.432		

b. $\alpha = 0.9$, $b_c = 4.0 \times 10^{-8}$cm , λ_1(Manning) = 0.439

C_s (M)	n	Σ	$\Delta\Sigma/\Delta\ln C_s$	λ_1
5.0×10^{-4}	34	3.327		
			} 0.489	0.426
1.0×10^{-3}	24	2.988		
			} 0.482	0.418
2.0×10^{-3}	17	2.654		
			} 0.468	0.400
5.0×10^{-3}	11	2.225		
			} 0.450	0.376
1.0×10^{-2}	8	1.913		
			} 0.504	0.443
2.0×10^{-2}	5	1.564		
			} 0.440	0.362
5.0×10^{-2}	3	1.161		
			} 0.408	0.312
1.0×10^{-1}	2	0.878		
			} 0.242	[illegible]
2.0×10^{-1}	2	0.710		
			} 0.345	0.187
5.0×10^{-1}	1	0.394		

Table 6 - 1 (continued 1)

c. $\alpha = 0.8$, $b_c = 4.5 \times 10^{-8}$cm , λ_1(Manning) = 0.369

C_s (M)	n	Σ	ΔΣ/ΔlnC$_s$	λ_1
5.0×10^{-4}	30	3.209		
			} 0.492	0.358
1.0×10^{-3}	21	2.868		
			} 0.475	0.335
2.0×10^{-3}	15	2.539		
			} 0.455	0.306
5.0×10^{-3}	10	2.122		
			} 0.463	0.318
1.0×10^{-2}	7	1.801		
			} 0.439	0.281
2.0×10^{-2}	5	1.497		
			} 0.433	0.271
5.0×10^{-2}	3	1.100		
			} 0.400	0.211
1.0×10^{-1}	2	0.823		
			} 0.179	0
2.0×10^{-1}	2	0.699		
			} 0.381	0.172
5.0×10^{-1}	1	0.350		

d. $\alpha = 0.7$, $b_c = 5.14 \times 10^{-8}$cm , λ_1(Manning) = 0.278

C_s (M)	n	Σ	ΔΣ/ΔlnC$_s$	λ_1
5.0×10^{-4}	26	3.075		
			} 0.468	0.229
1.0×10^{-3}	19	2.751		
			} 0.494	0.270
2.0×10^{-3}	13	2.409		
			} 0.480	0.248
5.0×10^{-3}	8	1.969		
			} 0.424	0.149
1.0×10^{-2}	6	1.675		
			} 0.460	0.216
2.0×10^{-2}	4	1.356		
			} 0.359	0
5.0×10^{-2}	3	1.027		
			} 0.388	0.070
1.0×10^{-1}	2	0.758		
			} 0.416	0.133
2.0×10^{-1}	1	0.470		

Table 6 - 1 (continued 2)

e. $\alpha = 0.6$, $b_c = 6.0 \times 10^{-8}$cm , λ_1(Manning) = 0.158

C_s (M)	n	Σ		$\Delta\Sigma/\Delta\ln C_s$	λ_1
5.0×10^{-4}	23	2.936			
			}	0.489	0.139
1.0×10^{-3}	16	2.597			
			}	0.489	0.139
2.0×10^{-3}	11	2.258			
			}	0.461	0.087
5.0×10^{-3}	7	1.835			
			}	0.440	0.043
1.0×10^{-2}	5	1.530			
			}	0.377	0
2.0×10^{-2}	4	1.269			
			}	0.457	0.079
5.0×10^{-2}	2	0.850			
			}	0.245	0
1.0×10^{-1}	2	0.680			
			}	0.384	0
2.0×10^{-1}	1	0.414			

f. $\alpha = 0.5$, $b_c = 7.2 \times 10^{-8}$cm , λ_1(Manning) = 0.010

C_s (M)	n	Σ		$\Delta\Sigma/\Delta\ln C_s$	λ_1
5.0×10^{-4}	19	2.757			
			}	0.495	0
1.0×10^{-3}	13	2.414			
			}	0.481	0
2.0×10^{-3}	9	2.081			
			}	0.437	0
5.0×10^{-3}	6	1.180			
			}	0.460	0
1.0×10^{-2}	4	1.361			
			}	0.385	0
2.0×10^{-2}	3	1.094			
			}	0.417	0
5.0×10^{-2}	2	0.712			
			}	0.345	0
1.0×10^{-1}	1	0.473			

Table 6 - 2 Helix conformation

a. $\alpha = 1.0$, $b_h = 1.5 \times 10^{-8}$cm , λ_1(Manning) = 0.790

C_s (M)	n	Σ	ΔΣ/ΔlnC_s	λ_1
5.0×10^{-4}	91	4.296		
			} 0.498	0.789
1.0×10^{-3}	64	3.951		
			} 0.495	0.788
2.0×10^{-3}	45	3.608		
			} 0.485	0.783
5.0×10^{-3}	29	3.163		
			} 0.496	0.788
1.0×10^{-2}	20	2.819		
			} 0.452	0.768
2.0×10^{-2}	15	2.506		
			} 0.490	0.786
5.0×10^{-2}	9	2.057		
			} 0.416	0.747
1.0×10^{-1}	7	1.796		
			} 0.437	0.760
2.0×10^{-1}	5	1.466		
			} 0.431	0.756
5.0×10^{-1}	3	1.071		

b. $\alpha = 0.8$, $b_h = 1.875 \times 10^{-8}$cm , λ_1(Manning) = 0.737

C_s (M)	n	Σ	ΔΣ/ΔlnC_s	λ_1
5.0×10^{-4}	73	4.076		
			} 0.499	0.737
1.0×10^{-3}	51	3.730		
			} 0.494	0.734
2.0×10^{-3}	36	3.388		
			} 0.485	0.729
5.0×10^{-3}	23	2.943		
			} 0.489	0.731
1.0×10^{-2}	16	2.604		
			} 0.447	0.706
2.0×10^{-2}	12	2.294		
			} 0.492	0.733
5.0×10^{-2}	7	1.843		
			} 0.442	0.703
1.0×10^{-1}	5	1.537		
			} 0.377	0.652
2.0×10^{-1}	4	1.276		
			} 0.460	0.715
5.0×10^{-1}	2	0.855		

Table 6 - 2 (continued 1)

c. $\alpha = 0.6$, $b_h = 2.50 \times 10^{-8}$cm , λ_1(Manning) = 0.650

C_s (M)	n	Σ	$\Delta\Sigma/\Delta\ln C_s$	λ_1
5.0×10^{-4}	54	3.786		
			} 0.494	0.646
1.0×10^{-3}	38	3.444		
			} 0.483	0.638
2.0×10^{-3}	27	3.107		
			} 0.487	0.641
5.0×10^{-3}	17	2.660		
			} 0.476	0.632
1.0×10^{-2}	12	2.330		
			} 0.440	0.602
2.0×10^{-2}	9	2.025		
			} 0.437	0.599
5.0×10^{-2}	6	1.625		
			} 0.455	0.615
1.0×10^{-1}	4	1.310		
			} 0.385	0.545
2.0×10^{-1}	3	1.043		
			} 0.358	0.511
5.0×10^{-1}	2	0.715		

d. $\alpha = 0.4$, $b_h = 3.75 \times 10^{-8}$cm , λ_1(Manning) = 0.475

C_s (M)	n	Σ	$\Delta\Sigma/\Delta\ln C_s$	λ_1
5.0×10^{-4}	36	3.387		
			} 0.478	0.451
1.0×10^{-3}	26	3.056		
			} 0.494	0.468
2.0×10^{-3}	18	2.714		
			} 0.491	0.465
5.0×10^{-3}	11	2.264		
			} 0.450	0.416
1.0×10^{-2}	8	1.952		
			} 0.426	0.384
2.0×10^{-2}	6	1.657		
			} 0.417	0.370
5.0×10^{-2}	4	1.275		
			} 0.382	0.313
1.0×10^{-1}	3	1.010		
			} 0.387	0.321
2.0×10^{-1}	2	0.742		
			} 0.355	0.260
5.0×10^{-1}	1	0.417		

Table 6 - 2 (continued 2)

e. $\alpha = 0.35$, $b_h = 4.29 \times 10^{-8}$cm , λ_1(Manning) = 0.400

C_s (M)	n	Σ	$\Delta\Sigma/\Delta \ln C_s$	λ_1
5.0×10^{-4}	32	3.261		
			} 0.501	0.401
1.0×10^{-3}	22	2.914		
			} 0.468	0.359
2.0×10^{-3}	16	2.590		
			} 0.479	0.373
5.0×10^{-3}	10	2.151		
			} 0.465	0.355
1.0×10^{-2}	7	1.829		
			} 0.440	0.318
2.0×10^{-2}	5	1.523		
			} 0.436	0.312
5.0×10^{-2}	3	1.125		
			} 0.404	0.257
1.0×10^{-1}	2	0.845		
			} 0.247	0
2.0×10^{-1}	2	0.674		
			} 0.334	0.101
5.0×10^{-1}	1	0.368		

f. $\alpha = 0.30$, $b_h = 5.0 \times 10^{-8}$cm , λ_1(Manning) = 0.300

C_s (M)	n	Σ	$\Delta\Sigma/\Delta \ln C_s$	λ_1
5.0×10^{-4}	27	3.106		
			} 0.488	0.282
1.0×10^{-3}	19	2.768		
			} 0.457	0.234
2.0×10^{-3}	14	2.451		
			} 0.466	0.249
5.0×10^{-3}	9	2.024		
			} 0.481	0.272
1.0×10^{-2}	6	1.691		
			} 0.462	0.242
2.0×10^{-2}	4	1.371		
			} 0.359	0.025
5.0×10^{-2}	3	1.042		
			} 0.391	0.105
1.0×10^{-1}	2	0.771		
			} 0.420	0.166
2.0×10^{-1}	1	0.480		

Table 6 - 2 (continued 3)

g. $\alpha = 0.25$, $b_h = 6.0 \times 10^{-8}$cm , λ_1(Manning) = 0.160

C_s (M)	n	Σ	ΔΣ/ΔlnC$_s$	λ_1
5.0×10^{-4}	23	2.936		
			} 0.489	0.141
1.0×10^{-3}	16	2.597		
			} 0.489	0.141
2.0×10^{-3}	11	2.258		
			} 0.461	0.089
5.0×10^{-3}	7	1.835		
			} 0.440	0.045
1.0×10^{-2}	5	1.530		
			} 0.377	0
2.0×10^{-2}	4	1.269		
			} 0.457	0.086
5.0×10^{-2}	2	0,850		
			} 0.245	0
1.0×10^{-1}	2	0.680		
			} 0.384	0
2.0×10^{-1}	1	0.414		

h. $\alpha = 0.20$, $b_h = 7.5 \times 10^{-8}$cm , λ_1(Manning) = 0.0

C_s (M)	n	Σ	ΔΣ/ΔlnC$_s$	λ_1
5.0×10^{-4}	18	2.713		
			} 0.486	0
1.0×10^{-3}	13	2.389		
			} 0.479	0
2.0×10^{-3}	9	2.057		
			} 0.437	0
5.0×10^{-3}	6	1.656		
			} 0.457	0
1.0×10^{-2}	4	1.339		
			} 0.385	0
2.0×10^{-2}	3	1.072		
			} 0.360	0
5.0×10^{-2}	2	0.742		
			} 0.410	0
1.0×10^{-1}	1	0.458		

coil(helix) parts and 3) between a charge on a coil part and one on an adjacent helix part, are as follows ;

$$1)\ \Sigma_{cc}(\Sigma_{hh}) \equiv \sum_{j=1}^{n-1} (1-j/n)\exp(-\kappa jb)/j \quad \text{when} \quad (n-1)b \le \kappa^{-1}$$

$$\equiv \{(n-n') \sum_{j=1}^{n'} \exp(-\kappa jb)/j + \sum_{n''=1}^{n'-1} \sum_{j=1}^{n''} \exp(-\kappa jb)/j\}/n \quad \text{when} \quad (n-1)b > \kappa^{-1} \tag{19}$$

where n is the number of charged groups on a coil or helical part and n′ is an integer which satisfies $n'b \simeq \kappa^{-1}$.

$$2)\ \Sigma_{cc'} \equiv \sum_{p=2}^{w} (p-1)\exp[-\kappa\{(n_h-1)b_h + pb_c\}]/\{n_h-1)b_h + pb_c\} \quad \text{when} \quad (n_h-1)b_h + 2b_c \le \kappa^{-1} \tag{20}$$

where $w = \{\kappa^{-1} - (n_h-1)b_h\}/b_c$.

$$\Sigma_{hh'} \equiv \sum_{q=0}^{z} (q+1)\exp[-\kappa\{(n_c+1)b_c + qb_h\}]/\{(n_c+1)b_c + qb_h\} \quad \text{when} \quad (n_c+1)b_c \le \kappa^{-1} \tag{21}$$

where $z = \{\kappa^{-1} - (n_c+1)b_c\}/b_h$.

$$3)\ \Sigma_{hc} \equiv \sum_{m=0}^{x} \sum_{m'=1}^{y} \exp\{-\kappa(mb_h+m'b_c)\}/(mb_h+m'b_c) \tag{22}$$

where $x = n_h - 1$ when $(n_h-1)b_h + b_c \le \kappa^{-1}$,

$= (\kappa^{-1} - b_c)/b_h$ when $(n_h-1)b_h + b_c > \kappa^{-1}$,

$y = n_c$ when $mb_h + n_cb_c \le \kappa^{-1}$,

$= (\kappa^{-1} - mb_h)/b_c$ when $mb_h + n_cb_c > \kappa^{-1}$.

With the above expressions, the sum of $g_{el} + g_{mix}$ corresponding to the transition region(Model 2 in Fig.9) is given as

$$g_{el} + g_{mix} = (n_c+n_h)^{-1}\{n_c\lambda_{1c}\ln(10^3\lambda_{1c}V_{pc}^{-1}/C_s) + n_h\lambda_{1h} \times \ln(10^3\lambda_{1h}V_{ph}^{-1}/C_s) + n_c\alpha_c\xi_c(1-\lambda_{1c})^2\Sigma_{cc} + b_c\alpha_c\xi_c \times (1-\lambda_{1c})^2\Sigma_{cc'} + 2e^2/DkT \times (1-\lambda_{1c})(1-\lambda_{1h})\Sigma_{hc} + n_h\alpha_h\xi_h(1-\lambda_{1h})^2\Sigma_{hh} + b_h\alpha_h\xi_h(1-\lambda_{1h})^2\Sigma_{hh'}\} \qquad (23)$$

where λ_{1c} and λ_{1h} are degrees of counter-ion condensation in coil and helical parts, respectively. The condition of free energy minimization is

$$d(g_{el} + g_{mix}) = \frac{\partial(g_{el}+g_{mix})}{\partial\lambda_{1c}} + \frac{\partial(g_{el}+g_{mix})}{\partial\lambda_{1h}} = 0 \qquad (24)$$

As λ_{1c} is expected to be 0 below $\alpha = 0.5$ for PLGNa,

$$1 + \ln(10^3\lambda_{1h}V_{ph}^{-1}/C_s) = 2\{\alpha_h\xi_h b_h n_h^{-1}\Sigma_{hc} + \alpha_h\xi_h(1-\lambda_{1h})\Sigma_{hh} + \alpha_h\xi_h b_h n_h^{-1}(1-\lambda_{1h})\Sigma_{hh'}\} \qquad (25)$$

However this equation cannot be solved by the method used for eq.(17), since in the above case $\Delta\Sigma_i/\Delta \ln C_s$ depends on C_s even in the lower limit of C_s investigated. Then only the contribution of electrostatic interaction to the helix-coil transition of PLGNa is to be estimated.

The helix-coil transition in charged polypeptides was theoretically treated by Zimm and Rice[9)], who, utilizing the Grand Partition Function in the matrix form, considered only electrostatic interactions within a unit composed of four contiguous monomer residues. Warashina et al.[10)] also analysed the helix-coil transition of PLGNa in aq. NaCl solution taking into account only the nearest-neighbor interaction. In systems with high ionic strength, these treatments could be justified, though short cutting-off of electrostatic interaction between charged groups should not be accepted in the lower C_s region relevant to the present study. The formulation in terms of Model 2 in Fig.9, however, requires a matrix of enormous order. In addition, the equilibrium constant for the growth of helical part, s, is likely to change with the length of helical part, as Model 2 suggests it. Therefore, it is not feasible to treat statistically the helix-coil transition of PLGNa in dilute NaCl solution based on Model 2. Then as a first approximation, a mean value of s′, the contribution of electrostatic interaction to s, which is obtained by the difference of electrostatic free energy of charged groups on a helical part and a coil part as shown in Model 2, is used to evaluate the contribution of electrostatic interaction to the slope, the left-hand side of eq.(11). The above assumption means

$$\ln \sigma' + \sum_{i=1}^{N_u} \ln s_i' = N_u \ln s' \qquad (26)$$

Hence s′ implicitly contains the contribution of σ′ to the free energy change. $d \ln s'/d \ln C_s$ can be estimated by the following equation,

$$d \ln s'/d \ln C_s = \{ \alpha_c^2 \xi_c (\Delta\Sigma_{cc} + b_c n_c^{-1} \Delta\Sigma_{cc'} + b_c n_c^{-1} \Delta\Sigma_{hc}) - \alpha_h^2 \xi_h (\Delta\Sigma_{hh} + b_h n_h^{-1} \Delta\Sigma_{hh'} + b_h n_h^{-1} \Delta\Sigma_{hc}) \} / \Delta \ln C_s \qquad (27)$$

Values of $N_u d \ln s'/d \ln C_s$ assumed to be equal to $d\ln(\theta/1-\theta)/d\ln C_s$ when the counter-ion condensation does not take place, are shown in Table 7, in which all the data needed to calculate eq.(27) are contained. As λ_{1h} (and λ_{1c}) decreases with decreasing α, it is worth while to compare the value of $N_u d \ln s'/d \ln C_s$ at $\alpha = 0.25$ with $d\ln(\theta/1-\theta)/d\ln C_s$ obtained experimentally. The calculated value, -0.3, appears to be in qualitative agreement with the observed small negative slope, -0.09, at $\alpha = 0.20$, if we consider the oversimplification in the model and errors in the experimental data.

Manning theory predicts that electrostatic interaction favors helix conformation rather than random coil with increasing C_s even in the α region where counter-ion condensation does not take place, while eq.(27) predicts that coil conformation will be favored with increasing C_s. Derivations of eq.(19)-eq.(27) are essentially similar to Manning's treatment^6) except that the present model takes account of hc term, that is, the contribution of electrostatic interaction between two charges which are fixed on adjacent parts in different conformations. Therefore it can be concluded that hc term plays a substantial role in the helix-coil transition of charged polypeptides with such low cooperativity as found for PLGNa and PLL in aqueous solution.

Here it will be of interest to calculate λ_{1h} which can explain experimental values of the slopes. Such values of λ_{1h} can be obtained by solving the following equation.

Table 7 Values of $d\ln s'/d\ln C_s$ calculated by eq.(27) and those of λ_{1h} by eq.(28)

α	$N_u d\ln s'/d\ln C_s$	λ_{1h}	$\sigma \times 10^3$	$-\Delta\Sigma_{hh}/\Delta\ln C_s$	$-\Delta\Sigma_{hh'}/\Delta\ln C_s$	$-\Delta\Sigma_{hc}/\Delta\ln C_s$	$-\Delta\Sigma_{cc}/\Delta\ln C_s$	$-\Delta\Sigma_{cc'}/\Delta\ln C_s$
0.25	-0.30	0.13	3.1	0.137	0.288	0.648	0.027	0.099
0.30	-0.36	0.18	2.4	0.113	0.307	1.188	0.066	0.146
0.35	-0.79	0.24	1.9	0.093	0.195	1.940	0.111	0.145
0.40	-1.4	0.28	1.4	0.062	0.014	2.457	0.210	0.124
0.45	-1.3	0.25	1.0	0.048	0	2.436	0.333	0.081

Values of θ, α_c and α_h used for calculation are shown in Table 5.

$$d\ln(\theta/1-\theta)/d\ln C_s = N_u[\ \alpha_h\lambda_{1h} + \alpha_c^2\xi_c\{\Delta\Sigma_{cc} + b_c n_c^{-1}\Delta\Sigma_{cc'} + b_c n_c^{-1}(1-\lambda_{1h})\Delta\Sigma_{hc}\}/\Delta\ln C_s - \alpha_h^2\xi_h\{(1-\lambda_{1h})^2\Delta\Sigma_{hh} + b_h n_h^{-1}(1-\lambda_{1h})^2\Delta\Sigma_{hh'} + b_h n_h^{-1}(1-\lambda_{1h})\Delta\Sigma_{hc}\}/\Delta\ln C_s\ ] \qquad (28)$$

Table 7 contains values of λ_{1h} thus obtained for PLGNa in aq. 1.0 x 10^{-3}M NaCl solution at 25°C. The decreasing trend of λ_{1h} with decreasing α agrees with the theoretical expectation, though quantitative discussion on these values is not to be made because of the overestimation of the contribution of electrostatic interactions.

4) The effects of alkali and alkaline earth metal salts on the helix-coil transition of PLGNa

In the above, dependence of the helix content of PLGNa on C_s, especially in the lower region of C_s studied, was semiquantitatively explained based on Model 2. In the following, results on the other systems will be discussed.

Fig.2 shows the results of CD measurements on PLGNa in aqueous solutions of alkali chlorides. The helix content at each i does not depend on salt species added in the region of $C_s < 5 \times 10^{-2}$M. This suggests that alkali metal cations condense on PLG to almost the same extent. The behavior in the higher C_s regions of these salts, however, is very complex and difficult to interpret. The helix content decreases in the order ; $Na^+ > K^+ \approx Rb^+ > Li^+ > Cs^+$, which must be explained by taking into account not only nonspecific interactions but also specific interactions between the salts and the polymer. Decrease of water activity with increasing salt concentration may affect the helix content. In higher region of C_s (0.1M ~ 1.0M), hydration number estimated from compressibility data[11)] for each salt decreases as follows ; $NaCl \approx KCl > LiCl \approx RbCl > CsCl$. But the activity change of water molecules liberated by the helix formation may be rather small if it is judged from the compressibility change mentioned in Chapter III. Therefore it is inferred that the decrease of water activity caused by the increase of C_s in its higher region will not exert very much influence on the dependence of the helix content on C_s.

The relative effectiveness of alkali metal cations on the conformational change in biopolymers is not unique. The melting temperature T_m of DNA decreases in the order[12)] $Li^+ > Na^+ > K^+ > Rb^+ > Cs^+$, and the stability of the collagen fold in gelatin increases in the order[13)] $Rb^+ < Na^+ < K^+ < Cs^+ < Li^+$. These examples indicate that conformation of biopolymers cannot be predicted simply based on the diameter or the hydration number of the relevant ion. Interactions between ions and polymer moieties, e.g., charged, polar and nonpolar groups, must be properly taken into account. Nandi and Robinson[14)] estimated the effects of alkali metal chlorides on the free energy of denaturation of ribonuclease by considering contributions from peptide groups and nonpolar groups.

The series of cation effectiveness obtained in this study should also be interpreted from such point of view. However, as can be seen from Fig.2, the effect of Cs^+ on the helix content is markedly large compared with the other cations. Fig.6 shows that the slope of the plot of pH vs. log I for PLGNa in aq. CsCl solutions becomes gentle with increasing C_s(I), while pH values for NaCl and LiCl linearly decrease with log I. (Though similar deviations are observed for NaCl solutions at i $\leq$ 0.30, they are attributed to the increasing α with increasing C_s.) Therefore the deviation from the linear dependence of pH on log I for PLGNa-CsCl solution may indicate that the degree of counter-ion condensation of Cs^+ decreases with increasing C_s in the higher region ($> 5 \times 10^{-2}$M). By the decrease of λ_1, the decrease of the helix content with increasing the concentration of added cesium cation can be explained. But then, it is not to be explained why Rb^+, which has properties by and large similar to Cs^+, does not exert such marked influence on the helix content as Cs^+. A research into the microscopic hydration structure in the vicinity of the polymer chain may throw light on this unsolved problem.

Fig.3 shows the dependence of the helix content on C_s for PLGNa in aq. $MgCl_2$ solutions. One finds much larger helix content in $MgCl_2$ solutions than in NaCl solutions in Table 2. This fact is explained by the enhanced degree of Mg^{++} condensation, which is predicted by eq.(5). Since the difference of λ_N between coil and helix conformations decreases with increasing N, the slope of $\ln \theta/1-\theta$ vs. $\ln C_s$ plot should be smaller in $MgCl_2$ solution than in NaCl solution, as shown by the following general forms of eq.(11).

$$
\begin{aligned}
d\ln(\theta/1-\theta)/d\ln C_s &= N_u\{(\xi_c^{-1} - \xi_h^{-1})/2N^2 - (\alpha_c - \alpha_h)/N\}. \\
&\quad \text{for} \quad N\alpha_h\xi_h > 1,\ N\alpha_c\xi_c > 1 \\
&= N_u\{(\alpha_h - 1/2N\xi_h)/N - \alpha_c^2\xi_c/2\} \\
&\quad \text{for} \quad N\alpha_h\xi_h > 1,\ N\alpha_c\xi_c \leq 1
\end{aligned}
$$

$$= (\alpha_h^2\xi_h - \alpha_c^2\xi_c)N_u/2$$
$$\text{for} \quad N\alpha_h\xi_h \leq 1,\ N\alpha_c\xi_c \leq 1 \qquad (29)$$

In fact, this is the case found in Table 4. However eq.(29) cannot explain the α dependence of the slope for PLGNa-$MgCl_2$ system because $\alpha_c - \alpha_h$ decreases with decreasing α as shown in Fig.5. Lack of data on σ of the helix-coil transition of PLGNa in aq. $MgCl_2$ solutions detracts us from estimating the contribution of electrostatic interactions to the helix-coil transition based on Model 2.

Fig.4 gives the results on PLGNa in the presence of the other divalent cations ; Ca^{++} and Ba^{++}. The helix content depends on the cation species even in the lower C_s region, which is a marked difference from the alkali metal cases. This result suggests that the enhanced helix content observed for PLGNa in aq. alkaline earth metal chlorides solutions be caused by specific interaction of the cations with the polymer. In fact, Jacobson[15)] reported that the enhanced helix content of PLG by addition of Mg^{++} must be interpreted by taking into account both the electrostatic interaction and the complex formation between Mg^{++} and charged groups on PLG. The complex formations of Cu^{++} and Ni^{++} with carboxylic groups are also well known. Fig.10 will be of use to shed light on the question whether the enhanced helix content is caused by the complex formation involving the covalent bond between Mg^{++} and carboxylic groups or by the counter-ion condensation as predicted by Manning theory. In the lower part of Fig.10, the helix content of PLGNa in the presence of small amount of Mg^{++} are plotted against NaCl

Fig.10 a. Plot of $\ln(\theta/1-\theta)$ vs. $\ln C_s$ for PLGNa in aq. NaCl solutions which contain small amount of $MgCl_2$ at i = 0.50 ; ———————— : $\ln \theta/1-\theta$ for PLGNa in aq. NaCl solution at i = 0.50.

b. Plot of pH vs. log I for the same systems as a.

---------- : pH for PLGNa in aq. NaCl solution at i = 0.50

—— - —— : pH for PLGNa in aq. $MgCl_2$ solution at i = 0.50

(●, ○) 3.86×10^{-4}M $MgCl_2$; (▲, △) 2.42×10^{-4}M $MgCl_2$

(■, □) 9.66×10^{-5}M $MgCl_2$.

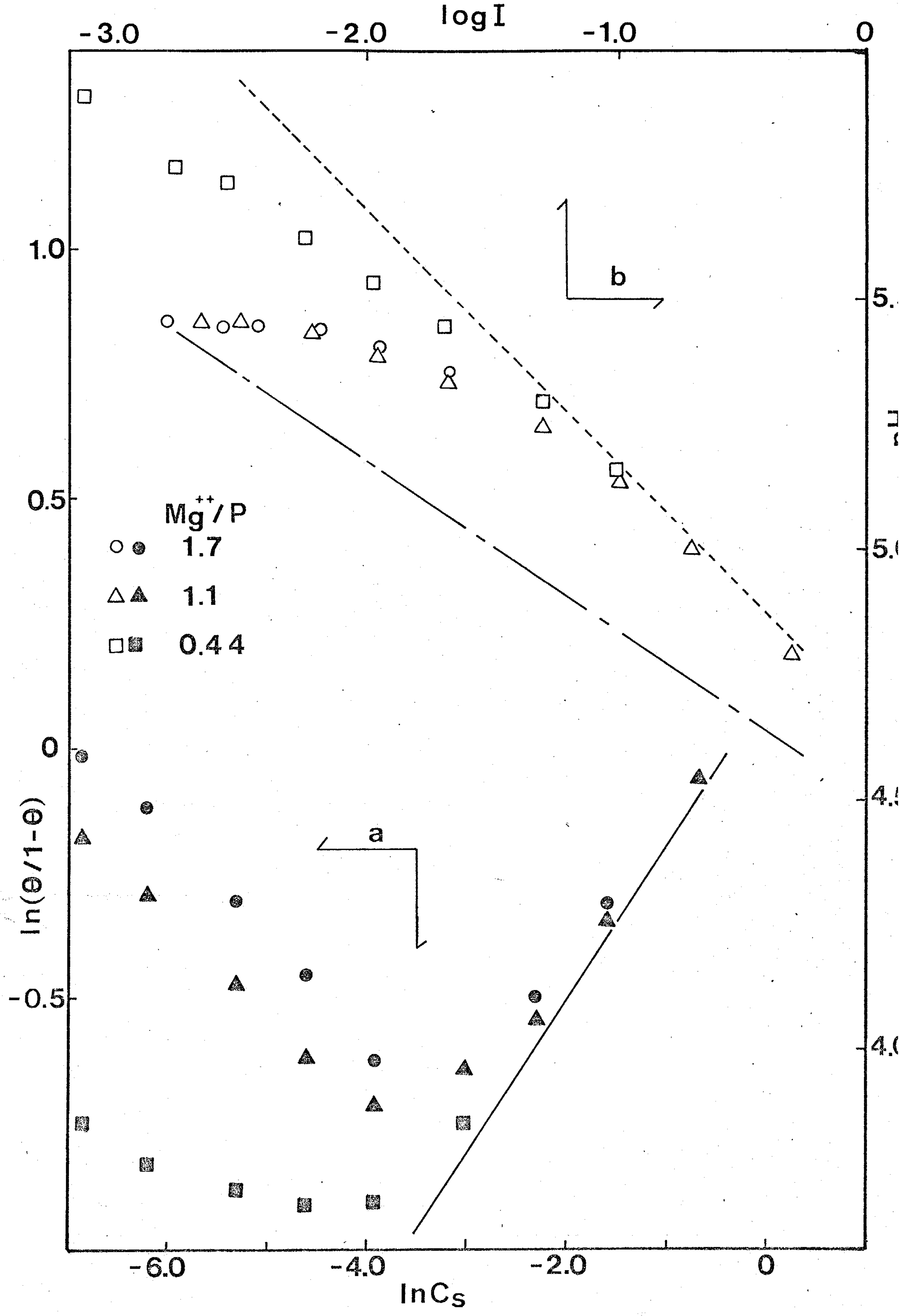
log I
-3.0
-2.0
-1.0
0
1.0
0.5
0
-0.5
ln(θ/1-θ)
-6.0
-4.0
-2.0
0
lnCs
b
a
Mg^{++}/P
○ ● 1.7
△ ▲ 1.1
□ ■ 0.44
5.
5.0
4.5
4.0

concentration. It is found that the larger the equivalent ratio of Mg^{++} to the charged groups of the polymer(Mg^{++}/P), the higher becomes the helix content. The decreasing trend of the helix content with increasing NaCl concentration(C_s) suggests that the degree of Mg^{++} binding be a decreasing function of C_s. If M_g^{++} is bound to carboxylic groups on PLGNa via covalent binding, addition of small amount of Na^+ which may not compete with Mg^{++} for the covalent bond, would not give rise to such a significant decrease of the helix content. Manning theory can explain the results ; The degree of counter-ion condensation λ_N is determined by a balance of g_{el} and g_{mix}. The entropic loss by the condensation can be compensated by the enthalpic gain from electrostatic interaction. It is this compensation that keeps the degree of counter-ion condensation constant in the lower C_s region($< 0.01M$). However when the ionic species condensed on the polyion is different from that added, the constancy in the degree of counter-ion condensation cannot be kept. Because in this case the decrease of electrostatic interaction free energy with increasing NaCl concentration does not accompany the decrease of the entropic loss of condensed Mg^{++}. Therefore with increasing C_s of NaCl, λ_2 of Mg^{++} decreases and eventually Na^+ begins to condense on the polymer. This seems to be the case, since Fig.10 shows asymptotic approach of the helix content to the linear dependence of the helix content on $\ln C_s$ for PLGNa solution containing only NaCl. The above discussion is based on the assumption that the enhanced helix content in the presence of Mg^{++} is caused by "binding" of Mg^{++} with carboxylic groups, which is supported by the result of pH measurements for the same systems shown in the upper insertion of Fig.10. The pH values for higher equivalent ratios of Mg^{++} to carboxylic groups on PLGNa, do not decrease with log I due to added NaCl at first, but afterward approach the dotted line which represents the dependence of pH on log I for PLGNa in aq. NaCl solution. The result can be interpreted in terms of decreasing λ_2 of Mg^{++} with increasing C_s of NaCl, since pH values of PLGNa in aq. $MgCl_2$ solution decrease with increasing C_s of $MgCl_2$ as indicated by the dot-dashed line. Thus, the enhanced helix content of PLGNa in the presence of Mg^{++} can be well explained by the increased λ_2 rather than the complex formation via covalent bond.

Manning theory predicts λ_N by eq.(5). If the dependence of the helix content of PLGNa on the ionic species is determined by λ_N, experimental results shown in Figs.2,4 and Table 2 suggest that eq.(5) is valid for PLGNa-alkali metal salts, but not for alkali earth metal salts, in the low C_s region. Manning6) has ascribed the slight dependence of T_m of DNA on ionic species(alkali metal cations) to the differential solvent structure in the local environment of DNA. However, Ikegami et al.16) found dehydration of Mg^{++} and Ba^{++} as counter-ions of poly(acrylic acid) from the refractive index measurements. According to their estimation, these divalent cations are completely dehydrated at i = 1.0, while dehydrated to much lesser extent at i = 0.25. The similar dehydration can well occur also in the case of PLGNa.(In Chapter III, we have inferred that the dehydration of Na^+ condensed on PLGNa is only slight. Ikegami17) also thought that Na^+ bound to the fixed charge on PAA is dehydrated only in the second hydration shell. Therefore in the case of monovalent cations, the dehydration effect on the dependence of the helix content on C_s can be safely neglected.) Since Manning has derived eq.(5) assuming that condensed counter-ions keep their hydration intact as in bulk, the balance of entropic gain and enthalpic loss due to the dehydration must be considered for the divalent cations condensed on PLGNa. The contribution to the helix-coil transition is given as

$$n_{deh}(\lambda_{2h} - \lambda_{2c})(\ln a_w - g_{hyd})$$

where n_{deh} is the dehydration number of the counter-ion, a_w the activity of bulk water, g_{hyd} the hydration energy per hydrated water molecule of the counter-ion and it is assumed n_{deh} is independent of the polymer conformation. This expression means that the larger n_{deh} is, the more coil conformation is favored, because the hydration free energy is negative. Therefore it is inferred from the experimental results that n_{deh} increases in the order ; $Ca^{++} < Mg^{++} < Ba^{++}$, which is in qualitative agreement with that by Ikegami et al.[16)].

Another feature in the C_s dependence of the helix content of PLGNa in aq. $MgCl_2$ solutions can be found by scrutinizing Fig.3. That is, the helix content is enhanced in the C_s region higher than 0.1M. In the corresponding region of log I , the pH values deviate from the linear dependence on log I as shown in Fig.7. Both these results can be explained in terms of enhanced degree of counter-ion "binding" in such a region of C_s. As such enhancement of the helix content was not observed in the case of monovalent cations, the nature of the "binding" might be the complex formation between the divalent cation and carboxyl groups on PLG, which does not take place in the lower C_s region as discussed in the preceding section. For the confirmatory discussion, it is necessary to ascertain if mass action low dominates the "binding" reaction by some methods.

In summary, the dependence of the helix content of PLGNa on the concentration of added salt has been discussed by taking the counter-ion condensation into account. But the application of Manning theory to the analysis turned out to be unsatisfactory. The modification of the theory based on the model polymer chain composed of alternating coil and helix portions, explained qualitatively the results obtained for PLGNa in aq. NaCl solutions. The limitations in the formalism of the counter-ion condensation theory for such helix forming poly(amino acid) as PLGNa was pointed out.

REFERENCES

1) ref. 1 ~ 10 and 12 in Chapter I

2) H. Kanehiro, J. Komiyama, O. Morikiyo and T. Iijima, Biopolymers, 15, 1005 (1976)

3) M. T. Record, Jr., T. M. Lohman and P. D. Haseth, J. Mol. Biol., 107, 145 (1976)

4) M. T. Record, Jr., C. P. Woodbury and T. M. Lohman, biopolymers, 15, 893 (1976)

5) M. T. Record, Jr., C. F. Anderson and T. M. Lohman, Q. Rev. Biophys., II, 103 (1978)

6) G. S. Manning, ibid., II, 179 (1978)

7) ref. 39 ~ 42 in Chapter I

8) G. S. Manning and B. H. Zimm, J. Chem. Phys., 43, 4250 (1965)

9) B. H. Zimm and S. A. Rice, J. Mol. Phys., 3, 391 (1960)

10) A. Warashina and A. Ikegami, Biopolymers, 11, 529 (1972)

11) J. O'M Bockris and P. P. S. Saluja, J. Phys. Chem., 76, 2140 (1972)

12) C. Zimmer and H. Venner, Naturwiss, 49, 86 (1962)

13) P. H. von Hippel and K. Y. Wong, Biochem., 1, 664 (1962)

14) P. K. Nandi and D. R. Robinson, J. Amer. Chem. Soc., 94, 1308 (1972)

15) A. L. Jacobson, Biopolymers, 1, 269 (1963)

16) A. Ikegami and N. Imai, J. Polym. Sci., 56, 133 (1962)

17) A. Ikegami, ibid., 2, 907 (1964)

CHAPTER V

Concluding Remarks

It is found that the unperturbed dimension of PLGNa in aq. NaCl solution is not dependent on the salt concentration, but linearly dependent on the degree of neutralization, i. It is also found that the charge induced helix-coil transition is characteristically affected by C_s. The last experimental fact has been successfully interpreted in terms of the counter-ion condensation and the electrostatic interaction between the charged groups. Thus, Manning's counter-ion condensation theory which assumes that charges on a polyion are partially compensated to keep the charge density constant by counter-ions condensed onto the polymer phase and interact with small ions conforming to the Debye-Hückel potential, turned out to be useful for the comprehension of the helix-coil transition phenomenon of PLGNa.

One of the results on the polymer dimension, however, is not compatible with the concept of the counter-ion condensation ; viscometric data on PLGNa in aq. NaCl solution show that the short-range interaction among polymer residues is influenced by electrostatic interaction. Therefore it is inferred that the compensation of fixed charges due to the counter-ion condensation leaves the short-range electrostatic interaction in some portion which increases with the charge density. The counter-ion concentration in the condense phase, which governs the short-range electrostatic interaction between fixed charges, is much higher than that in bulk, especially when it is lower than 0.1M. Manning$^{1)}$ has estimated the local concentrations of counter-ion for various polynucleotides as being 0.1 ~ 4 M. Since the degree of counter-ion condensation has little dependence on C_s, the unperturbed dimension should practically be independent of C_s, which was actually observed for PLGNa in aq. NaCl solution in the present study. Similar results have been obtained for other polyelectrolyte systems, e.g., poly(acrylic acid) studied by Nagasawa et al.$^{2)}$ and a sulfonate-containing homopolymer and an acrylic acid-containing copolymer by Tan et al.$^{3)}$.

On the basis of these interpretations, some results obtained in Chapter II are reexamined in the following.

1. The dependence of α_η^3 on i

As shown in Table 6 in Chapter II, α_η^3 of PLGNa increases with decreasing i. According to the counter-ion condensation theory, the long-range electrostatic interaction should not be affected bi i in the experimental range. However, the enhanced flexibility of the polymer chain by the decrease of i results in the increased α_η^3, since $\alpha_\eta^3 = \{\eta\}/\{\eta\}_0$ and $\{\eta\}_0$ is decreased by the enhanced flexibility.

2. Negative excluded volume effect estimated by linear extrapolation of the viscometric data to infinite concentration of added salt.

We have obtained extrapolated values of $\{\eta\}$, α_η^3 and B at infinite salt concentration by the linear plots against $C_s^{-1/2}$. However experimental points at C_s = 1.0 M deviate from the linear plots as can be seen from Figs. 5, 6 and 7 in Chapter II. Such deviations can be interpreted by taking account of counter-ion condensation ; the driving force of counter-ion condensation is reduced free energy in the electrostatic interactions as expressed by eqs.(2) and (16) in Chapter IV. Therefore with increasing C_s, the extent of the counter-ion condensation decreases. For example, at C_s which is equal to that of "condense phase", uncompensated charges will interact one another because no distinction between condense phase and bulk one exsists any more. Then, in the higher C_s region, the decreasing trend of $\{\eta\}$, α_η^3 and B with increasing C_s, will be relaxed, because the effective charge density increases. Therefore the upward deviations of experimental points at $C_s = 1.0$ M from the linear plots can be interpreted as caused by the increase of the effective charge density, and the linear extrapolations used to estimate the nonelectrostatic excluded volume effect can be justified.

3. Viscometric results for PLGNa in aq. organic solvents.

As described in Chapter II, the electrostatic part of α_η^3, $\alpha_{\eta el}^3$, has been expressed as a function of $\alpha/b_0\sqrt{C_s D}$ or $\alpha^2/C_s b_0^{3/2}$. Due to the counter-ion condensation, the effective charge density α is constant in the condensation region and can be calculated from eqs.(1) and (5) in Chapter IV. Assuming that the nonelectrostatic part of α_η^3, $\alpha_{\eta nel}^3$, can be neglected compared with $\alpha_{\eta el}^3$ and that b_0 is independent of solvent, the intrinsic viscosities for PLGNa in aq. organic solvents were calculated with the two functions for $\alpha_{\eta el}^3$. In the calculation, α_η^3 values for PLGNa in aq. 0.05M NaCl solution were used as a standard. The resulta are given in Table 1. Qualitative agreements with experimental results are obtained in both cases, though quantitative agreement is better when $\alpha_{\eta el}^3 \propto \alpha^2$ is assumed than $\alpha_{\eta el}^3 \propto \alpha/\sqrt{D}$. For further examination of these results, it is necessary to study effects of the specific interaction of organic solvent and the dielectric constant upon $\alpha_{\eta nel}^3$ and $\alpha_{\eta el}^3$, respectively.

Table 1 Comparison of calculated values of $\{\eta\}$ for PLGNa in aq. 0.05M NaCl-20vol.% organic solvents

	Ethylene Glycol			iso-PrOH			t-BuOH			Dioxane		
i	$\{\eta\}_{exp}$	$\{\eta\}_1$	$\{\eta\}_2$	$\{\eta\}_{exp}$	$\{\eta\}_1$	$\{\eta\}_2$	$\{\eta\}_{exp}$	$\{\eta\}_1$	$\{\eta\}_2$	$\{\eta\}_{exp}$	$\{\eta\}_1$	$\{\eta\}_2$
1.00	29.3	31.6	28.7	26.6	30.8	26.0	25.5	30.4	25.0	24.0	29.6	22.7
0.90	27.6	28.7	26.1	24.8	27.9	23.6	24.2	27.6	22.6	22.1	26.9	20.6
0.80	25.8	26.2	23.8	23.0	25.5	21.5	22.6	25.2	20.6	20.5	24.6	18.6

$\{\eta\}_{exp}$; Experimental values

$\{\eta\}_1$; Calculated by assuming $\alpha_{\eta el}^3 \propto \alpha/b_\circ\sqrt{C_s D}$

$\{\eta\}_2$; Calculated by assuming $\alpha_{\eta el}^3 \propto \alpha^2/C_s b_\circ^{3/2}$

These examples show that certain results on the dimension of PLGNa in solution can be well interpreted by taking account of the counter-ion condensation.

Bailey[4)] has proposed a theory of polyelectrolyte expansion which assumes the Debye-Hückel potential and counter-ion binding as described by Manning theory. However he, assuming the short-range electrostatic interaction as well as the long-range one by the Debye-Hückel screened potential, did not make distinction between the short-range and the long-range electrostatic interactions. Fixman et al.[5)] have formally made the distinction ; it is well known that application of the Debye-Hückel screened coulomb potential to the excluded volume effect in polyelectrolytes gives too large excluded volume effect. The authors argued that the failure of this application should not be attributed to the potential itself but to the assumption in the excluded volume theory that a segment negligibly interacts with its immediate neighbors. They managed to make the assumption available for polyelectrolytes by dividing the chain into segments which consist of many monomer units and the length of which is much larger than the Debye screening length. They estimated electrostatic interaction between the segments, or rods, and obtained excluded volume per one segment, by which the viscometric data of Nagasawa et al.[2)] could be semi-quantitatively reproduced. Such treatments by Fixman et al. seem to be an equivalent to a distinction between the short-range and the long-range electrostatic interactions. It is, however, very difficult to take explicitly the two types of interactions into consideration, because the short-range interaction may not be described by the Debye-Hückel screened potential and an artificial border line must be drawn between the short-range and the long-range interactions.

Another important limitation of the counter-ion condensation theory is that the model and actual polyelectrolytes have certain differences in their structures ; this theory is based on a structure model that charged beads are uniformly strung along a straight wire, which is, however, inappropriate for polyelectrolytes with long side chains bearing charged groups. In the case of PLGNa, the actual distances between charges are given by Zimm and Rice6) as about 10 Å for first three neighbors in random coil conformation and 10.1 Å, 13.1 Å, 7.9 Å, 7.5 Å, 14.3 Å and 14.4 Å for first six neighbors in the α-helix conformation. Given these values, eqs. (4) and (17) in Chapter IV do not predict counter-ion condensation. Therefore the success obtained for various polyelectrolyte systems might be originated in the other assumptions used together in the theory. One is the Debye-Hückel potential and another is the use of D in bulk phase. Particularly the latter seems to leave much to be disputed. Conway et.al.7) assumed that the dielectric constant in the first layer of electrostrictly hydrated water to polyion is lower than 55 due to dielectric saturation. Such a low dielectric constant must have a great influence on the electrostatic interactions of relatively short range. However either experimental or theoretical study on this subject have rarely performed, and it is the present situation that dielectric constant in bulk phase is used together with the Debye-Hückel potential which also should be taken as only an approximation as applied to polyelectrolytic systems.

Another assumption in the two phase model by Manning is that condensed counter-ions are not desolvated. In Chapter III, we have found that this assumption is available for PLGNa. At the same time, however, we have observed that divalent cations, Mg^{++}, Ca^{++} and Ba^{++}, differently stabilize the helix conformation of PLG, which was interpreted by the various extents of counter-ion condensation of these cations caused by the difference in hydration.

As can be seen from the above, there is rather few systems of polyelectrolytes to which Manning theory can be straightforwardly applied. Then, we must choose one of two ways ; one is the use of Manning theory with regard to the simplicity, and discrepancies between theory and experiment are interpreted on occasion by some appropriate reasons such as invalidity of model or assumption of the theory in a given polymer system. The other is improvements of the theory without regard to the resultant complication. We have chosen the former way in Chapter IV, but it is the latter way that is needed for development of polyelectrolyte theory. Since it is beyond doubt that elabolation of Manning theory makes excluded volume theories of polyelectrolytes advance and throw light upon conformational transitions of ionized polypeptides, theoretical progress and accumulation of experimental data should be unified at every stage of the polyelectrolyte study. This I have intended in my thesis.

REFERENCES

1) G. S. Manning, Q. Rev. Biophys., II, 179 (1978)

2) I. Noda, T. Tsuge and M. Nagasawa, J. Phys. Chem., 74, 710 (1970)

3-a) J. S. Tan and S. P. Gasper, J. Polym. Sci., Polym. Phys. Ed., 13, 1705 (1975)

3-b) idem., ibid., 12, 1785 (1974)

4) J. M. Bailey, Macromolecules, 10, 725 (1977)

5) M. Fixman and J. Skolnick, ibid., 11, 863 (1978)

6) B. H. Zimm and S. A. Rice, J. Mol. Phys., 3, 391 (1960)

7) B. E. Conway, J. E. Desnoyers and A. C. Smith, Phil. Trans. Roy. Soc., 256, 389 (1964)

GLOSSARIES

a ; Mark-Sakurada-Houwink parameter

a_+, $a_\pm$; Activities of cation and salt, respectively.

b_0, b_h ; Effective sebment lengths per monomer residue in unperturbed and helical polymer chains, respectively. (Chapter II)

b_c, b_h ; Mean charge spacings of random coil and helical polymer chains. (Chapter IV)

B ; A parameter related to the second virial coefficient.

C_s, C_p ; Concentration of salt and polymer in mol/l or basemol/l, respectively.

d ; Density.

D ; Dielectric constant.

i ; Degree of neutralization of polyelectrolyte.

I ; Ionic strength.

n_c, n_h ; Numbers of charged groups in a coil and a helical parts of a polymer chain.

N ; Degree of polymerization (Chapter II) or valence of counterion (Chapter IV).

N_u ; Number of monomer residues in a cooperative unit of coil-helix transition.

$\langle R^2 \rangle$; Mean square end-to-end distance of polymer chain.

s, s' ; Equilibrium constant for growth of helical part and the contribution of electrostatic interaction to s, respectively.

α ; Degree of dissociation of polyelectrolyte.

α_c ; Expansion factor of random coil polymer chain. (Chapter II)

α_c, α_h ; Degrees of dissociation of charged groups in random coil and helical parts, respectively. (Chapter IV)

GLOSSARIES (continued)

α_η ; Hydrodynamic expansion factor of polymer chain.

β ; Adiabatic compressibility.

$[\eta]$, $\{\eta\}$; Intrinsic viscosities in dl/g and l/basemol, respectively

κ ; Debye screening parameter.

λ_N ; Number of N-valence counter-ions associated with a fixed charge on polyelectrolyte.

ϕ ; Apparent molar compressibility.

σ ; Cooperativity parameter of coil-helix transition of polypeptide.

Σ ; Electrostatic energy of a fixed charge on polyelectrolyte.

θ ; Helix content.

ξ ; A dimensionless structural parameter proportional to axial charge density of linear polyelectrolyte.

ACKNOWLEDGEMENTS

This investigation has been performed under the direction of professor Toshiro Iijima. I wish to express my sincerest gratitude and appreciation to him for his continued concern, encouragement and guidance.

I wish to express my hearty thanks to Dr. Jiro Komiyama for many enlightening discussions throughout this work.

Thanks are also due to Mr. Yoshiyuki Morimoto and Miss Naoko Maki for their experimental assistance.

I am greatly indebted to Mr. Yukinori Usuda for the computer programming for calculating electrostatic energy based on the models in Chapter IV. His quick performance has largely contributed to the completion of this thesis.

The collaboration of all the research fellows and students in Professor Iijima's laboratory is gratefully acknowledged.